Department of Chemical Engineering

Experimental Investigation of Pipeline Emulsions Flow Behaviours

Lim Jit Sen

This thesis is presented for the Degree of
Master of Philosophy
of
Curtin University

April 2016

Declaration

To the best of my knowledge and belief, this thesis contains no material previously published by any other person except where due acknowledgment has been made.

This thesis contains no material which has been accepted for the award of any other degree or diploma in any university.

ABSTRACT
Experimental Investigation of Pipeline Emulsions Flow Behaviours

by
Lim Jit Sen
Curtin University, Sarawak Malaysia

Emulsification occurs when one immiscible liquid is dispersed as droplets (dispersed phase) in the other continuous phase of immiscible liquid. In the oil production industry, crude oil is usually produced together with water from the reservoir, and the immiscible mixtures of oil and water result in emulsions flow in the pipelines as well as other major processing facilities. Emulsions cause higher pressure drop, create difficulties in water-oil separation process, require more retention time in the separation vessels, take larger volume in separators and pipelines, and affect the flow behaviours due to changes in density and viscosity of the fluid. The presence of stable emulsions also reduces the quality of crude oil and causes more problems in the downstreams refinery operations, such as corrosion and higher heat capacity. In this research work, a lab-scale flow loop was constructed to investigate the formation of emulsions solely through flow shear, and the effect of emulsions on pressure drop. Behaviours of emulsions such as the stability and phase inversion were studied under different parameters of oil-water content and flow rate. The effect of emulsions on flow pressure drop is established too, with the presentation of flow pressure drop profile and dissipation energy profile. This research work shows that stable emulsions droplets were formed at higher flow rate (or higher kinetic energy); at lower flow rate, more emulsion droplets settled out and separated into phases of oil and water. Higher flow rate also brought the emulsions system to an earlier phase inversion, where in the experiment, samples with 60% water volumetric content experienced phase inversion at flow rate above 80 L/m. Stable water-in-oil (W/O) emulsions, which require dissipation energy to form, resulted in significant pressure drop. The dissipation energy is directly proportional to the pressure drop and flow velocity. The peak maximum pressure drop was experienced at the phase inversion point, where it could increase as much as 142.86% from the pressure drop value of pure crude oil. After the phase inversion, the pressure drop started to decrease, until it reached the pressure drop of pure water, due to the presence of unstable emulsions, irregular size distribution of emulsion droplets, non-aggregated emulsions with less dense packing, and water as the continuous phase. The flow pressure drop profile is an important optimization tool in the industry to determine the values of flow rate and pump discharge pressure, in mitigating the unwanted formation of emulsions and higher additional pressure loss.

ACKNOWLEDGEMENT

TABLE OF CONTENTS

LIST OF FIGURES

LIST OF TABLES

LIST OF ABBREVIATIONS

Abbreviation	Definition
BS&W	Basic Sediments and Water
CII	Colloidal Instability Index
EOR	Enhanced Oil Recovery
g/mol	Gram per Mol (molecular weight)
HPLC	High Performance Liquid Chromatography
L/m	Litre per Minute (flow rate)
LCD	Liquid Crystal Display
m/s	Meter per Second (velocity)
MCOT	Miri Crude Oil Terminal
MLC	Miri Light Crude
O/W	Oil-in-Water Emulsions
O/W/O	Oil-in-Water-in-Oil Emulsions
SARA	Saturates, Aromatics, Resins, and Asphaltenes
SG	Specific Gravity
SMAW	Shielded Metal Arc Welding
SS	Stainless Steel
Vac	Voltage Alternating Current
Vdc	Voltage Direct Current
WAT	Wax Appearance Temperature
W/O	Water-in-Oil Emulsions
W/O/W	Water-in-Oil-in-Water Emulsions

LIST OF SYMBOLS

Symbol	Definition
D	Diameter
du/dy	Shear rate
E	Dissipation energy for emulsification
f	Friction factor
g	Gravitational acceleration constant
h_f	Head loss
K	Loss coefficient
K_0	Hydration factor
$K_f(\gamma)$	Flocculation factor
ℓ_e	Entrance length
m	Flow consistency index
n	Flow behaviour index
r	Radius (pipe radius)
Re	Reynolds number
V	Flow mean velocity
ΔP	Pressure drop
ε	Surface roughness
η_c	Continuous phase's viscosity
η_d	Droplets' viscosity
η_e	Emulsions' viscosity
η_r	Relative emulsion viscosity
μ	Viscosity (dynamic viscosity)
ρ	Density
τ	Shear stress
ϕ	Dispersed droplets' volume fraction

CHAPTER 1

INTRODUCTION

1.1 Introduction to Emulsions Flow in Pipeline

Emulsion is defined as a system, where one immiscible liquid is dispersed as droplets (dispersed phase) in the other continuous phase of immiscible liquid. To form stable emulsions, there must be enough agitation or mixing energy to disperse one phase into the other, and emulsifying agents (surface active agents) such as asphaltic materials, resinous substances, oil-soluble organic acids or finely dispersed solid materials must be present (Abdel-Aal *et al*., 2003). Emulsions can be encountered, either desirable or undesirable, in many areas of daily life such as food, cosmetics, pulp and paper, pharmaceutical, agricultural as well as oil and gas industry (Mat *et al*., 2006).

Pipeline emulsions flow is inevitable for upstream oil production system transporting immiscible mixtures of crude oil and water. The turbulence, mixing, as well as agitation through downhole wellbores, surface chokes, valves, pumps and pipes will emulsify either the oil phase or water phase, depending on the volumetric amount of the phases (Fingas *et al*., 1993). Oil is usually produced together with water from the reservoirs, and towards the end of the reservoirs' life, the amount of produced water will increase, especially if the reservoirs are driven by natural water aquifer. This scenario will induce the formation of water-in-oil emulsions, and it is undesirable. Water-in-oil emulsions occur when water droplets are dispersed in the continuous oil phase (refer to Figure 3 for graphical representation).

Treating stable water-in-oil emulsions can be expensive as well as difficult, and some major oil producers are reported to reduce the selling price of their oil for not meeting the required oil quality. To bring down emulsions to the acceptable level, equipment such as free-water knock-out vessel, heater and electrostatic treater have to be used, in addition to strong dosage of demulsifier chemical treatment. In Malaysia, the oil quality is determined from basic sediments and water parameter (BS&W), where the BS&W must not exceed 0.5% (Mat *et al*., 2006). Oil with high content of emulsions will be retained in the treatment process, and this may delay the oil export, as well as affect the capacity of the treatment plant to accept more feed. Apart from treatment and separation difficulties, emulsions may also affect the

effectiveness of corrosion inhibitor and biocide, which are common types of offshore chemical injection used to protect the integrity of pipelines.

Figure 1 shows a common 3-phase separator used in the upstream oil industry, where separation between the gas, water, and oil phases occurs by virtue of momentum change, density difference, gravity difference, and gravity settling. Gas and liquid can be readily separated due to their large density difference, but separation between oil and water is more challenging. Although sufficient retention time in the separator has been allowed, there will be oil contaminant in the water outlet, as well as water contaminant in the oil outlet. The presence of emulsions further reduces the density difference, which makes separation of oil and water even more difficult. Repeated separation, longer retention time, larger vessels, and the use of auxiliary treatment such as heater and electrostatic method will be required.
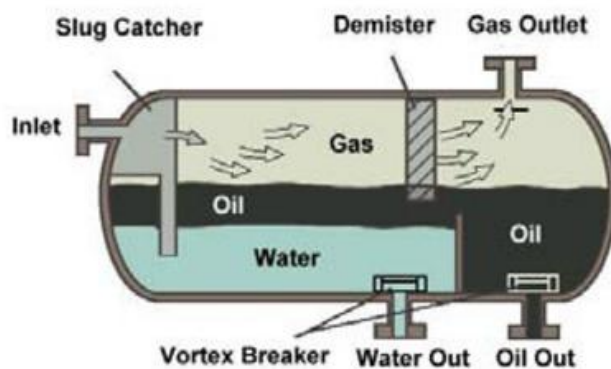
Figure 1: 3-phase separator (from Devold, 2013).

Oil contaminant in the water outlet will affect the water discharge quality and cause environmental issues, if poor water quality is discharged into the sea. Meanwhile, water contaminant in the oil outlet will reduce the quality and specifications of the exported oil.

In the oil production industry, crude oil transportation to the downstream customers plays a major role in determining the economic viability of the operations. Emulsions can pose considerable flow assurance problems and greatly affect the capacity of separators, pumps and pipelines. For example, Boukadi *et al*. (2012) calculated separator sizing using modified Arnold-Stewart's method, and claimed that the retention time was increased from base case of 3 – 20 minutes to 8 – 53 minutes, when emulsions' viscosity was taken into consideration. Longer retention time results in larger separator size, and larger footprint area to

accommodate the separator. Besides that, higher concentration of emulsions is also correlated to larger value of pressure drop (Russell *et al*., 1959; Pal, 1993; Nädler and Mewes, 1997; Keleşoğlu *et al*., 2012; Plasencia *et al*., 2013). Higher pressure drop is proportional to higher pumping power requirement, or lower flow rate. The negative consequences are higher operating expenditure and more oil deferment.

Although water-in-oil emulsions are mostly encountered in the oil production industry, there are also cases of oil-in-water emulsions. Oil-in-water emulsions are formed when oil droplets are dispersed in the continuous water phase. This occurs due to the presence of large amount of water, which can happen if water injection is used as the secondary drive. As the water amount continues to be increased, the water-in-oil emulsions will reach phase inversion point. This is the point where a catastrophic inversion will occur, resulting in crude oil to become the dispersed phase, while water will become the continuous phase, *i.e*. oil-in-water emulsions (Alwadani, 2009).

It is interesting to note that while water-in-oil emulsions are undesirable, oil-in-water emulsions on the flip side can be beneficial. The application of oil-in-water emulsions resolves the challenges of transporting highly viscous crude, as the effective viscosity of oil-in-water emulsions system is much lower than the single-phase viscosity of heavy crude (Lamb and Simpson, 1963; Ahmed *et al*., 1999).

As emulsions significantly affect the flow behaviours and flow properties, which differ compared to two-phase stratified or annular oil-water flow [shown in studies by Russell *et al.* (1959), Rose and Marsden (1970), Pilehvari *et al.* (1988), Sanchez and Zakin (1994) as well as Nädler and Mewes (1997], this research will investigate the formation of emulsions in pipeline flow, and the corresponding flow characteristics of emulsions. Understanding of emulsions flow behaviours can give significant contribution to pipeline flow assurance studies. Although emulsions cannot be fully eradicated in the upstream pipelines, but the emulsions can be controlled and manipulated through flow rate optimization, to allow efficient transportation and pumping operations.

1.2 Problem Statement

To improve the economic viability of offshore mature fields, the number of pipelines is often rationalized, and in this process, it is very important to be able to correctly estimate the pressure drop of a given pipeline (PETRONAS, 2015). Wrong estimation may lead to failures in crude oil export, if the existing pumps are not able to meet the required discharge pressure. This situation is commonly termed as "backpressure" in the industry, as the pumps fail to provide the driving force to transport the crude to its destination.

The estimation of pressure drop of a given pipeline takes into account the flow frictional losses of crude and water, but there is no consideration on the effect of emulsions (PETRONAS, 2015). This causes under-optimized operations, as the pressure effect of emulsions is not mitigated, or controlled so that the benefits can be enhanced.

This deficiency can be addressed by studying the formation and stability of emulsions (for water-in-oil emulsions and oil-in-water emulsions), and understanding their effect on the pressure drop.

1.3 Research Objectives

This research aims to present the effect of emulsions formation on pressure drop, and establish a flow pressure drop profile for water-and-oil emulsions system. The flow pressure drop profile is an essential optimization tool in the oil production industry, as the operators can exercise more control over the presence of emulsions and pressure drop, by manipulating the flow rate (*e.g.* pump speed).

The specific objectives of this research are:
   i) To analyze the formation and stability of water-and-oil emulsions in a continuous flow loop of water and crude oil mixtures.

   In a number of previous studies, emulsification takes place separately in a mixing tank. Less attention has been given on flow-induced emulsification to replicate the real practical field conditions. To date, in the best efforts of the author's literature review, only Nädler and Mewes (1997), Keleşoğlu *et al.* (2012) and Plasencia *et al.* (2013) studied on water-in-oil emulsification solely from flow shear in lab-scale pipeline.

Plasencia *et al.* (2013) attempted to replicate flow-induced emulsions, but full spectrum analysis was not available, as the water content could not be increased beyond 60% due to prohibitive backpressure to the pump. Other researchers have been focusing on emulsification from stirring or mixing.

ii) To determine the phase inversion from water-in-oil emulsions to oil-in-water emulsions, as the water content is increased in a continuous flow loop of water and crude oil mixtures.

In this research work, emulsification is induced by the virtue of flow shear, which is achieved through a flow loop. A 90°-constriction, which replicates a choke valve, is introduced in the flow loop. Full perspective of various types of emulsions and phase inversion points are investigated under different cases of flow rate (20 L/m – 100 L/m) and water content (0% – 100%).

iii) To establish the effect of emulsions formation on pressure drop along a pipe length, and its relationship with dissipation energy.

This research work also studies the effect of emulsions formation on pressure drop along a test section of the horizontal pipe length, under various scenarios of flow rate and water content.

The relationship between emulsions formation, pressure drop, and the dissipation energy in forming the emulsions is further deliberated to contribute more understanding to the field of flow assurance research.

1.4 Research Significance

i) This study is very significant in the context of Malaysian oil and gas industry, as local offshore crude oil is used in the research. Sarawak's offshore crude, classified by PETRONAS as Miri Light Crude (MLC), is studied to analyze its emulsification behaviours and the effect on flow properties.

ii) Next, this work also explores flow-induced emulsification across a constriction, and this particular research area has not received much attention yet. Existing literature shows studies done on annular or stratified flow of water and oil phases, and growing research on emulsions flow. More research needs to be done on emulsions flow, especially on flow-induced emulsification, so that the results can reflect real practical conditions as much as possible.

iii) Finally, the understanding of pressure drop with respect to emulsions formation will contribute extensively to the flow assurance research in the transportation of immiscible liquids. More robust simulation and prediction of pressure drop can be obtained from the flow pressure drop profile, more efforts to optimise the operations can be realised, and more efficient facilities design can be achieved. In today's use of demulsifier chemical, emulsions still cannot be totally inhibited, but emulsions can be controlled and manipulated by optimizing the flow rate, to allow efficient transportation and pumping operations.

1.5 Overview of Thesis Outline

The thesis starts with this introductory chapter, Chapter 1, which introduces the issues and challenges of emulsions in the oil production industry. Chapter 1 also provides the objectives and significance of performing this research on pipeline emulsions flow.

Chapter 2 gives the theoretical background on crude oil, emulsions formation process, types of emulsions and the characteristics, demulsification process, as well as emulsions treatment methods used in the oil production industry.

Chapter 3 discusses the literature review on relevant past researches on emulsions, such as studies on the effects of emulsions, factors influencing emulsions' stability and external effects on emulsions.

Chapter 4 provides the comprehensive methodology for the execution of this research. The equipment fabrication solutions, resources, design considerations, technical sizing, technical selection, installation procedures and experimental procedures are presented in detailed manner.

Results and discussion are deliberated in Chapter 5, which covers the crude oil properties, emulsions formation and stability analysis, emulsification effect on pressure drop for various scenarios, flow pressure drop profile, and dissipation energy in emulsification.

Chapter 6 finalizes this research with conclusion and further recommendations. References and Appendix are provided at the end of the chapter.

CHAPTER 2
BACKGROUND

2.1 Introduction to Emulsions

Emulsion occurs when one immiscible liquid is distributed or dispersed, in the form of droplets, in another substantially immiscible liquid (Aske, 2002). The droplets are usually referred to as the dispersed phase or the internal phase. The droplets are suspended in a medium known as the continuous phase or the external phase. According to Schramm (1992), emulsions are a special type of colloidal dispersions, and their diameters range from 1 nm to over 1000 nm.

The three major factors contributing to the formation of emulsions are (Schubert and Armbruster (1992);

1) the presence of two immiscible liquids,
2) the presence of emulsifying agents, which are surface active agents, and
3) the involvement of sufficient mixing energy to disperse one liquid into another liquid phase as droplets

In the oil and gas industry, pipeline emulsions flow is a very common occurrence. As the crude oil continues to be produced towards the end of the reservoirs' life, the amount of produced water increases as well, especially if the reservoirs are driven by water aquifer. Although crude oil and water are immiscible and initially present in separated phases, but the turbulence, mixing, as well as agitation through downhole wellbore, surface chokes, valves, pumps and pipes will cause emulsions to form (Fingas *et al.,* 1993).

The mixing and flowing of crude oil together with water result in the formation of water-in-oil (W/O) emulsions, oil-in-water (O/W) emulsions, oil-in-water-in-oil (O/W/O) emulsions and water-in-oil-in-water (W/O/W) emulsions. O/W/O and W/O/W emulsions are also called multiple emulsions.

Figure 2 gives an overview of surface facilities to produce crude oil, from oil wellhead until pipeline.
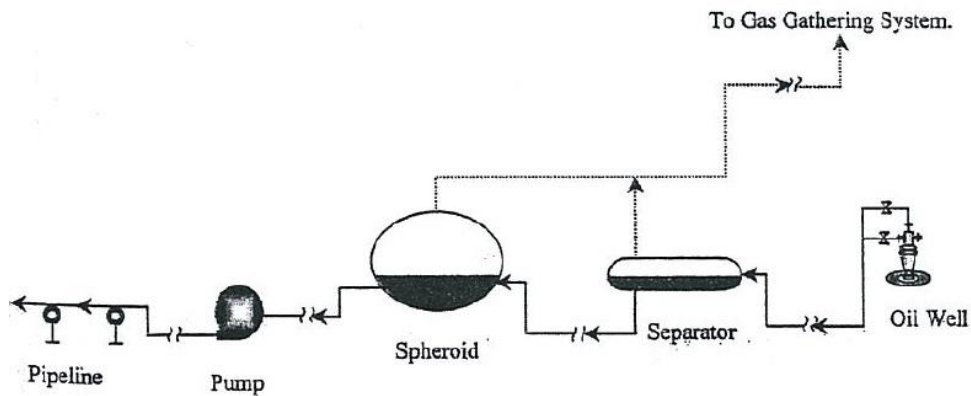
Figure 2: Overview of crude oil surface production facilities (from Abdel-Aal *et. al.,* 2003)

Water-in-oil emulsions are formed when water droplets are dispersed in the continuous oil phase. Reversely, oil-in-water emulsions are formed when oil droplets are dispersed in the continuous water phase. Volume fraction is a factor which determines the type of emulsions. The smaller liquid volume fraction will be dispersed as droplets, while the bigger liquid volume fraction will be the continuous phase.

Figure 3 shows the schematic representation of oil-in-water and water-in-oil emulsions.

Oil-in-Water (O/W)   Water-in-Oil (W/O)
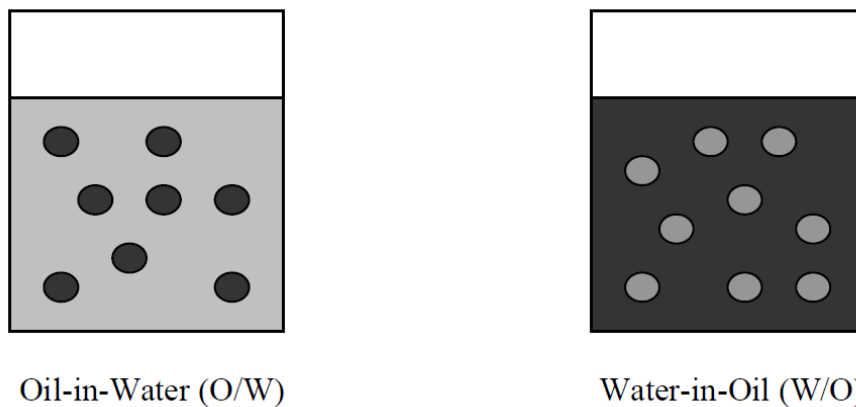
Figure 3: O/W emulsions and W/O emulsions (from Mat *et al*., 2006)

Crude oil production from the reservoirs may have little or negligible produced water in the beginning of the field life. However, as production continues for years, water breakthrough will occur, resulting in formation water to be produced. At low water cut production, water-in-oil emulsions will be present. The water cut will continue to increase, until subsurface intervention is performed on the particular reservoirs. Apart from formation water, the use of Enhanced Oil Recovery (EOR) method such as water injection also causes more amount of water to be produced together with the crude oil. At high water cut production, oil-in-water emulsions will be formed.

As the water cut continues to be increased, water-in-oil emulsions will reach the phase inversion point. This is the point where a catastrophic inversion occurs, resulting in crude oil to become the dispersed phase, while water will become the continuous phase (*i.e.* O/W) emulsions). According to Alwadani (2009), the phase inversion point is reached when the dispersed phase volume fraction (*i.e.* water volume fraction) exceeds the limit of critical close-packing. Close-packing refers to the maximum dense arrangement of theoretical spheres. When the limit is exceeded, the droplets of the dispersed phase will compress against each other and deform the interfaces. The value of this critical close-packing limit varies, depending on the packing nature of the droplets. For identical-size droplets with rhombohedral packing, the limit is 0.74 (Schramm, 1992). Interestingly, studies by Pal *et al.* (1986), Pilehvari *et al.* (1988) and Plegue *et al.* (1989) show that the limit can go as high as 0.90, especially if the droplets are polyhedral.

The emulsions produced from the oil fields are stabilized by natural emulsifying agents, such as asphaltenes, resins, clays and / or waxes (Bhardwaj and Hartland, 1998). Untreated emulsions can have the stability ranging from few minutes to years, depending on the physical and chemical characteristics of the emulsifying agents present in the crude oil.

2.2 Understanding the Nature of Crude Oil

Prior to engaging in further discussion on emulsification and demulsification mechanisms, it is of paramount importance to understand the nature of crude oil, and how the constituents of crude oil affect the emulsions. The presence of natural emulsifying agents, or surface active agents, such as asphaltenes, resins, waxes and clays, in either dissolved or particulate form, has significant impact on the formation and stability of emulsions (Bhardwaj and Hartland, 1998; Lee, 1999). Researchers have also identified that the emulsions will be more stable, if the above surface active agents appear in the particulate form (Ali and Alqam, 2000).

Crude oil is complex fluid consisting of light hydrocarbons, asphaltenes, resins, waxes, napthenic acid, aromatic compounds, phenols, carboxylic acids, sulphur, nitrogen compounds and metals (*e.g.* nickel, vanadium, copper and iron). The elements and composition of crude oil can vary widely for each reservoir, due to its maturity, depth and place of origin (Speight, 2014). The hydrocarbons can be present in the gaseous, liquid or solid state, depending on the molecular weight and arrangement of carbon atoms in the molecules (Mat *et al.,* 2006). Common types of hydrocarbons are paraffin (saturated hydrocarbons), olefin (unsaturated hydrocarbons) and aromatics. Paraffin has the generic formula of C_nH_{2n+2}, where each carbon atom is linked with the maximum number of hydrogen atoms. Olefin has the generic formula of $C_n H_{2n}$, where not every carbon atom is linked to the maximum number of hydrogen atoms, due to the presence of double bonds (Mat *et al.,* 2006).

A well-accepted classification method for crude oil is to distinguish the crude oil based on its API gravity. API gravity is a dimensionless quantity, and it compares the density or specific gravity of oil to water. API gravity is given as (Speight, 2014):

$$\text{API Gravity} = \frac{141.5}{SG} - 131.5 \tag{1}$$

where SG refers to the specify gravity of oil with respect to water (at the same reference temperature and pressure).

$$\text{Specific Gravity (SG)} = \frac{Density_{crude}}{Density_{water}} \tag{2}$$

The reference density for water is taken at 4 °C.

Although API gravity is a dimensionless quantity, it is often expressed in degree (°) in the industry's usage. If the API gravity is more than 10°, the crude oil has less density compared to water. Reversely, if the API gravity is less than 10°, the crude oil has more density compared to water. Crude oil typically has the API gravity of more than 20°. Heavy and viscous crude oil has the API gravity ranging between 10° to 20°. Bitumen, one of the heaviest hydrocarbon compounds in crude oil, has the API gravity of less than 10° (Speight, 2014).

Besides API gravity, SARA fractionation is also widely used to classify the crude oil. By taking advantage of the polarity difference and solubility difference in the solvent, SARA fractionation separates crude oil into four major categories, known as Saturates (including waxes), Aromatics, Resins and Asphaltenes (Auflem, 2002). SARA fractionation is very useful for understanding the emulsification characteristics of a given type of crude oil, as SARA analysis displays the amounts of asphaltenes, resins and saturates, which are the surface active agents responsible for emulsifying and stabilizing the emulsions. However, one limitation of SARA analysis is, the fractionation of crude oil components is based on physical properties (*e.g.* solubility), and not chemical properties. Without full appreciation of the chemical structures and interactions of various molecules of crude oil components, full understanding of emulsions' stability remains a challenge (Lee, 1999; Mat *et al.,* 2006).

2.2.1 Understanding the Nature of Asphaltenes

Asphaltenes display the colour of dark brown to black, and they are amorphous particles suspended as microcolloid in the crude oil. The colloidal suspension is stabilized by the adsorbed resin on the surfaces. Asphaltene particles have the size of approximately 3 nm, and each particle is made up of 1 or more aromatic sheets of asphaltene monomers (Speight, 1994; Aske, 2002). The specific gravity of asphaltenes is just above unity and their molecular weight ranges from 1,000 g/mol to 10,000 g/mol. Asphaltene particles do not have a definite melting point, but they will decompose at temperatures above 300 °C to 400 °C (Speight, 1994).

Asphaltenes have been identified as the major contributory cause for stabilized emulsions, due to asphaltenes' highly polar fraction and active interfacial components (Auflem, 2002). Auflem (2002) also agreed that when the thermodynamic equilibrium is interrupted, asphaltenes may be deposited and flocculated. The interfacial active components of the asphaltenes reach the most active peak during the initial flocculation process (Schorling *et al.,* 1999).

To date, the structure of asphaltenes is not fully understood yet, but several possible structures have been proposed (Gafonova, 2000; Mat *et al.,* 2006). According to Aske (2002), asphaltenes molecules are claimed to be held together by π-bonds, hydrogen bonds, and electron donor-acceptor bonds. An example of hypothetical molecular structure of asphaltenes is shown in Figure 4 (Gafonova, 2000), which includes nitrogen, sulphur and oxygen in the asphaltenes.
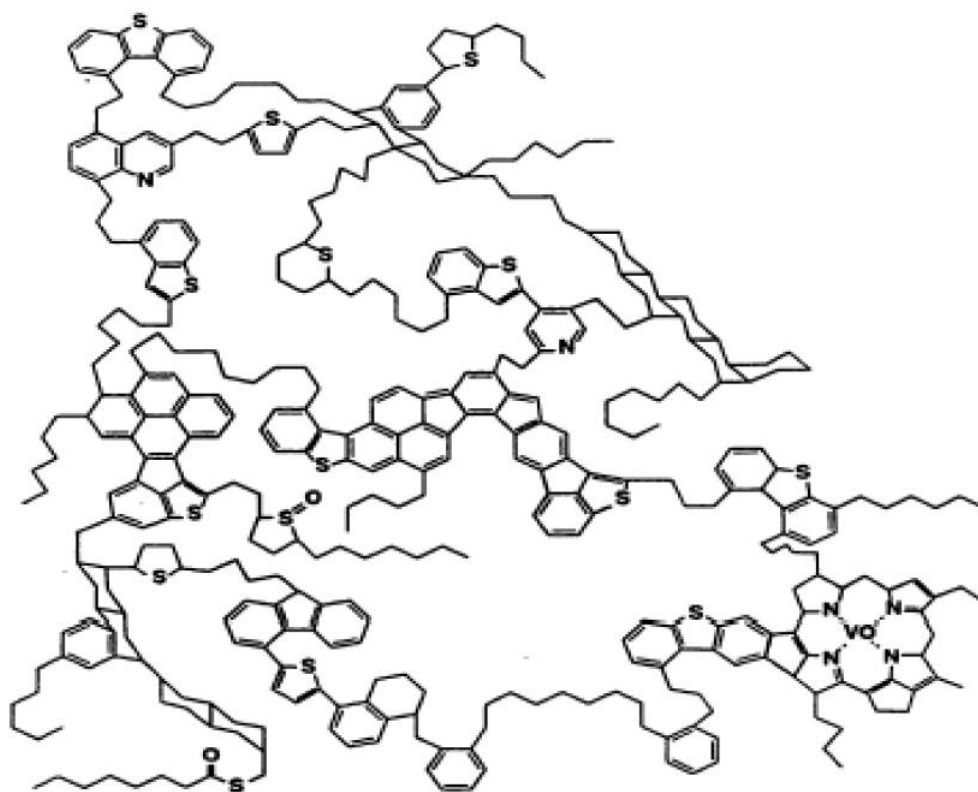
Figure 4: Hypothetical representation of molecular structure of asphaltenes (Gafonova, 2000)

2.2.2 Understanding the Nature of Resins

Resins appear in black or dark brown colour, non-volatile, semi-solid, and they have strong adhesive characteristics. The molecular weight of resins ranges from 500 g/mol to 2,000 g/mol, and their specific gravity is near unity (Gafonova, 2000). Resins display some similarities with aromatics, but resins have higher molecular weight, greater polarity, higher heteroatom content and lower H/C ratio (Mat *et al.,* 2006).

Resin molecules are highly polar (although they have a long non-polar end), and carbon, hydrogen, oxygen, nitrogen, sulphur, ester, ketone as well as napthenic acids are present in the structures of resins. Nitrogen exists in pyrolle and indole groups, while sulphur exists in cyclic sulfides (Gafonova, 2000). According to Speight (1994), it is believed that the aromatization and maturation of resins will form asphaltenes.

Figure 5 shows the hypothetical representation of molecular structure of resins. Resins are assumed to be long paraffinic chain molecules with the presence of napthenic rings and condense aromatics (Gafonova, 2000).
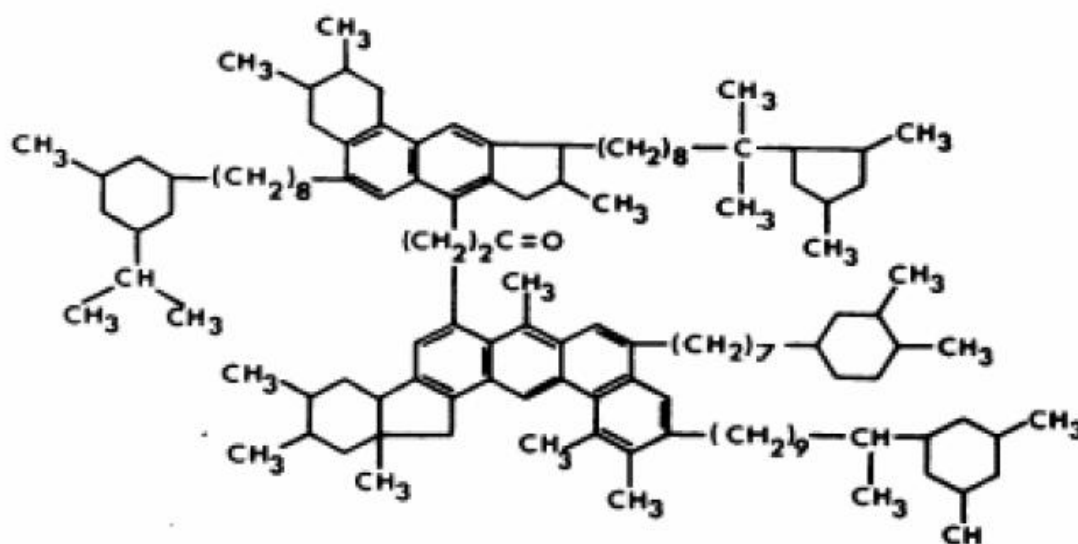
Figure 5: Hypothetical representation of molecular structure of resins (Gafonova, 2000).

2.2.3 Understanding the Nature of Waxes

Wax can be considered as sub-class of the saturates (from the SARA fractionation), and wax is made up of mostly straight-chain monoxidized alkanes, mainly ranging from C20 to C30, resulting in its high molecular weight properties. The alkanes, which can be present in the forms of submatic, hetero-cyclic or polymeric poly-sulfide parents, are usually monoxidized alkanes due to the anaerobic conditions during the biodegradation of organic materials to form crude oil (Becker, 1997). Becker (1997) also explained that wax does contain long-chain esters, (above C16), monohydric (one hydroxyl group), or long-chain alcohols (above C16) and fatty acids. The structures of wax are formed due to the various solubility and inductive forces experienced by the wax.

At low temperatures, wax will precipitate as solid, and the solid precipitates have been proven to enhance the stability of emulsions (Zaki *et al.,* 2000). The emulsions' interfacial films can be further stabilized when the fatty tails of the carboxylic acids are incorporated with the wax molecules (Becker, 1997; Mat *et al.,* 2006). In the oil production industry, chemicals such as wax dissolver and pour point depressant can be injected to mitigate the formation of wax.

2.3 The Process of Emulsification

As stated before, the three major factors contributing to the formation of emulsions are (Schubert and Armbruster (1992);

1) the presence of two immiscible liquids,
2) the presence of emulsifying agents, which are surface active agents, and
3) the involvement of sufficient mixing energy to disperse one liquid into another liquid phase as droplets

To disperse one liquid into another liquid phase as droplets, an amount of energy is required to overcome the pressure gradient between the external (convex) and the internal (concave) sides of an emulsion droplet's interface (Becher, 1955). This energy is actually the mixing or agitation energy, and higher mixing energy results in the formation of smaller and more stable emulsion droplets.

In the formation of emulsions through cylindrical pipe flow, which is achieved via flow shear, Johnsen and Rønningsen (2003) discussed on the dissipation energy required to disperse the emulsion droplets. The dissipation energy for emulsification, E, can be related by:

$$E = 2f \frac{V^3}{D}$$
(3)

where f stands for Fanning friction factor, V stands for flow velocity and D stands for internal diameter of the pipe.

The presence of emulsifying agents or surface active agents will help to reduce the required dissipation or mixing energy, thus favouring the formation of emulsions. According to (Becher, 1955), emulsifying agents (surface active agents such as asphaltenes, resins, waxes and clays) will be adsorbed to the oil-water interface, forming an elastic film that encapsulates the emulsion droplets. This interfacial film will stabilize the emulsion droplets, and can reduce the required mixing energy by a factor of at least 10 (Becher, 1955). The stability of emulsions depends largely on the rigidity and structure of this film. Asphaltenes are the main emulsifying agents which stabilize the interfacial film, preventing it from rupturing (Sjöblom *et al.,* 1992; Auflem, 2002). Without rupturing the film, the emulsion droplets will remain stable and will not be able to coalesce.

Due to the complexity of crude oil components, their chemical structures and molecular interactions have not been fully understood yet, especially the interactions taking place in the interfacial film (Lee, 1999; Gafonova, 2000; Mat *et al.,* 2006). It is believed that asphaltenes remain soluble in pure crude oil. However, the presence of water will cause asphaltenes to be aggregated and adsorbed to the oil-water interface, because of the amphiphilic characteristics of asphaltenes' molecular structures (Gafonova, 2000).

2.4 The Process of Demulsification

The demulsification process takes place in the following order (Ese *et al*., 1999);

a) flocculation of emulsion droplets,

b) deformation and rupturing of the interfacial film which encapsulates the emulsion droplets, and

c) coalescence of emulsion droplets

The demulsification process is mainly affected by the kinetics of the emulsion droplets. As the number of emulsion droplets increases, there will be more collisions, leading to aggregation and flocculation. In flocculation, the emulsion droplets will be aggregated, but without causing any change in the total surface area. The identity of the emulsion droplets remains, but the emulsion droplets lose their kinetic independence, as the droplets now move as an aggregated cluster (Ese *et al*., 1999). Creaming or sedimentation may occur, depending on the density difference.

If the interfacial films of the emulsion droplets break during flocculation, the emulsion droplets will start to coalesce. For the interfacial films to break, it is necessary for the interfacial films to be drained and subsequently ruptured (Auflem, 2002). Factors affecting the rate of film drainage include interfacial tension, tension gradient, viscosity, film's elasticity, and other rheological properties (Aveyard *et al.,* 1992). Pressure gradient will drive the drainage of interfacial films, and the films will be thinner as they continue to be drained out, to the point of rupture. Upon rupture, the capillary pressure difference will drive the surrounding droplets to be immediately fused together as one new and larger droplet, known as coalescence.

In coalescence, the droplets combine together to form larger droplets with reduced total surface area. After coalescence, the larger droplets, which have less surface tension, will start to settle out, separating into 2 distinct phases of oil and water. Demulsification of the droplets is deemed complete at this point.

Throughout the demulsification process, emulsifying agents (e.g. asphaltenes, resins, waxes or clays) may hinder the demulsification by stabilizing the interfacial films, or by causing electrical double-layer repulsion between the droplets due to their long polar molecular chains (Auflem, 2002). Repulsion between droplets will prevent the droplets from having effective aggregation or flocculation.

Figure 6 shows the graphical representation of demulsification process, from flocculation of emulsion droplets, which results in creaming or sedimentation, and subsequently coalescence of emulsion droplets, and finally the separation into distinguished liquid phases.
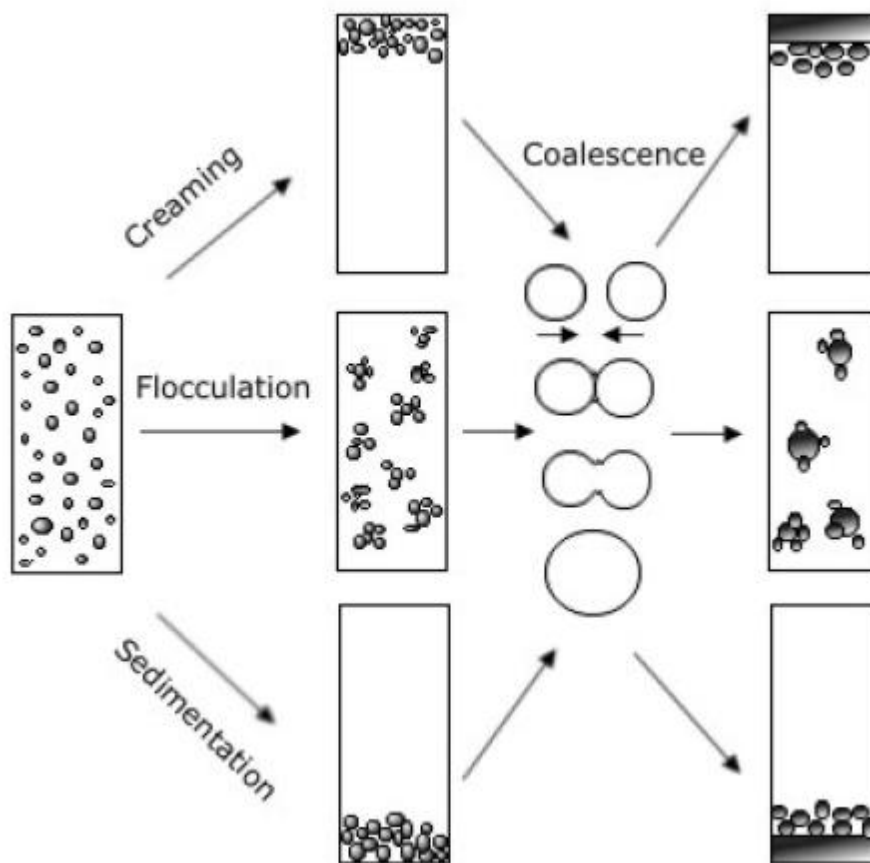
Figure 6: Graphical representation of demulsification process (Auflem, 2002)

2.5 Common Emulsions Treatment Methods in the Industry

Common emulsions treatment procedures employed in the oil production industry involve the use of chemical, thermal, electrical and mechanical methods. There are also studies on treating emulsions through filtration, membrane separation, and pH adjustment (Gafonova, 2000). To ensure effective and efficient emulsions treatment method, understanding of the properties and characteristics of a particular crude oil stock and the related emulsions is very important.

It is highly recommended to treat emulsions as early as possible, as emulsions pose various capacity, flow assurance, and operational difficulties. Apart from that, matured emulsions can be more difficult to be treated. In the upstream oil production industry, emulsions are best treated by using chemical injection, which is known as demulsifier injection. Electrical, thermal and mechanical methods are very likely impractical in the offshore (upstream) facilities, as space and additional power supply are limited.

Demulsifier chemical is usually injected in the very initial stage of crude oil production, namely at the wellheads. Injecting demulsifier chemical at the wellheads allows complete mixing, as the fluids are transported to the separation vessels and pumping facilities, and finally to the pipelines. This enhances the effectiveness of the demulsifier chemical. The type and concentration of demulsifier chemical depend on the crude oil's properties, and usually a trial-and-error methodology is required to determine the optimum parameters (Mat *et al.,* 2006). In the recent development, the use of non-toxic and environmental-friendly demulsifier chemical is emphasized by most oil operating companies, resulting in the trend of rejecting demulsifier consisting of benzene, toluene, or xylene traces, although these aromatic structures are actually effective in destabilizing the emulsions (Gafonova, 2000).

Demulsifier is actually a type of surfactant, and the four common categories of demulsifier are anionic, cationic, non-ionic and amphoteric (Porter, 1994). Demulsifier generally contains polyglycols, polyglycol esters, ethoxylated alcohols, amines, ethoxylated resins, ethoxylated phenols, formaldehyde resins, ethoxylated nonylphenols, polyhydric alcohols, ethylene oxides, propylene oxides, copolymer fatty acids, fatty alcohols, fatty amines and sulfonic acid salts (Porter, 1994; Mat *et al.,* 2006).

Demulsifier chemical acts by adsorbing at the interfacial films of the emulsion droplets, effectively decreasing their interfacial tension gradient and viscosity (Ese *et al.,* 1999; Zaki *et al.,* 1996). This increases the rate of film drainage, and finally causes the interfacial films to rupture, paving the way for coalescence of droplets to occur (Aveyard *et al.,* 1992; Ese *et al.,* 1999).

For water-in-oil emulsions, using oil-soluble demulsifier will be more effective. Conversely, for oil-in-water emulsions, using water-soluble demulsifier has been proven to give better results (Mercant *et al.,* 1988). The basis is to use the type of demulsifier which can be readily dissolved in the continuous phase without much resistance. The demulsifier should also be able to cause sufficient diffusion flux at the interface and suppress the interfacial tension gradient (Krawczyk *et al.,* 1991).

When the crude oil has been received at onshore facilities, various emulsions treatment methods can be used, as space is no longer a constraint. Furthermore, it is necessary to separate all emulsions and remove the entrained water droplets, to meet the crude export quality. The crude export quality is Malaysia is dictated by the BS&W (basic sediments and water) parameter, where the BS&W must not exceed 0.5% (Mat *et al.,* 2006). At onshore facilities, in additional to chemical treatment, electrical, thermal and mechanical treatment methods are implemented too.

For electrical treatment method, electrostatic is used to disrupt the emulsion droplets' surface tension, and re-orient the polar molecules of the interfacial films. This weakens the interfacial films, allows more film drainage, and facilitates to attract oppositely-charged molecules after inducing the orientation (Grace, 1992). This assists the coalescence process of the emulsion droplets.

For thermal treatment method, heat is applied to achieve temperatures above 50 °C – 65 °C to destabilize the emulsions (Grace, 1992). Higher temperature leads to lower viscosity, higher rate of interfacial film drainage, more collisions between the droplets to enhance coalescence, and increased density difference between oil and water (due to the volatility nature of oil, higher temperature causes oil's density to decrease at greater rate compared to water). The increased density difference between oil and water induces these two immiscible liquids to be separated into two distinguished phases.

For mechanical treatment methods, physical separation equipment is used, such as centrifugal separator, corrugated plate interceptor, and settling tank. Physical separation equipment usually works on the principle of physical properties such as density difference (Auflem, 2002). The equipment is sized based on the calculated effective settling time. Mechanical treatment methods are only feasible to be used at onshore facilities, as they require large footprint areas.

CHAPTER 3
LITERATURE REVIEW

3.1 Reviewing Existing Research Studies on Emulsions Flow in Pipeline

This chapter deliberates and critically reviews the existing research studies and findings concerning emulsions flow in pipeline. Emulsions cause significant changes to the flow properties, compared to the equivalent flow rate of single-phase liquid or stratified flow of two-phase liquid (Russell *et al.*, 1959; Rose and Marsden, 1970; Pilehvari *et al,* 1988; Sanchez and Zakin, 1994; Nädler and Mewes, 1997). More importantly, the effects of emulsions are profound, only if the emulsions are stable. The flow conditions, either physical or chemical factors, dictate whether the emulsions will remain stable or be settled out into two distinct liquid phases.

Pure light crude oil is generally Newtonian fluid, except at low temperatures of less than 15 °C, where it starts showing shear thinning behaviours (Keleşoğlu *et al*., 2012). Paso *et al.* (2009) postulated that at low temperatures, heavier components will partially solidify, and their interactions may result in non-Newtonian shear thinning observation. Figure 7 shows the relationship between shear stress, τ, and shear rate, du/dy of Newtonian and non-Newtonian fluids.
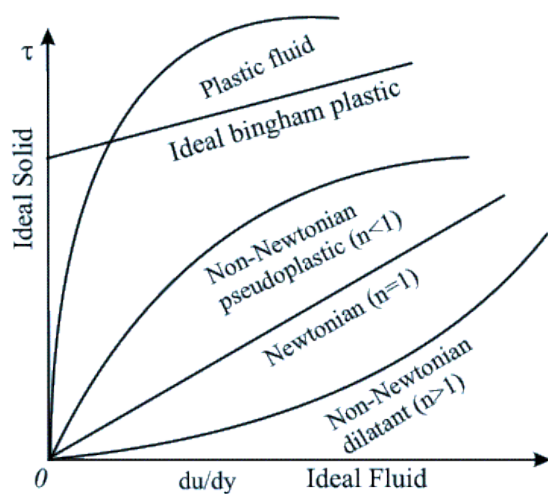
Figure 7: Shear stress and shear rate of Newtonian and non-Newtonian fluids (Som and Biswas, 2003)

Newtonian fluid exhibits proportional linear relationship of shear stress, τ, and shear rate, du/dy, and complies with the following equation (Som and Biswas, 2003):

$$\tau = \mu \frac{du}{dy} \tag{4}$$

where τ stands for shear stress, μ stands for viscosity and du/dy is the shear rate.

Non-Newtonian fluid which does not obey the linear relationship above can be described by using Power-Law model or Ostwald-de Waele model (Som and Biswas, 2003):

$$\tau = m\left(\frac{du}{dy}\right)^{n-1} \frac{du}{dy} \tag{5}$$

where τ stands for shear stress, m stands for flow consistency index, n stands for flow behaviour index, and du/dy is the shear rate.

The emulsions system is generally Newtonian fluid, except at high concentration of emulsion droplets, where non-Newtonian shear thinning behaviours will be observed (Pal, 1987; Pal and Hwang, 1999; Wong et al., 2015b). This now-Newtonian flow regime, if occurs, is only applicable at specific and limited range of high emulsion droplets' concentration. High emulsion droplets' concentration is usually unstable and will bring the emulsions system to its phase inversion point (Alwadani, 2009). Once the phase inversion point is reached, the dispersed phase of emulsion droplets will be inverted to become the continuous phase, and thus the emulsions system may start to behave as Newtonian fluid again.

Emulsions flow can be classified as laminar, transitional or turbulent flow based on its Reynolds number (Re). Reynolds number is the ratio of inertia force to viscous force (Som and Biswas, 2003; Cheng and Heywood, 1984):

$$Re = \frac{\rho VD}{\mu} \tag{6}$$

where ρ stands for density, V stands for mean velocity of fluid flow, D stands for internal diameter, and μ stands for mean dynamic viscosity of fluid.

Laminar flow occurs when the Re is less than 2100, and turbulent flow occurs when the Re is more than 4000. Transitional flow is the regime where the Re ranges from 2100 to 4000.

Figure 8 shows the comparison of velocity profiles (u denotes the velocity) for laminar and turbulent flows.
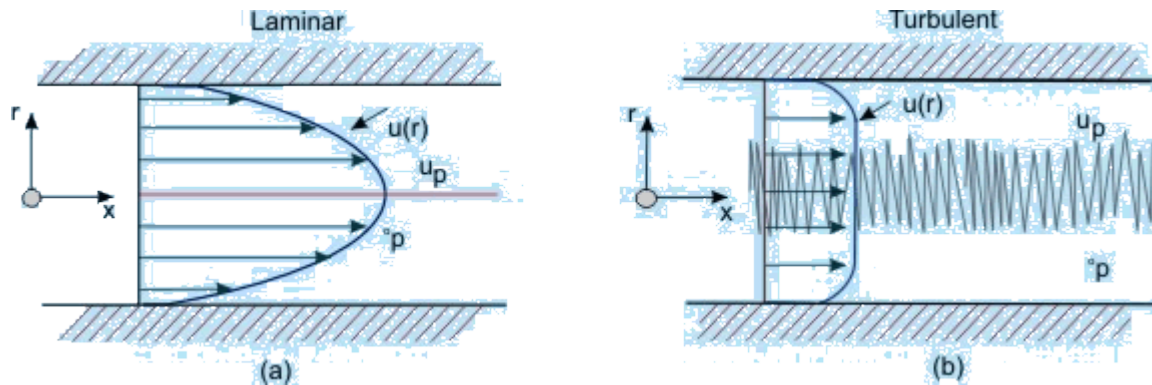
Figure 8: Comparison of velocity profiles for laminar and turbulent flows (Som and Biswas, 2003)

In fully-developed laminar flow, Re can be related to friction factor, f, through the Hagen-Poiseuille equation (Darby, 1996; Wilkes, 1999):

$$f = \frac{16}{\text{Re}} \tag{7}$$

For laminar flow, the friction factor is independent of the surface roughness of the pipe, except if the surface roughness is too severe to the extent it significantly alters the pipe's internal diameter. The independency is caused by the thick laminar sublayer, which covers the surface roughness and irregularities (Som and Biswas, 2003).

In turbulent flow, the laminar sublayer decreases and diminishes, thus allowing the surface irregularities to be more prominent. So, for turbulent flow, Re is related to both friction factor and surface roughness of the pipe. However, at high degree of surface roughness, which is known as rough zone, higher Re becomes insignificant. For this type of turbulent flow, the friction factor is dictated by the surface roughness alone (Som and Biswas, 2003). In fully-developed turbulent flow, the relationship between Re, friction factor and surface roughness can be studied from models such as Moody's diagram or Colebrook equation (Keleşoğlu *et al.*, 2012).

Colebrook equation is given as:

$$\frac{1}{f^{1/2}} = -2\log\left[\frac{\varepsilon/D}{3.7} + \frac{2.51}{\text{Re}\left(f^{1/2}\right)}\right] \tag{8}$$

where f stands for friction factor, ε stands for pipe's surface roughness, D stands for pipe's internal diameter, and Re stands for Reynolds number.

In a straight horizontal pipeline flow, pressure drop or head loss, h_f, is caused by the friction over the horizontal length. The relationship is given as (Som and Biswas, 2003):

$$h_f = \frac{\Delta P}{\rho g} = f\frac{L}{D}\left(\frac{V^2}{2g}\right) \tag{9}$$

where ΔP denotes pressure drop, ρ denotes density, g denotes gravitational constant, f denotes friction factor, L denotes horizontal length, D denotes pipe's internal diameter, and V denotes mean velocity.

3.2 The Effects of Emulsions on Flow Properties

As explained in the previous introductory section, at low concentration of emulsion droplets, the emulsions system can be assumed to behave as Newtonian fluid. However, as the concentration of emulsion droplets is increased, the emulsions system starts to exhibit non-Newtonian behaviours. In a research done by Pal (1987), the oil-in-water emulsions system was Newtonian when the oil droplets' concentration was less than 55.14% volume. But, as the oil droplets' concentration was further increased, the emulsions system became non-Newtonian pseudoplastic. The viscosity decreased when higher shear stress was applied. This shear thinning non-Newtonian behaviour is further confirmed in later research by Pal and Hwang (1999). Tadros (1994) contributed more understanding in this area by proposing that this shear thinning observation is the result of close packing of high concentration of dispersed droplets in the continuous phase. Similar observations were recorded by Keleşoğlu *et al.* (2012).

Omer and Pal (2013) reported there was significant delay in the transition from laminar to turbulent regime in water-in-oil emulsions flow. The delay became even greater with bigger pipe diameter. This view is supported by Pouplin *et al.* (2010), who reported that the transition to turbulent flow could be delayed up to Re of 5000. But, interestingly, such transitional delay was not observed for the case of oil-in-water emulsions.

Plasencia *et al.* (2013) reported that as the water-in-oil emulsions' concentration was increased towards the inversion point, the pressure drop increased up to 8 times higher than the pressure drop of pure oil. Higher pressure drop can cause operational difficulties, especially if the pressure drop is more than the pump's design discharge head. The flow rate will become lower, and possibly the crude will not be able to be transported downstream. This scenario is termed as "production deferment" in the oil production industry, and can result in financial losses.

However, if the water volume fraction is increased further beyond the phase inversion point (the inversion from W/O emulsions to O/W emulsions occurs), Charles *et al.* (1961) and Nädler and Mewes (1997) found that the pressure drop would decrease, to as low as the pressure drop of pure water. Nädler and Mewes (1997) explained this observation as drag-reduction behaviour, where a continuous water layer is flowing at the lower section of the pipe wall, and this water layer minimises the viscous dissipation effects of the emulsions. This phenomenon has been greatly leveraged to facilitate the transportation of heavy and viscous crude oil via pipelines, by emulsifying the oil to be concentrated oil-in-water emulsions (Marsden and Raghavan, 1973; Sifferman, 1981; Simon and Poynter, 1970). The practical application of this idea has been implemented in Indonesia (20-in diameter and 283-km length pipeline) as well as California (8-in diameter and 20.9-km length pipeline) (Lamb and Simpson, 1963; Ahmed *et al.*, 1999).

The viscosity of concentrated oil-in-water emulsions can be several orders of magnitude lower than the viscosity of the single-phase oil. This shows that the emulsions flow's viscosity strongly depends on the viscosity of the continuous phase (Ashrafizadeh and Kamran, 2010). Yaghi and Al-Bemani (2002) claimed that in some cases, the viscosity could be reduced up to 90%, while Zhang *et al.* (1991) reported that the pressure drop could be as much as 30% lower. Messick (1982) recommended that for the purpose of feasible crude transportation via pipeline, the viscosity of the flow should not be more than 200 cP.

From the observation on the flow properties, emulsions cause significant effects on friction factor and viscosity of the flow. The most obvious measurable impact is the pressure drop.

3.2.1 The Effects of Emulsions on Flow Friction Factor

The effects of emulsions on the flow friction factor, f, have been studied by Cengel *et al.* (1962), and the results were re-confirmed by Pal (1993), Pal (2007) as well as Omer and Pal (2010). Friction factor data of emulsions flow were compared against the calculated values of single-phase Hagen-Poiseuille and Blasius equations. Both equations give the relationship between friction factor, f, and Reynolds number, Re.

Hagen-Poiseuille equation is valid for laminar flow of Newtonian fluids, and it is given earlier in Equation 7:

$$f = \frac{16}{\text{Re}} \tag{7}$$

Blasius equation is an empirical relationship for turbulent flow of Newtonian fluids in smooth pipes, and it is given by (Darby, 1996; Wilkes, 1999):

$$f = 0.079\,\text{Re}^{-0.25} \tag{10}$$

The results show different behaviours between unstable emulsions and surfactant-stabilized emulsions at turbulent flow regime. For unstable emulsions in turbulent flow, the measured friction factor data were much lower than the calculated values of single-phase Blasius equation. This phenomenon is known as drag-reduction behaviour, and it was aggravated with increased concentration of emulsion droplets (Cengel *et al.*, 1962).

However, for surfactant-stabilized emulsions in turbulent flow, little or no drag-reduction behaviour was observed. The only exception to this observation is documented in a research conducted by Zakin *et al.* (1979), where they reported the occurrence of drag-reduction behaviour in surfactant-stabilized emulsions. They worked on non-Newtonian oil-in-water emulsions, and they postulated viscoelasticity to be a reason of that behaviour. But Pal (1993) questioned the significance of droplet viscoelasticity's role in drag-reduction, and doubted the existence of droplet-droplet microstructure in high shear rates of turbulent flow. Pal (1993)

further suggested that the emulsions might not have been fully stabilized, thus causing drag-reduction behaviour to be observed.

More recent studies by Omer and Pal (2013; 2010), Pal (2007) and Pal (1993) all agreed that drag-reduction behaviour is only exhibited in unstable emulsions. According to Pal (1993), unstable emulsions experience frequent and dynamic break-up as well as coalescence of dispersed droplets, and this may have suppressed the turbulence, eventually causing the drag-reduction behaviour. Pal (1993) also compared the extent of drag-reduction between water-in-oil emulsions and oil-in-water emulsions. He found out that the extent of drag-reduction was higher for water-in-oil emulsions. He attributed this to the more frequent coalescence activities occurring for water-in-oil emulsions, as water droplets tend to coalesce rapidly in the non-polar continuous oil phase due to negligible potential energy barrier (Sherman, 1970). Conversely, for oil-in-water emulsions, the coalescence activities are less frequent, due to resistance from electrical double-layer effect in the continuous water phase (Sherman, 1970; Tadros and Vincent, 1983).

Little or no drag-reduction behaviour is observed for the case of surfactant-stabilized emulsions, as the dispersed droplets are smaller (due to lower interfacial tension), so they flow along with turbulent eddies and do not affect the turbulence suppression, resulting in negligible drag-reduction. This is especially true when the dispersed droplets are smaller than the scale of turbulence (Omer and Pal, 2013).

Ashrafizadeh *et al.* (2012) gave an alternative explanation on the reason of no drag-reduction behaviour for surfactant-stabilized emulsions, by virtue of the higher viscosity. They found out that the viscosity of emulsions increased with higher surfactant concentration, and this observation agrees with a previous work done by Otsubo and Prud'homme (1994). One possible cause is the higher surfactant concentration resulted in smaller dispersed droplets, leading to more interaction energy among the droplets.

Drag-reduction phenomenon can be interpreted as less frictional losses along the flow, which will lead to lower pressure drop of the flow.

3.2.2 The Effects of Emulsions on Flow Viscosity

For water-in-oil emulsions, prior to the phase inversion point, the increase of water volume fraction causes the viscosity of emulsions to increase, and subsequently results in higher pressure drop (Keleşoğlu *et al*., 2012; Lim *et al.,* 2015). In water-in-oil emulsions flow experiment conducted by Plasencia *et al.* (2013), as the water content was increased towards the inversion point, the effective viscosity became larger, to the extent that the flow turned to laminar. Towards the inversion point, the pressure drop increased sharply.

Emulsions flow's viscosity can be correlated to the volume fraction or the concentration of dispersed droplets by using various models or empirical equations. Relative emulsion viscosity (η_r) is generally defined as:

$$\eta_r = \frac{\eta_e}{\eta_c} \tag{11}$$

where η_e stands for emulsions' viscosity and η_c stands for continuous phase's viscosity.

Einstein (1906) developed the following correlation of emulsions flow's viscosity and dispersed droplets' volume fraction:

$$\eta_r = 1 + 2.5\phi \tag{12}$$

where η_r stands for relative emulsion viscosity and ϕ stands for dispersed droplets' volume fraction.

Taylor (1932) presented a more refined relationship of relative emulsion viscosity, η_r:

$$\eta_r = 1 + 2.5\phi \left(\frac{\eta_d + 0.4\eta_c}{\eta_d + \eta_c} \right) \tag{13}$$

where ϕ stands for dispersed droplets' volume fraction, η_d stands for droplets' viscosity and η_c stands for continuous phase's viscosity.

Richardson (1933) proposed the following correlation for relative emulsion viscosity and dispersed droplets' volume fraction:

$$\eta_r = e^{k\phi} \tag{14}$$

where k is constant and ϕ stands for dispersed droplets' volume fraction.

Broughton and Squires (1938) improved on the earlier correlation by Richardson (1933), and modified to the equation to be:

$$\ln \eta_r = A + k\phi \tag{15}$$

where A and k are constants and ϕ stands for dispersed droplets' volume fraction.

Pal and Rhodes (1989) developed empirical correlations on relative emulsion viscosity, which are applicable for Newtonian as well as non-Newtonian fluids:

$$\eta_r = \left[1 + \frac{(\phi/\phi^*)}{1.187 - (\phi/\phi^*)} \right]^{2.49} \tag{16}$$

where ϕ stands for dispersed droplets' volume fraction and ϕ^* stands for dispersed droplets' volume fraction at which relative viscosity becomes 100.

$$\eta_r = \left(1 - K_0 K_f(\gamma)\phi \right)^{-2.5} \tag{17}$$

where K_0 stands for hydration factor, $K_f(\gamma)$ stands for flocculation factor, and ϕ stands for dispersed droplets' volume fraction. K_0 is fluid-dependent, and it is dictated by the emulsifier type. $K_f(\gamma)$ is only applicable for non-Newtonian emulsions.

Besides the water volume fraction, the viscosity of emulsions is also affected by single-phase viscosities of oil and water, viscosity of the continuous phase, temperature, droplet size, droplet size distribution, amount of solids in the crude and the applied shear rate (Kokal, 2005). Crude with higher asphaltenes content is shown to exhibit higher emulsions' viscosity when emulsification occurs, especially for aggregated asphaltenes (Plasencia *et al.*, 2013).

The increment of emulsions flow's viscosity can be understood from the hydrodynamic forces working on the emulsion droplets. As the droplets experience collision and shear flow, hydrodynamic forces cause two droplets to make a doublet rotating around their mutual centre of mass (Krieger and Dougherty, 1959; Lee, 1969). The rotating doublets dissipate more energy as the number of emulsion droplets increases, contributing to higher emulsions flow's viscosity. The viscosity can also be influenced by the deformation and rearrangement of network structures of emulsion droplets' interfacial film (Otsubo and Prud'homme, 1994).

Zaki (1997) supported the earlier findings, by concluding that high interaction of emulsion droplets would increase the flow's effective viscosity. Pal (1998) added to this research area by showing that the effect of droplet size on emulsions flow's viscosity is only important when the droplets are stable, with dispersed droplets' concentration of more than 60%. This hypothesis is in agreement with Keleşoğlu *et al*. (2012) and Plasencia *et al*. (2013), who put forward that droplet size distribution, which is affected by velocity, has negligible effect on emulsions flow's viscosity at low concentration of emulsion droplets.

However, the understanding of the relationship between droplet size distribution and concentration of dispersed droplets is still unclear. As examined by Keleşoğlu *et al*. (2012), who researched into droplet size distribution by using Nuclear Magnetic Resonance (NMR) and Digital Video Microscopy (DVM) techniques, as the emulsion droplets' concentration was increased, the droplet size distribution largely remained the same. Although there were some inconsistencies in the results obtained using the NMR technique, Keleşoğlu *et al*. (2012) justified that it could be caused by the validity of short-time approximation, which failed to take into account the curvature and finite surface relaxivity.

3.3 Factors Influencing the Stability of Emulsions Flow in Pipeline

Stability of emulsions can be understood as the ability of the emulsion droplets to resist against coalescence. This can only happen if the interfacial films encapsulating the droplets remain intact. Aggregated emulsions can still be considered stable, as long as there is no further kinetics movement towards coalescence (Schramm, 1992). Schramm (1992) viewed stable emulsions as kinetically stable, but thermodynamically unstable. Only micro-emulsions are able to achieve thermodynamic-stability.

NRT Science & Technology Committee (1997) classified the stability of emulsions into three categories;
  a) stable emulsions,
  b) unstable emulsions, and
  c) meso-stable emulsions

Basically, the stability of emulsions is classified based on the observation of duration taken for the emulsions droplets to remain suspended, before coalescing. Although there is no firm time duration to distinguish between stable and unstable emulsions, but it is generally accepted that stable emulsions can last for days, while unstable emulsions can last for not longer than few hours (Wong *et al.,* 2015a).

Untreated stable emulsions can last for many days, especially if the volatile light hydrocarbons get evaporated from the liquid, and the heavier polar components become more prevalent (Schramm, 1992). The heavier polar components will further stabilize the interfacial films, preventing possibility of coalescence between the emulsion droplets.

Meso-stable emulsions have the highest probability of existence in an emulsions system, and they are at a stage between stable and unstable emulsions. Further interfacial film strengthening will improve them to be stable emulsions, and on the flip side, increased disturbance and kinetics movement will lead them to coalesce and settle out as distinct liquid phases.

The adverse and beneficial effects of emulsions can be realized only if the emulsions are stable. If the emulsions are unstable, they will soon separate into two distinct phases of water and oil, and thus the effects discussed in Section 3.2 will no longer be applicable. The stability of emulsion interestingly ranges from few minutes up to a number of years (Bhardwaj and Hartland, 1998).

Stability of emulsions can be affected by a variety of factors, such as emulsifying agents, flow rate, temperature, pH, salt concentration and phase inversion point. Generally, smaller emulsion droplets are more stable (Ashrafizadeh and Kamran, 2010; Briceno *et al*., 1997; Pal *et al*., 1992). Larger, irregular droplet size distribution and unstable emulsion droplets may be formed when the continuous phase has higher interfacial tension (Plasencia *et al*., 2013). However, the listed stability factors are not exhaustive, given the fact that crude oil contains complex compounds, and their molecular interactions are not fully understood yet. The molecular interactions do play a role in either stabilizing or destabilizing the emulsions.

3.3.1 The Influence of Natural Emulsifying Agents and Solids

Crude oil is a complex compound, which is produced from the reservoirs together with other components such as sand, scale, clay, acids, resins, wax and asphaltenes. These components, especially when present in small solid particles, serve to be natural surfactants and good emulsifying agents (Mouraille *et al*., 1998; Ali and Alqam, 2000; Sjöblom *et al.,* 2001; Aske *et al*., 2002; Kokal, 2005). Although the chemistry and clear correlation of the effect of natural emulsifying agents on emulsions' stability have not been fully established, it is widely accepted that polar compounds such as asphaltenes play a major determining role. The interfacial activities will strengthen the films encapsulating the emulsion droplets, thus further stabilizing the emulsions (Schramm, 1992).

Precipitated and aggregated asphaltenes are believed to be main contributor of stable emulsions. Lee (1999) proved this hypothesis, by showing that emulsions failed to form after asphaltenes particles were removed from the crude oil by using a silica column. However, asphaltenes alone is not the deciding factor for emulsions' stability. It is rather the interactions between asphaltenes and other crude oil components that affect the emulsions' stability.

Ali and Alqam (2000) argued that although resins can be an emulsifying agent, but if resins are present in an amount which increases asphaltenes' solubility, the emulsions will be less stable. Thus, higher concentration of resins will not necessarily induce stable emulsions, but may instead work to destabilize the emulsions. This view is agreed by Gafonova (2000) as well as Kilpatrick and Spiecker (2001).

The adsorption of asphaltenes particles at the droplets' interfacial films will increase the films' viscosity, reduce the film drainage rate and stabilize the films. But to date, the molecular interactions at the interfacial films are not fully comprehended yet (Gafonova, 2000).

It is pertinent to emphasize that emulsifying agents, such as asphaltenes, can be effective, only when they are present in the solid form. Pal *et al.* (1992) explained that small solids have higher yield stress, and will give higher viscosity and stability to the emulsions system. Besides that, small solids also act as mechanical barriers to prevent the emulsion droplets from coalescing.

Another possible emulsifying agent is wax crystals, which will precipitate and solidify when the temperature falls below the Wax Appearance Temperature (WAT). However, dissolved wax in the crude oil will not affect the emulsions' stability (Mouraille *et al*., 1998; Sjöblom *et al.,* 2001; Sjöblom, 2006). WAT of crude oil typically lies in the range of 40 °C to 50 °C. At temperatures above 60 °C to 90 °C, microcrystalline wax will start to melt (Ali and Alqam, 2000). In the oil production industry, formation of wax crystals is usually mitigated by injecting wax dissolver or pour point depressant chemicals.

In conclusion, an effective emulsifying agent shall have polar compounds, and must appear in solid form, such as precipitated asphaltenes.

3.3.2 The Influence of Flow Rate and Velocity

Higher flow rate or velocity causes more shear rate, resulting in smaller sizes of emulsion droplets. Smaller emulsion droplets, which have higher interfacial area, are more stable (Ashrafizadeh and Kamran, 2010; Briceno *et al*., 1997; Pal *et al*., 1992). In studies conducted by Ashrafizadeh and Kamran (2010), fully stabilized emulsions (no separated water observed in 24 hours) were achieved by mixing at more than 10,000 rpm for longer than 30 minutes.

To date, in the best efforts of the author's literature review, only Nädler and Mewes (1997), Keleşoğlu *et al*. (2012) and Plasencia *et al*. (2013) studied on water-in-oil emulsification solely from flow shear in lab-scale pipeline. Other researchers have been focusing on emulsification from stirring or mixing.

In experimental research conducted by Keleşoğlu *et al*. (2012), it was recorded that higher flow rate did not affect emulsions flow's viscosity, but unexplainably, the pressure drop would increase. Plasencia *et al*. (2013) later confirmed the findings on the non-dependency of emulsions flow's viscosity on flow rate. Flow rate or velocity does not have any effect on emulsions flow's viscosity, except at very high emulsion droplets' concentration, where the fluids start to exhibit non-Newtonian behaviours.

3.3.3 The Influence of Temperature

Higher temperature reduces the emulsions' viscosity, eventually destabilizing and breaking the emulsions. This thermal method is well practised in the oil refinery industry (Mat *et al.*, 2006). According to Grace (1992), temperatures above 50 °C to 65 °C may completely destabilize the emulsions. Mat *et al.* (2006) highlighted that the film drainage rate of emulsion droplets is directly proportional to the temperature rise.

3.3.4 The Influence of pH

Sakka (2002) and Yang *et al.* (2007) suggested that higher pH (alkaline) would give more stability to the emulsions. According to Yang *et al.* (2007), for oil-in-water emulsions, higher pH would promote more affinity of surfactant molecules towards aggregation, resulting in more stable emulsions. Sakka (2002) attributed the emulsions' stability to the increased absolute value of zeta potential of the droplets in the alkaline region, *i.e.* pH 9.

However, Tambe and Sharma (1993) offered a different observation. Tambe and Sharma (1993) maintained that in their studies, low pH values of 4 − 6 favoured oil-in-water emulsions, while high pH values of 8 − 10 favoured water-in-oil emulsions. They found out that for the case of oil-in-water emulsions, the stability was increased as the pH was increased from 4 to 6. But beyond pH 6 to pH 10, oil-in-water emulsions became less stable, and on the flip side, water-in-oil emulsions were favoured.

Sjoblom *et al.* (1990) put forward another point of view, which generally believed that intermediate pH would cause instability, while either very high or very low pH values would help in stabilizing the emulsions. In later research, Sjöblom *et al.* (2003) discussed about the possibility of natural acids such as naphthenic acids in contributing to emulsions' stability.

3.3.5 The Influence of Salt Concentration

The water which accompanies the oil production from the reservoirs can be salty, and it is termed as brine in the oil industry. There are various conflicting ideas and theories surrounding the effect of salt concentration on the stability of emulsions. Nevertheless, the presence of salt in oilfield emulsions is real and should not be overlooked.

In a research conducted by Bink (1993), he claimed that higher salt concentration resulted in oil-in-water droplets to increase in size, while water-in-oil droplets to decrease in size. Bink (1993) showed that higher salt concentration would destabilize oil-in-water emulsions, but stabilize water-in-oil emulsions.

However, later research by Ahmed *et al*. (1999) does not agree with Bink (1993). Ahmed *et al*. (1999) found out that higher salt concentration would result in lower interfacial tension of the oil droplets and the continuous water phase, facilitating the formation of smaller oil droplets. Smaller oil droplets made the oil-in-water emulsions to be more stable.

Ashrafizadeh and Kamran (2010) echo the views by Ahmed *et al*. (1999). Ashrafizadeh and Kamran (2010) reported that at higher salinity of the water phase, the viscosity of oil-in-water emulsions was increased, and the amount of separated water was reduced as well. Oil-in-water emulsions became more stable at higher salinity of the water phase. Ashrafizadeh and Kamran (2010) postulated that the phenomenon could be caused by salt ions acting as barriers among the oil droplets and the continuous water phase, thus increasing the emulsions' stability.

More recently, Ashrafizadeh *et al*. (2012) contributed additional information into this interesting discussion, by showing the effect of chemical reactions between the salt (NaCl) ions and the surfactants. The stability of emulsions is not affected by the salt concentration alone, but its chemical reactions with the surfactants do play an important role. In their research, sodium carbonate (Na_2CO_3) was used as the surfactant, where the formed carboxylate ions would be adsorbed at the interface of oil-water, promoting the reduction of the oil droplets' mean diameter and increasing the emulsions' stability. But, as the salt (NaCl) concentration was increased, the excess sodium ions would induce the precipitation of carboxylate ions as sodium carboxylate, thus hindering the carboxylate ions from acting as good surfactant. So, in this special case, high salt concentration would destabilize the oil-in-water emulsions.

3.3.6 The Influence of Phase Inversion Point

Phase inversion point is defined as the stage where the dispersed phase is changed to be the continuous phase, as the dispersed phase's concentration is continuously increased (Alwadani, 2009). For example, in the case of water-in-oil emulsions, if the water content is continuously increased, there will be a point where the emulsions system will be inverted to be oil-in-water emulsions. After a phase inversion, there is also high possibility for multiple emulsions to form.

A stable emulsions system will have a later phase inversion point, and the system is able to accept more dispersed droplets. Phase inversion generally occurs when the dispersed phase's concentration is increased above 50%. However, it depends on the chemical characteristics of the fluids, and this particular research area is not fully understood yet. Plasencia *et al*. (2013) argued that there is no strong correlation between continuous phase's viscosity and phase inversion point. Plasencia *et al*. (2013) further proposed that phase inversion point is affected by the ability of an emulsions system to keep the large emulsion droplets stable. If the emulsions system allows the dispersed droplets to keep increasing and aggregating without coalescing, it will have a later phase inversion point.

3.3.7 Overall Knowledge Gap

In this research field on crude oil-and-water emulsions, a relevant and important knowledge gap is still the stability of emulsions. To date, there is no universal agreement on emulsions' stability criteria (Wong *et al.,* 2015a). Next, as mentioned in the earlier sections, the chemistry and molecular interactions contributing towards emulsions' stability are not fully understood yet (Gafonova, 2000). The stability of emulsions directly affects the droplet size distribution, concentration of dispersed droplets, phase inversion point and other various flow behaviours.

This research thesis aims to further contribute to this field, by investigating the stability of emulsions due to flow shear, and the effects on phase inversion point as well as pressure drop.

CHAPTER 4
RESEARCH METHODOLOGY

4.1 Introduction

This chapter provides the procedures and methodology to effectively fabricate a closed-circuit flow loop, to induce the formation of water-and-oil emulsions via flow shear, and to study the flow pressure profile of water-and-oil emulsions.

The chapter begins with design basis of the closed-circuit flow loop and experimental equipment setup, followed by the required materials and resources, and finally the experimental methodology.

4.2 Experimental Equipment Setup

One of the main objectives of this research is to induce emulsification by the virtue of flow shear, which can be achieved by circulating mixtures of crude oil and water in a closed-circuit flow loop. To date, to the best of the author's literature review, flow-induced emulsification has not been widely studied yet; the results of flow-induced emulsions were only reported by Nädler and Mewes (1997), Keleşoğlu *et al.* (2012) and Plasencia *et al.* (2013).

This section details out the basis of design considerations to fabricate a lab-scale pipeline flow loop. To replicate the pipeline used in the oil and gas industry, metal pipe is used for this research purpose. Stainless steel (SS) pipe has been selected over other types of metals due to the following reasons:

a) SS is less susceptible to corrosion and stains

b) Markey survey reveals that most laboratory pumps and flow meters are provided with SS joints or SS connectors. This allows SS pipes to be easily connected, without the threat of galvanic corrosion, as there are no dissimilar metals

The pressure-measurement part of this flow loop is the most critical segment as it is the main focus of this research thesis, and this segment largely dictates the sizing of the flow loop.

To fabricate a lab-scale pipeline flow loop, the design considerations shall cover:

a) Sizing of the flow loop (diameter and length of pipes, including the constriction)

b) Sizing of the tank

c) Technical selection of the flow meter

d) Overall pressure drop estimation and technical selection of the pump

e) Installation of the pressure transmitter and pressure indicator

4.2.1 Sizing of the Flow Loop

Two important criteria in sizing the flow loop are:

a) Space limitation of the laboratory room.

The flow loop shall be safely installed in the laboratory room, without affecting the walkway or personal ergonomics.

b) The pressure-measurement segment shall have sufficient straight horizontal length, for the flow to be fully-developed.

A fully-developed flow is the flow outside of entrance flow region. When the fluid flows into a different conduit character (*e.g.* pipe bend or change in diameter), the fluid will experience entrance flow region. Entrance length is given by (Som and Biswas, 2003):

$$\frac{\ell_e}{D} = 0.06 \, \mathrm{Re} \quad \text{for laminar flow (for Re} < 2100) \tag{18}$$

$$\frac{\ell_e}{D} = 4.4(\mathrm{Re})^{1/6} \quad \text{for turbulent flow (for Re} > 4000) \tag{19}$$

where ℓ_e denotes entrance length, D denotes pipe diameter and Re denotes Reynolds number.

Studies of velocity profile and pressure distribution in the entrance region can be quite complex (Som and Biswas, 2003), and not within the scope of this research. Estimation of entrance length is given in Table 1 below.

Table 1: Comparison of entrance length between 2"-pipe and 3"-pipe

Pipe Diameter Size	Entrance Length for Pure Crude Oil	Entrance Length for Pure Water
2" (50.8 mm)	At velocity of 1 m/s: Re is 10,615.52 (turbulent flow). The entrance length, ℓ_e is 1.0479 m. At velocity of 0.5 m/s: Re is 5307.76 (turbulent flow). The entrance length, ℓ_e is 0.9335 m.	At velocity of 1 m/s: Re is 56,912.26 (turbulent flow). The entrance length, ℓ_e is 1.3863 m. At velocity of 0.5 m/s: Re is 28,456.13 (turbulent flow). The entrance length, ℓ_e is 1.2350 m.
3" (76.2 mm)	At velocity of 1 m/s: Re is 15,923.29 (turbulent flow). The entrance length, ℓ_e is 1.6817 m. At velocity of 0.5 m/s: Re is 7961.64 (turbulent flow). The entrance length, ℓ_e is 1.4982 m.	At velocity of 1 m/s: Re is 85,368.38 (turbulent flow). The entrance length, ℓ_e is 2.2248 m. At velocity of 0.5 m/s: Re is 42,684.19 (turbulent flow). The entrance length, ℓ_e is 1.9821 m.

In the calculations used in Table 1, the kinematic viscosities of crude oil and water are assumed to be 4.78545 cSt and 0.8926 cSt, respectively, at 25°C. The internal diameter of the pipe is assumed to be similar to the nominal diameter, although in real situation, the internal diameter will be smaller, depending on the wall thickness of the pipe.

To optimize on the space limitation in the laboratory room, 2"-pipe diameter is selected, so that sufficient straight horizontal length for pressure-measurement segment can be provided, after accommodating the entrance length. Based on Table 1, it is decided that 3.50 m is the adequate length for the pressure-measurement segment, as this gives more than 1-m length of fully-developed flow.

A right-angle constriction is included in the flow loop, to further contribute to the formation of water-and-oil emulsions. This right-angle constriction, which narrows down the diameter of the pipe from 2" to 1", causing sudden contraction and expansion in the flow, serves to replicate the usage of choke valves in the oil and gas industry. Choke valves have been regarded as one of the important components which induces emulsification, because of the intense agitation and turbulence caused by them (Fingas *et al.,* 1993). The constriction can be graphically represented in Figure 9.
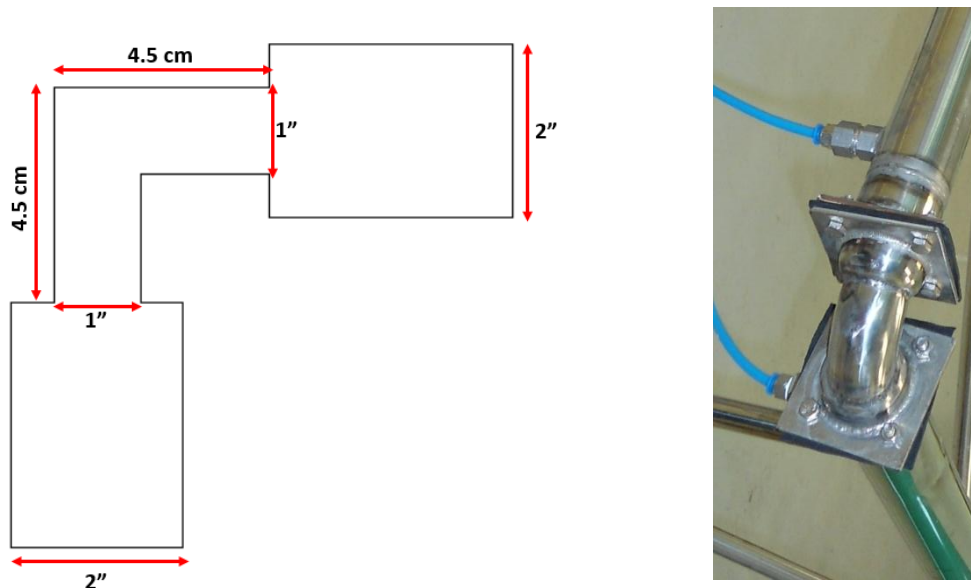
Figure 9: Schematic diagram of the constriction (dimensions are not to scale) and the actual fabricated constriction

The schematic diagram of the overall flow loop is given in Figure 10. In this closed-circuit flow loop, liquid will be circulated by a pump, through a digital flow meter and the pressure-measurement segment (Segment K). To control the flow rate, a bypass line is provided (Segments D and E), which will circulate a portion of the flow back to the tank, depending on the extent of the valve opening.

Segments M, N and O are independent segments, which are not normally used when the main focus is to obtain the pressure measurement of the flow. The purpose of having segments M, N and O is to allow visualization of the emulsions flow. Segment N has a straight horizontal length of 350 cm, and it is transparent as it is fabricated from acrylic glass (also known as Plexiglas®).

In the final procurement, the nominal 2"-stainless-steel pipe has outer diameter (OD) of 51.04 mm, and internal diameter (ID) of 48.80 mm. The nominal 2"-acrylic-glass pipe has outer diameter (OD) of 49.95 mm, and internal diameter (ID) of 43.46 mm. As the actual ID is smaller than the diameter used for calculating entrance lengths in Table 1, the actual entrance lengths will be shorter, thus giving more leverage and advantage to the pressure-measurement segment (Segment K).

The tank is equipped with a refill line, drain line, and level gauge, so that the appropriate volumetric amounts of water and oil can be manipulated.
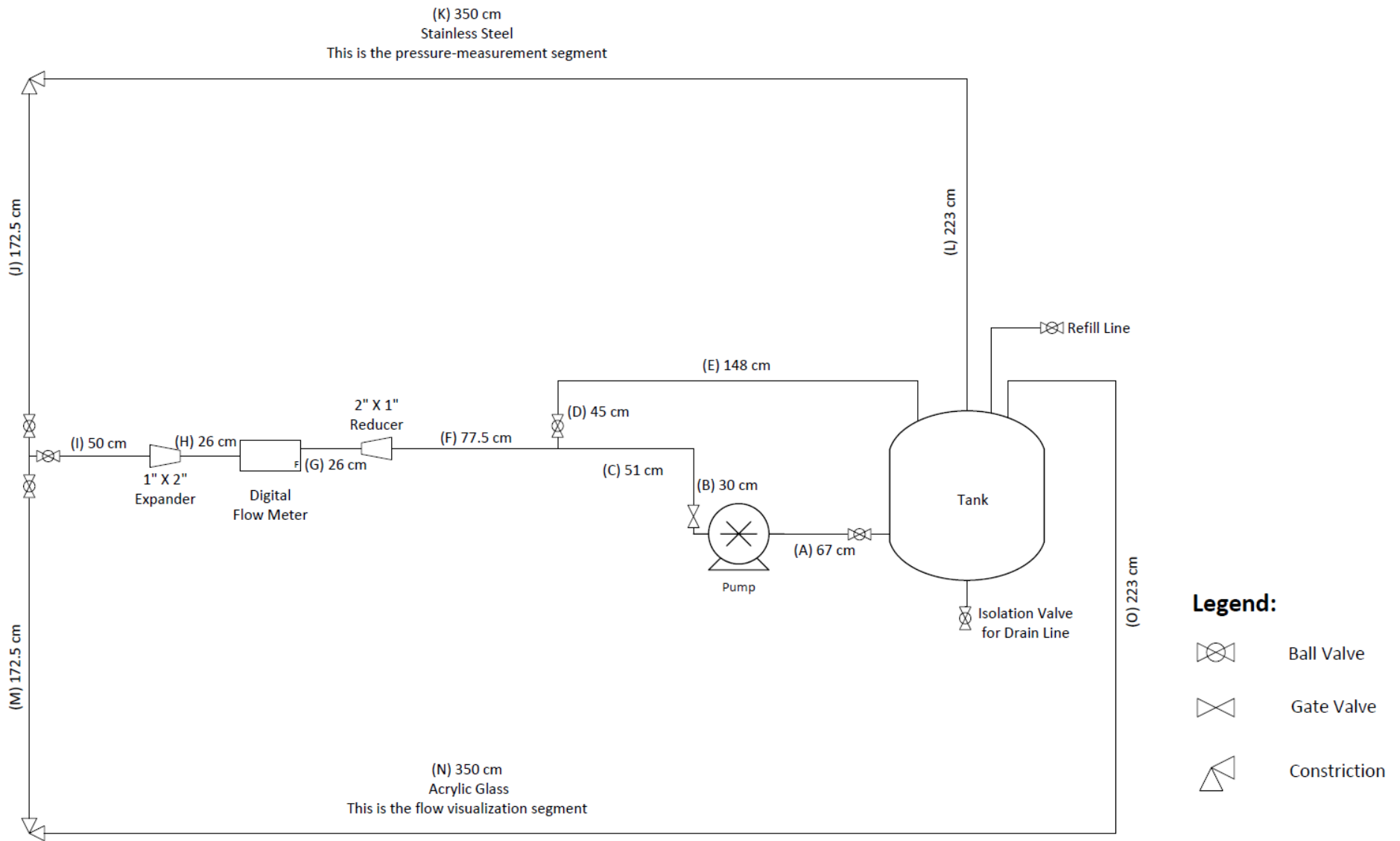
Figure 10: Schematic diagram of the flow loop (dimensions are not to scale)

4.2.2 Sizing of the Tank

For emulsions to effectively affect the behaviours and properties of the flow, it is important to ensure that all emulsion droplets remain suspended in the continuous phase. However, unstable emulsion droplets may settle out and be separated into distinct liquid phases, if there is insufficient agitation energy or flow rate. In this respect, as the liquid is circulated in the closed-circuit flow loop, its residence time in the tank shall be minimized, to prevent the unstable emulsion droplets from settling out.

To minimize the residence time in the tank, the volume of the tank shall be sized according to the total expected liquid volume of the closed-circuit flow loop. The total expected liquid volume is the volumetric summation of all segments of the flow loop.

The volume of each segment is calculated by using Equations 20 and 21:

$$\text{Volume, V} = \text{Area}_{\text{cross-sectional}} \text{ X Length} \tag{20}$$

$$\text{Area}_{\text{cross-sectional}} = \pi r^2 \tag{21}$$

where r denotes the radius of the pipe

The volumetric summation of all segments gives approximate 38.8 Litres. With 30% of contingency, the tank is sized to be 50.44 Litres.

In the final fabrication, a cylindrical tank is made, with the height of 85 cm and diameter of 28.5 cm. This gives the actual tank volume to be 54.23 Litres.

The tank is shown in Figure 11.
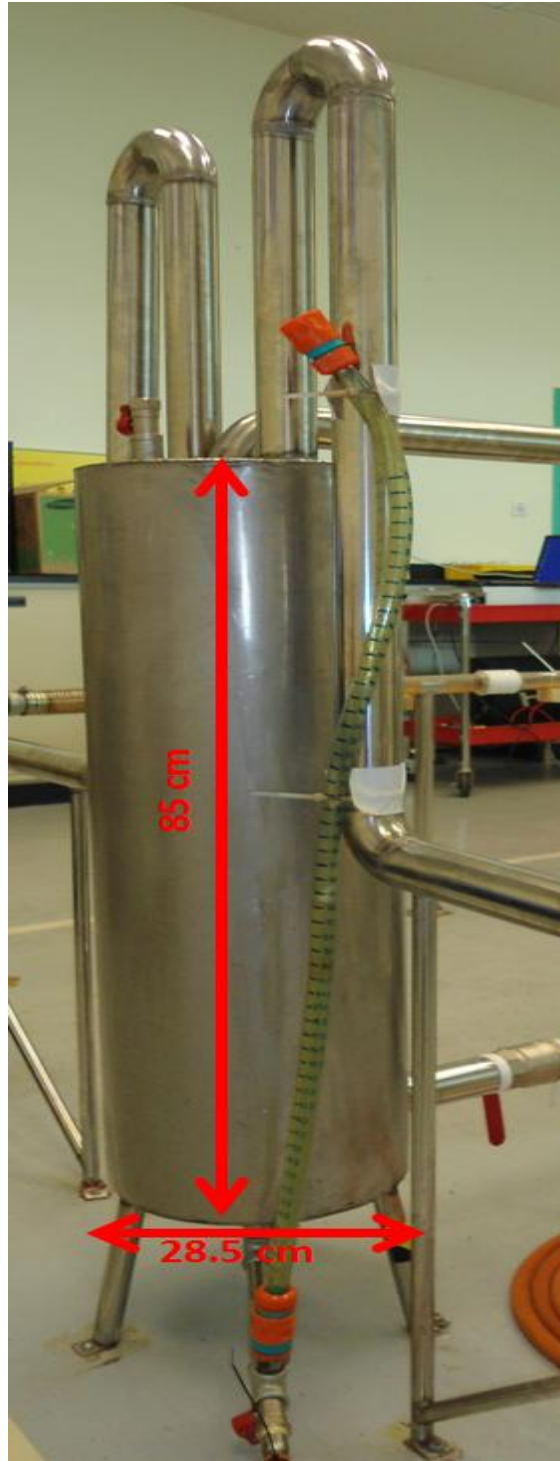
Figure 11: Photo of the cylindrical tank

4.2.3 Technical Selection of the Flow Meter

Criteria on selecting a digital flow meter include its measurable flow rate range, the maximum pressure drop across the meter, and price valuation.

GPI® A100 digital flow meter is selected to be used in this research project. This 1"-turbine-type flow meter is equipped with lithium-battery-powered Liquid Crystal Display (LCD), and it is able to measure flow rate in the range of 10 L/m to 190 L/m. At the maximum flow rate of 190 L/m, the highest pressure drop across the meter is expected to be 5 psi. This flow meter has been calibrated by the manufacturer, and its accuracy is ±1.5% of the reading, with repeatability of ±0.2%. It can withstand pressure up to 21 barg, and its allowable operating temperature ranges from -40 °C to 121 °C.

GPI® A100 digital flow meter is suitable to be used for crude oil service; the bearing is made of ceramic, the shaft is made of tungsten carbide, the rotor is made of nylon, and the ring is made of 316 stainless steel.

To maintain the accuracy and repeatability of the meter, the manufacturer's recommendations on the piping configuration and meter installation are adhered to (Computer Electronics Owner's Manual, 2010):

a) The meter must be installed at least 6 inches away from other electronic equipment. This is to avoid interference from other possible electromagnetic sources.

b) Adequate straight-run of pipes must be connected to both inlet and outlet of the meter. To meet this requirement, straight horizontal pipes, with the length of 10D (10 X pipe diameter), are provided at both sides of the meter. As the bore size of the meter is 1" (2.54 cm), straight horizontal pipes with the length of 26 cm are fabricated and connected to the inlet and outlet of the meter. Refer to Segments G and H in Figure 10.

Without having adequate straight-run of horizontal pipes, the presence of swirl and flow profile distortion will reduce the accuracy of the meter.

The installed digital flow meter is shown in Figure 12.

Figure 12: Photo of GPI® A100 digital flow meter

4.2.4 Overall Pressure Drop Estimation and Technical Selection of the Pump

To ensure correct technical selection of the pump, the criteria include maximum discharge pressure, maximum discharge flow rate and electrical power compatibility (*e.g.* voltage and frequency). The maximum discharge pressure of the pump shall be able to overcome the total pressure drop and pressure loss in the flow loop.

Pressure drop, or head loss, in the flow loop comes from frictional loss experienced by the flow at various pipe bends and pipe fittings. The equations for head loss, ΔH are given by (Som and Biswas, 2003):

$$\Delta H = K \frac{V^2}{2g} \tag{22}$$

where K stands for loss coefficient, V stands for average flow velocity, and g stands for gravitational acceleration.

Common values for the loss coefficient, K, can be referred from various literature sources.

$$\Delta H = f \frac{L_e}{D} \frac{V^2}{2g} \tag{23}$$

where f stands for friction factor, L_e stands for pipe equivalent length, D stands for pipe diameter, V stands for average flow velocity, and g stands for gravitational acceleration.

The friction factor, f, can be obtained from the Moody's diagram.

Taking the case of velocity at 1 m/s and pipe internal diameter of 48.8 mm, the calculated head loss due to frictional loss is approximately:

a) Head loss encountered due to pipe fittings, including valves and constriction (K value of 24 is selected): 4.8930

b) Head loss encountered due to pipe bends (K value of 0.9 is selected): 0.7798 m

c) Head loss encountered due to T-junction (K value of 1.8 is selected): 0.2752 m

d) Head loss encountered due to flow along a straight length (f is calculated to be 0.031): 0.6548 m

e) Head loss encountered due to pipe entrance and exit: 0.2548 m

The summation of head loss due to frictional loss is 6.8576 m.

Apart from frictional loss, based on piping configuration, elevation changes result in additional head of 2.35 m.

Thus, the total head loss, or pressure drop in the flow loop, is 9.2076 m.

Walrus® TQ1500 pump is selected to be used in this research project. This regenerative turbine pump is able to give maximum discharge head of 32 m and maximum discharge flow rate of 230 L/m. Its power requirement is 1.5 kW, and it is compatible with the existing laboratory's electrical power supply (voltage of 240 V at frequency of 50 Hz).

Figure 13: Photo of Walrus® TQ1500 pump

4.2.5 Installation of the Pressure Transmitter and Pressure Indicator

On the pressure-measurement segment (Segment K in Figure 10), to effectively measure the pressure drop along the length of 350 cm, 8 pressure-tapping points are provided. The 8 pressure-tapping points are connected to a manifold via impulse lines (flexible tubings). At the manifold, valves or switches are provided to select the required pressure point to be sensed by a digital pressure transmitter. The digital pressure transmitter is wired to a digital pressure indicator to provide pressure readings in the appropriate measurement unit.

The 8 pressure-tapping points are provided at different lengths of Segment K, as shown in Figure 14 and Figure 15 below:
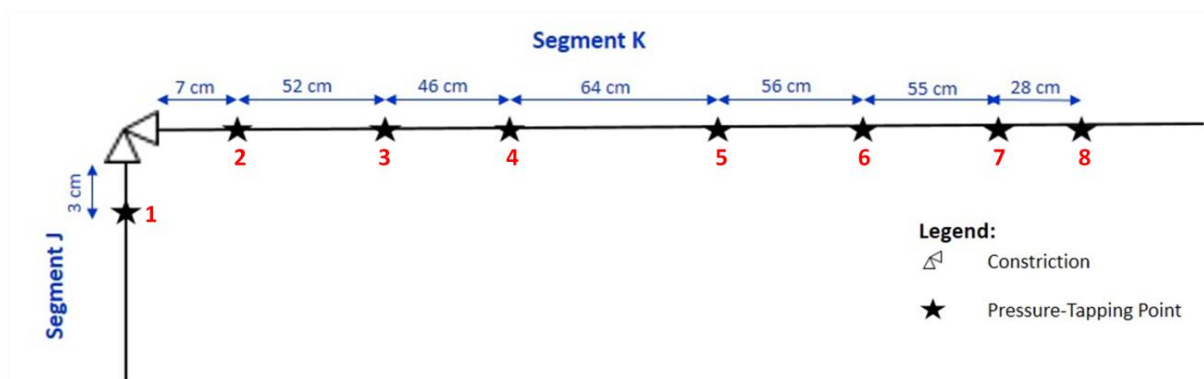
Figure 14: Location of the pressure-tapping points
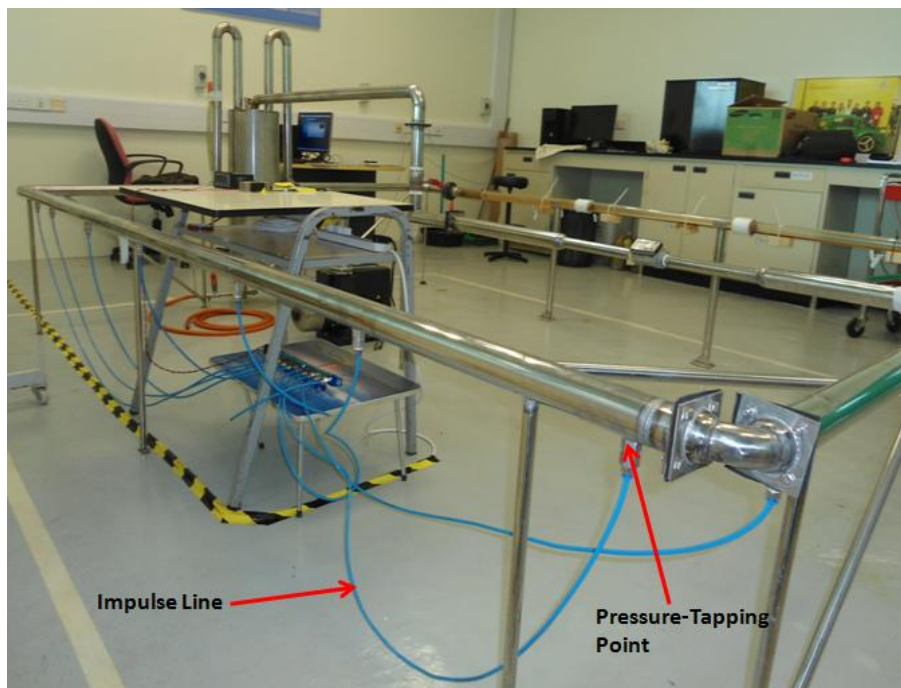
Figure 15: Photo of actual pressure-tapping points and impulse lines (flexible tubings)

Figure 16 shows the actual manifold, which is connected to the impulse lines. The impulse lines are flexible tubings with diameter of 0.125". The manifold has 8 impulse lines for the 8 pressure tapping points, 1 drain line, selection valves, and a digital pressure transmitter.
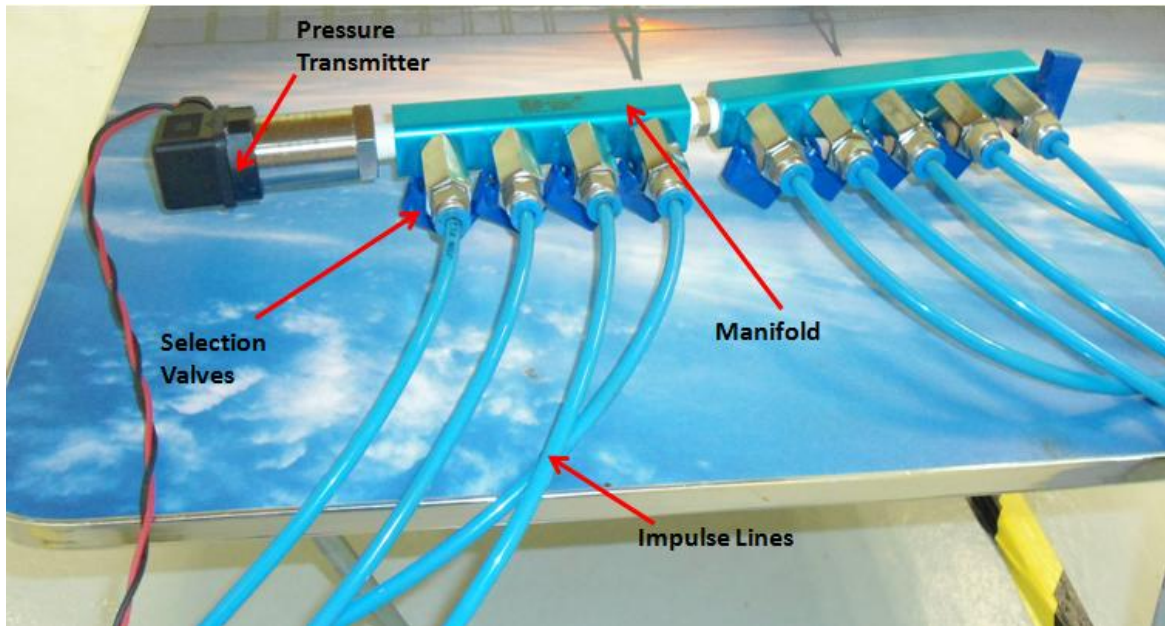
Figure 16: Photo of actual manifold, impulse lines, selection valves and pressure transmitter

BCM 130C digital pressure transmitter is used in this research project. This transmitter is able the measure pressures ranging from 0 to 4 bar, by giving 4 to 20 mA of output. Its accuracy is ±0.5% of the full-scale output, and its allowable operating temperature range is -40 °C to 125 °C. BCM 130C digital pressure transmitter requires 12 Vdc to 36 Vdc of supply voltage, and it gives the measured output in 4 to 20 mA. A voltage converter is provided, to convert the laboratory power supply voltage from 240 Vac to 24 Vdc. To display the output in the appropriate pressure measurement unit (bar), a digital pressure indicator has to be connected.

Autonics MT4W-DA-41 digital pressure indicator is used for the purpose of converting the current signal to the pressure measurement unit. It receives input of 4 to 20 mA from BCM 130C pressure transmitter, and displays the output range of 0.00 to 4.00 bar (sensitivity up to 2 decimal points). At temperature of 23 °C ± 5 °C, its display accuracy is ±0.1% of the reading. Its allowable operating temperature range is -10 °C to 50 °C. Autonics MT4W-DA-41 pressure indicator is powered by laboratory power supply voltage of 240 Vac. Figure 17 shows Autonics MT4W-DA-41 pressure indicator.

Figure 17: Photo of Autonics MT4W-DA-41 pressure indicator

The 3 electronic components, namely BCM 130C pressure transmitter, Autonics MT4W-DA-41 pressure indicator and 24 Vdc voltage converter, are wired and connected as shown in Figure 18 and Figure 19.
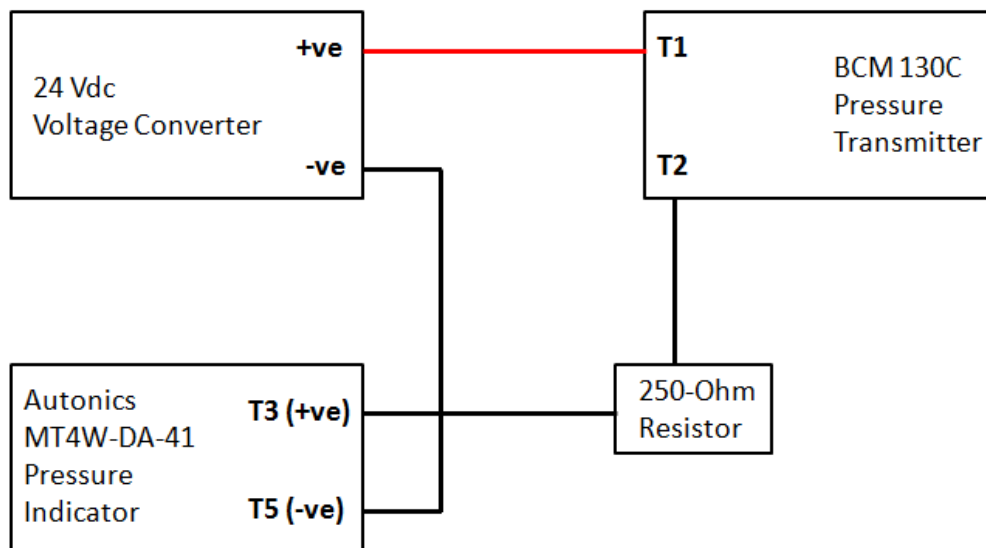
Figure 18: Schematics connection / wiring of pressure-measurement electronic components

Positive terminal is indicated by "+ve", and negative terminal is indicated by "-ve". Other terminal blocks are numbered according to the respective manufacturer's operating manual. Wire size of AWG 20 (0.50 mm^2) is used for connecting the terminal of the 3 electronic components.
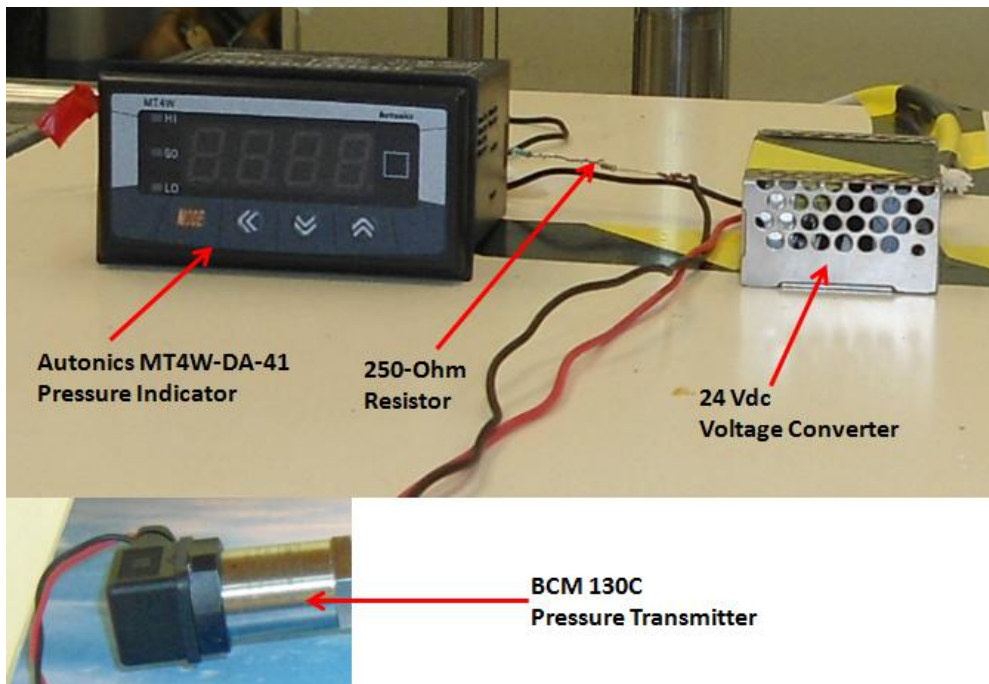
Figure 19: Photo of actual setup of the pressure-measurement devices

To ensure the accuracy and precision of the pressure-measurement devices, the setup has been tested by using a hand-pump calibrator, and also compared with a pneumatic locally-mounted pressure gauge. 5-point-test from the calibrator is employed, to determine the responses of Autonics MT4W-DA-41 pressure indicator at 0%, 25%, 50%, 75% and 100% of the full output range (0.00 – 4.00 barg). The results are satisfactory with 0% error, as shown in Table 2.

Table 2: Calibration results of pressure-measurement devices

Calibrator Pressure	Autonics MT4W-DA-41 Pressure Indicator
At 0% of the full output range: 0 barg	Pressure display: 0.00 barg
Calibrator pressure: 0 psig / 0 barg	
At 25% of the full output range: 1 barg	Pressure display: 1.00 barg
Calibrator pressure: 14.5 psig / 0.9997 barg	
At 50% of the full output range: 2 barg	Pressure display: 2.00 barg
Calibrator pressure: 29 psig / 1.9995 barg	
At 75% of the full output range: 3 barg	Pressure display: 3.00 barg
Calibrator pressure: 43.5 psig / 2.9992 barg	
At 100% of the full output range: 4 barg	Pressure display: 4.00 barg
Calibrator pressure: 58 psig / 3.9990 barg	

4.2.6 Final Installation and Equipment Setup

The final installation and overall equipment setup is shown in Figure 20.
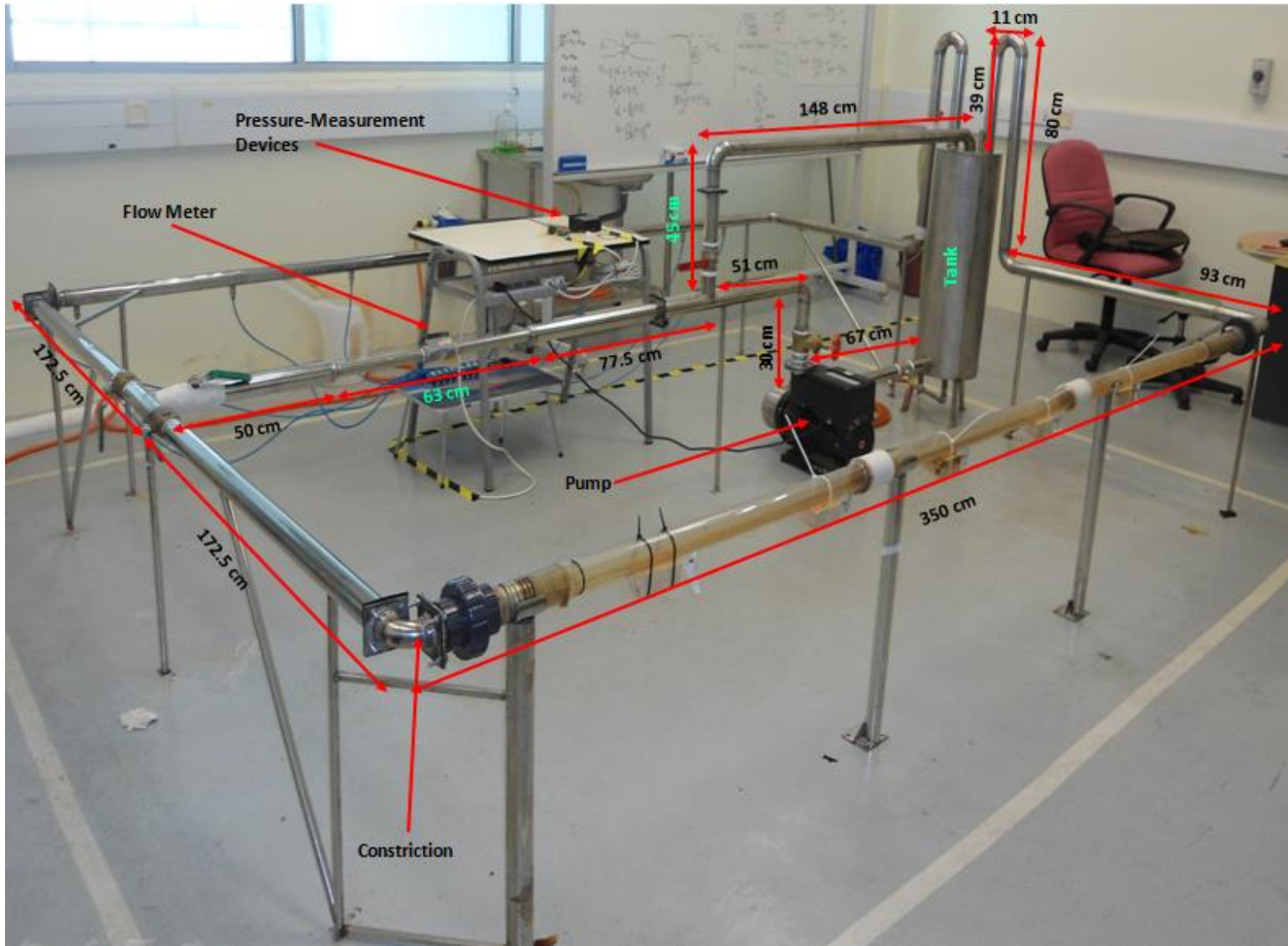
Figure 20: Photo of final installation and equipment setup

4.3 Materials and Resources

The required materials for running the experiment are crude oil stock, filtered tap water and oil-soluble cleaning agents.

Crude oil stock is obtained from PETRONAS Miri Crude Oil Terminal (MCOT), which is classified as "Miri Light Crude (MLC)". MLC is homogenous mixture of stabilized crude oil produced from Miri offshore platforms. The measurement of physicochemical properties, characterization, and compositional analysis of MLC are performed by an external industrial laboratory, complying with international testing standards such as American Society for Testing and Materials (ASTM). The external industrial laboratory is Petrotechnical Inspection (M) Sdn. Bhd., which is located in Labuan.

Table 3 shows the physicochemical properties and content of the crude oil.

Table 3: Physicochemical properties and content of the crude oil

No.	Parameter	Test Method	Unit	Result
1	Density @ 15 °C	ASTM D 5002	g/cm^3	0.8768
2	API Gravity @ 60 °F	Calculated	Degree	29.79
3	Total Sulphur	ASTM D 4294	wt %	0.0771
4	Nitrogen Content	ASTM D 5762	ppm wt	255
5	Total Acid Number	ASTM D 664	mgKOH/g	0.24
6	Nickel (Ni)	ASTM D 5863	ppm wt	< 1.0
7	Vanadium (V)	ASTM D 5863	ppm wt	1
8	Flash Point	IP 170	°C	< -20
9	Pour Point	ASTM D 5853	°C	-30
10	Colour ASTM	ASTM D 1500	-	D 8.0
11	Reid Vapor Pressure @ 37.8°C	ASTM D 5191	kPa	9.2
12	Salt Content	ASTM D 3230	lb/1000bbls	3.5
13	Ash Content	ASTM D 482	wt %	0.002
14	Mercaptan Sulphur	UOP 163	ppm wt	23
15	MCRT - 100% Sample	ASTM D 4530	wt %	0.23
16	Wax Content	UOP 46	wt %	4.5
17	Kinematic Viscosity @ 25°C	ASTM D 445	cSt	4.785

18	Kinematic Viscosity @ 40°C	ASTM D 445	cSt	3.958
19	Kinematic Viscosity @ 70°C	ASTM D 445	cSt	2.303
20	Characterisation Factor	UOP 375	-	11.5
21	Gross Calorific Value	ASTM D 240	MJ/kg	44.482
22	Asphaltenes	IP 143	wt %	0.43
23	Sodium (Na)	ASTM D 5863	ppm wt	14.0
24	Potassium (K)	ASTM D 5863	ppm wt	< 1.0
25	Copper (Cu)	ASTM D 5863	ppm wt	< 1.0
26	Lead (Pb)	ASTM D 5863	ppm wt	< 1.0
27	Iron (Fe)	ASTM D 5863	ppm wt	1.2
28	Basic Sediment & Water	ASTM D 4007	vol. %	0.05
29	Water Content	ASTM D 4006	vol. %	0.10

The cude oil stock has API of 29.79 °, thus it is classified as light crude oil (Speight, 2014). Results of full crude compositional analysis by gas chromatography method are provided in the Appendix section.

The source of tap water is from local municipal water supply, and the tap water is filtered to remove unwanted rust and sediment particles, before introducing it into the flow loop. In this experimental research, the composition and characteristics of water (*e.g.* salinity) are not the main parameters to be focused.

To ensure repeatability, precision and accuracy, the flow loop and measurement devices have to be cleaned from time to time, to avoid clogging or scaling. Oil-soluble cleaning solvent, such as kerosene, is easily available and used to remove the stubborn traces of crude oil in the flow loop and measurement devices.

The experimental research is performed using the flow loop setup deliberated in Section 4.2. Materials used in fabricating the flow loop are stainless steel pipes (with nominal diameters of 1" and 2"), stainless steel plates (to fabricate the flange faces and tank), cylindrical acrylic glass (with nominal diameter of 2"), pipe coupling, flexible hose fittings, ball valves (sizes of 2" and 0.75"), and gate valves (size of 2"). Threaded joints and welded joints are used to

complete the flow loop. Shielded Metal Arc Welding (SMAW) technique is employed to weld the stainless steel components.

4.4 Experimental Methodology

The experimental methodology is prepared with the aim of addressing:

    i)   Formation of emulsions via flow shear only

    ii)   Pressure drop measurement

    iii)   Variation of volumetric amount to reach and go beyond the phase inversion point

The turbulence and intense agitation experienced by the flow, especially when going through the constriction, are studied to evaluate their effects on the formation of emulsions. For this purpose, the flow will be circulated for 25 minutes at constant flow rate and constant volumetric ratio of oil and water. Samples will be taken at the end of the period to determine the extent of emulsification, followed by pressure drop measurement. During pressure drop measurement, Segments M, N and O (refer to Figure 7) can be isolated, as these segments are only required for visualization of the emulsions flow.

The similar steps will be repeated for another pre-determined flow rate and volumetric ratio of oil and water, according to the variables matrix in Table 4. The volumetric amount of water will be increased beyond the phase inversion point, to study the behaviours of emulsions when phase inversion occurs.

For each repeat at different flow rate or volumetric ratio, new mixtures of separated oil and water shall be used, to rule out the presence of existing emulsions. Total liquid volume in the flow loop shall be kept above 40L, to ensure the liquid fully occupy the piping. Besides that, the temperature of the flow shall be monitored closely, as continuous circulation will cause the temperature to rise. Higher temperature may invalidate the experiment results. It is thus recommended to allow the flow loop system to cool down to room temperature after each run.

Table 4: Experiment variables matrix

Volumetric Ratio	Flow Rate (Litres / minute)
100% Crude Oil	100 L/m
0% Water	80 L/m
	60 L/m
	40 L/m
	20 L/m
80% Crude Oil	100 L/m
20% Water	80 L/m
	60 L/m
	40 L/m
	20 L/m
60% Crude Oil	100 L/m
40% Water	80 L/m
	60 L/m
	40 L/m
	20 L/m
40% Crude Oil	100 L/m
60% Water	80 L/m
	60 L/m
	40 L/m
	20 L/m
20% Crude Oil	100 L/m
80% Water	80 L/m
	60 L/m
	40 L/m
	20 L/m
0% Crude Oil	100 L/m
100% Water	80 L/m
	60 L/m
	40 L/m
	20 L/m

4.4.1 Basis of Assumptions

The experimental methodology is performed with the following assumptions:

a) Flow circulation temperature shall not exceed 35 °C. The flow loop system shall be allowed to cool down before the next run.

b) For all batches, the properties and characteristics of the crude oil and water are assumed to be constant. To avoid variances, all batches shall be taken from the same crude oil stock obtained in the similar time period.

c) The composition and characteristics of water (*e.g.* salinity) are not the main parameters to be focused. The values are assumed to be constant for the filtered tap water stock obtained in the similar time period.

CHAPTER 5
RESULTS AND DISCUSSION

5.1 Introduction

This chapter provides the SARA analysis of the crude oil used in this research, the results of emulsions formation in the closed-circuit flow loop, the stability of emulsions, the effect of emulsions on pressure drop, the dissipation energy in forming the emulsions, as well as the corresponding discussion on the results. The experiment was performed according to Section 4.4.

The properties of the crude oil will give the understanding of the nature of the crude oil, and the presence of its surface active agents. Next, emulsification test was performed by circulating the oil and water mixtures in the closed-circuit flow loop. The types, quantity and stability of emulsions were observed and deliberated. Then, flow pressure drop was measured, and the relationship between emulsions and pressure drop was studied. Pressure drop data was further analyzed to obtain the dissipation energy of emulsions.

5.2 SARA Analysis of Crude Oil

SARA (Saturates, Aromatics, Resins and Asphaltenes) analysis was also conducted by employing High Performance Liquid Chromatography (HPLC) method. It shall be highlighted that the HPLC method has certain limitations such as inability to separate the macro/micro-crystalline wax, naphthenates and volatiles. Besides that, some volatile components may be lost, as the sample will be heated to 60 °C, centrifuged and filtered through sodium sulfate powder at 60 °C, before the final distillation process. The result of SARA analysis is given in Table 5.

Table 5: SARA analysis

Component	Unit	Result
Saturates	wt%	69.30
Aromatics	wt%	26.60
Resins	wt%	3.65
Asphaltenes	wt%	0.43

From the SARA analysis, the Colloidal Instability Index (CII) is calculated to be 2.3. CII is the ratio of saturates and asphaltenes fraction to aromatics and resins fraction (Asomaning and Watkinson, 1999). Refer to Equation 24 below.

$$CII = \frac{Saturates + Asphaltenes}{Aromatics + \mathrm{Re}\sin s} \qquad (24)$$

According to Bennett *et al.* (2006), crude oils with CII exceeding the value of 2 have higher tendency to foul due to precipitation of asphaltenes. It has been well-proven and accepted that precipitation of asphaltenes will favour the emulsification process (Lee, 1999; Ali and Alqam, 2000; Gafonova, 2000; Kilpatrick and Spiecker, 2001). Thus, the crude oil stock used in this research is expected to have the natural tendency of forming emulsions.

5.3 Formation of Emulsions and Observations

After circulating the flow of crude oil and water mixtures for 25 minutes, samples were taken to observe the extent of emulsification. The samples were taken for each different flow rate and different volumetric content ratio of oil and water. Immediate observation was made to maintain the actual representation of emulsions in the flow loop, as static condition would result in the emulsions to aggregate, coalesce, and finally settle out into two distinct phases of oil and water. Another observation was made after 5 hours, to assess the stability of emulsions, after the settling out of unstable emulsion droplets.

To determine the extent of emulsification, the sample was collected into a graduated 100-mL measuring cylinder. The volumetric amounts of water, oil and emulsions were visually observed, which is possible due to density differences among the 3 phases. This is actually a standard practice adopted in the oil production industry, and it is even implemented for custody transfer metering in crude sales.   For each flow rate and volumetric ratio, 3 samples were taken, to ensure the samples were representative of the emulsions in the flow loop.

5.3.1 Emulsification Observation for 20% Water and 80% Crude Oil
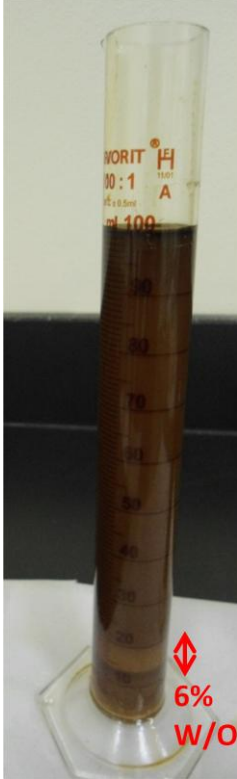
100 L/m Flow Rate	80 L/m Flow Rate	60 L/m Flow Rate	40 L/m Flow Rate	20 L/m Flow Rate
Water-in-oil emulsions were formed, and emulsion droplets took up 34% of the volume fraction.	Water-in-oil emulsions were formed, and emulsion droplets took up 9% of the volume fraction.	Water-in-oil emulsions were formed, and emulsion droplets took up 6% of the volume fraction.	No appreciable formation of emulsions.	No appreciable formation of emulsions.

Figure 21: Emulsification observation for 20% water and 80% crude oil

5.3.2 Emulsification Observation for 40% Water and 60% Crude Oil

100 L/m Flow Rate	80 L/m Flow Rate	60 L/m Flow Rate	40 L/m Flow Rate	20 L/m Flow Rate
Water-in-oil emulsions were formed, and emulsion droplets took up 63% of the volume fraction.	Water-in-oil emulsions were formed, and emulsion droplets took up 54% of the volume fraction.	Water-in-oil emulsions were formed, and emulsion droplets took up 31% of the volume fraction.	Water-in-oil emulsions were formed, and emulsion droplets took up 6% of the volume fraction. There was also observation of non-aggregated droplets.	There was observation of finely dispersed non-aggregated water-in-oil emulsion droplets, but the droplets did not aggregate to constitute significant volume fraction.

Figure 22: Emulsification observation for 40% water and 60% crude oil

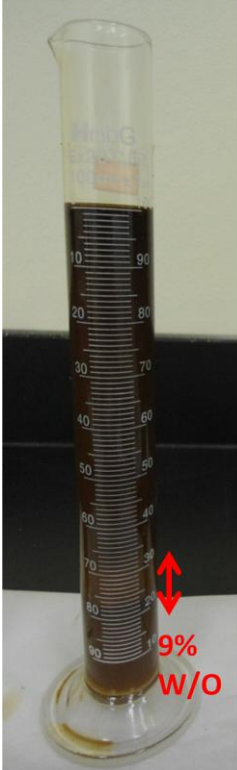### 5.3.3 Emulsification Observation for 60% Water and 40% Crude Oil
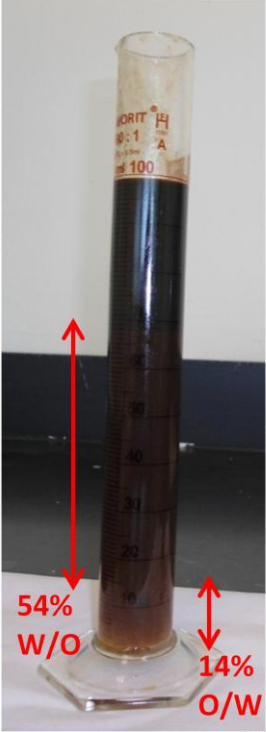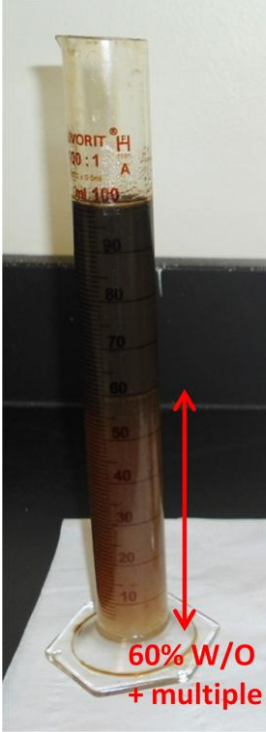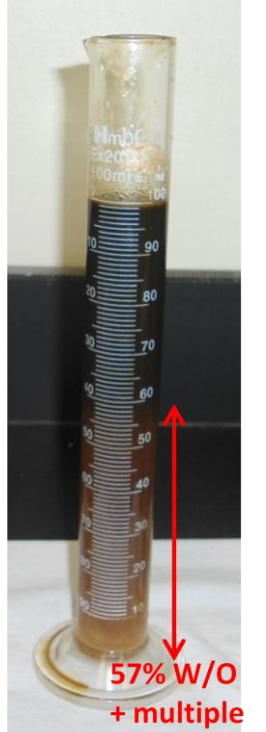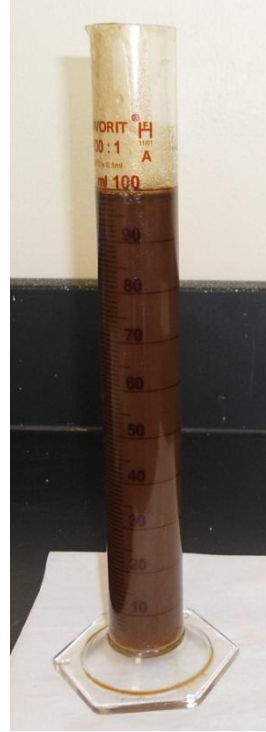
100 L/m Flow Rate	80 L/m Flow Rate	60 L/m Flow Rate	40 L/m Flow Rate	20 L/m Flow Rate
Multiple emulsions were formed. Emulsion droplets took up 68% of the volume fraction. Water-in-oil emulsions occupied 54% volume fraction, while oil-in-water emulsions occupied 14% volume fraction.	Multiple emulsions were formed. Emulsion droplets, mostly water-in-oil emulsions, took up 60% of the volume fraction. Oil-in-water emulsion droplets were present, but non-aggregated.	Multiple emulsions were formed. Emulsion droplets, mostly water-in-oil emulsions, took up 57% of the volume fraction. Oil-in-water emulsion droplets were present, but non-aggregated.	Multiple emulsions were formed. Emulsion droplets, mostly water-in-oil emulsions, took up 54% of the volume fraction. Oil-in-water emulsion droplets were present, but non-aggregated.	There was observation of finely dispersed non-aggregated water-in-oil emulsion droplets, but the droplets did not aggregate to constitute significant volume fraction.

Figure 23: Emulsification observation for 60% water and 40% crude oil

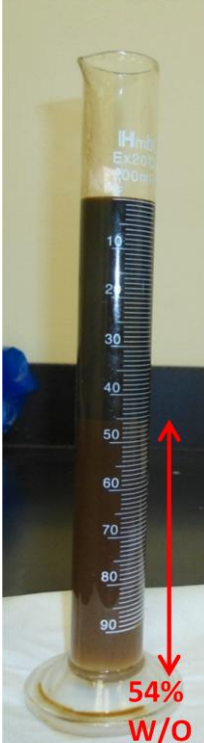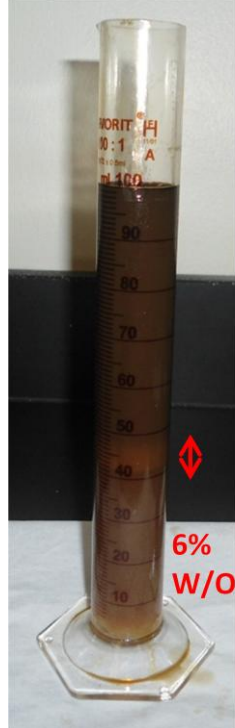## 5.3.4 Emulsification Observation for 80% Water and 20% Crude Oil
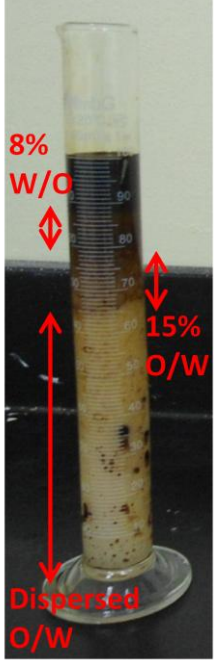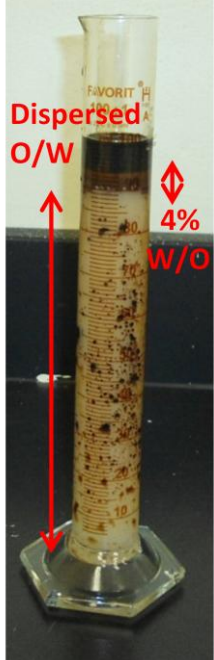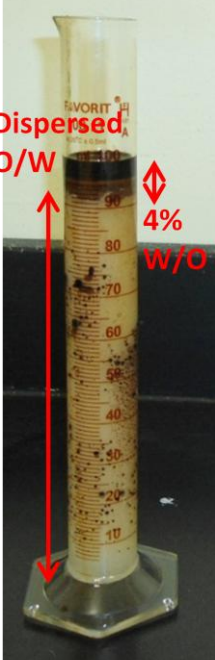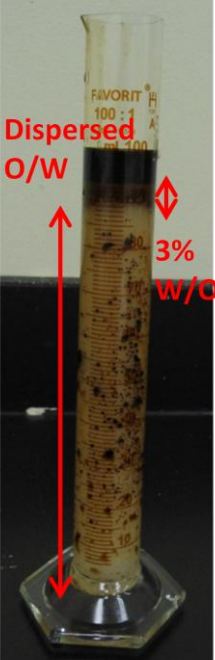
100 L/m Flow Rate	80 L/m Flow Rate	60 L/m Flow Rate	40 L/m Flow Rate	20 L/m Flow Rate
Multiple emulsions were formed. Emulsion droplets took up 23% of the volume fraction. Water-in-oil emulsions occupied 8% volume fraction, while oil-in-water emulsions occupied 15% volume fraction.	Multiple emulsions were formed. Water-in-oil emulsions occupied 4% volume fraction, while oil-in-water emulsions were dispersed. Oil-in-water emulsions had started to aggregate.	Multiple emulsions were formed. Water-in-oil emulsions occupied 4% volume fraction, while oil-in-water emulsions were dispersed.	Multiple emulsions were formed. Water-in-oil emulsions occupied 3% volume fraction, while oil-in-water emulsions were dispersed.	Multiple emulsions were formed. Water-in-oil emulsions occupied 2% volume fraction, while oil-in-water emulsions were dispersed. The packing of emulsion droplets was less dense.

Figure 24: Emulsification observation for 80% water and 20% crude oil

5.3.5 Discussion on Emulsions Formation

The results obtained in this research would add on to the understanding of emulsification by flow shear. Agreeing with previous works (Nädler and Mewes, 1997; Keleşoğlu *et al*., 2012; Plasencia *et al*., 2013), this research shows that higher flow rate causes more stabilized emulsion droplets to form.

At 20% and 40% of water volumetric content, more water-in-oil emulsion droplets were formed as the flow rate was increased. For 20% of water volumetric content, at maximum flow rate of 100 L/m (or 0.8910 m/s), water-in-oil emulsion droplets took up 34% of the sample's volume fraction. It is assumed that this sample is representative of the flow inside the pipe loop. At lower flow rate, the volume occupied by emulsion droplets was less, and below 40 L/m (or 0.3564 m/s), there was no appreciable formation of emulsion droplets.

For 40% of water volumetric content, at maximum flow rate of 100 L/m (or 0.8910 m/s), water-in-oil emulsion droplets took up 63% of the sample's volu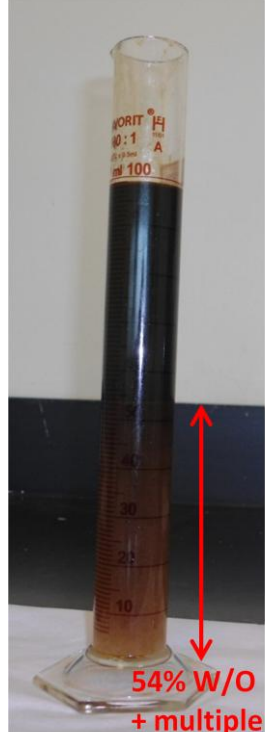me fraction. Emulsion droplets were present in all samples, including in the sample taken at the lowest flow rate of 20 L/m (or 0.1782 m/s). Similar to the previous emulsification trend, the volume occupied by emulsion droplets was reduced as the flow rate was decreased. At flow rate of 20 L/m (or 0.1782 m/s), water-in-oil emulsion droplets did not occupy any volume fraction; they were dispersed throughout the sample and were unstable.

The results strengthen the view that higher shear rate (higher flow rate or velocity) gives more dissipation energy to disperse the water phase into the continuous oil phase as emulsion droplets (Ashrafizadeh and Kamran, 2010; Briceno *et al*., 1997; Pal *et al*., 1992). Apart from forming more emulsion droplets, the droplets are also more stable when formed at higher flow rate. The stability observation of emulsion droplets is given in Table 6. Comparison is made between the initial volume occupied by emulsion droplets, and the final occupied volume after 5 hours, i.e. after settling out of unstable emulsions. A stable emulsions system has less percentage of reduction of emulsions (the emulsion droplets will remain suspended in the continuous phase).

Table 6: Stability observation of emulsion droplets

Volumetric Ratio	Flow Rate (Litres / minute)	%Volume by Emulsions	%Volume by Emulsions After 5 hours	% Reduction of Emulsions
80% Crude Oil 20% Water	100 L/m	34%	30%	11.76%
	80 L/m	9%	5%	44.44%
	60 L/m	6%	2%	66.67%
	40 L/m	Nil	Nil	Nil
	20 L/m	Nil	Nil	Nil
60% Crude Oil 40% Water	100 L/m	63%	60%	5.00%
	80 L/m	54%	42%	22.22%
	60 L/m	31%	20%	35.48%
	40 L/m	6%	1%	83.33%
	20 L/m	Dispersed	0%	100.00%
40% Crude Oil 60% Water	100 L/m	68%	65%	4.41%
	80 L/m	60%	55%	8.33%
	60 L/m	57%	50%	12.28%
	40 L/m	54%	45%	16.67%
	20 L/m	Dispersed	0%	100.00%
20% Crude Oil 80% Water	100 L/m	23%	18%	21.74%
	80 L/m	4%	3%	25.00%
	60 L/m	4%	3%	25.00%
	40 L/m	3%	2%	33.33%
	20 L/m	2%	1%	50.00%

At 20% and 40% of water volumetric content, it is observed that at higher flow rate, more emulsion droplets were formed with larger occupied volume, and the amount of settled-out emulsions (reduction of emulsions) was less.

It is also noted that, as the water volumetric content was increased from 20% to 40%, more water-in-oil emulsion droplets were formed with higher stability. This indicates that the system was favourable towards water-in-oil emulsions, as the water volumetric content was increased to 40%. Increasing the water content would cause more asphaltenes, which were soluble in crude oil, to be aggregated and adsorbed to the oil-water interface, mainly due to asphaltenes' amphiphilic characteristics (Gafonova, 2000). Also, as explained in Section 5.2, from the SARA analysis, the type of crude oil used in this research had Colloidal Instability Index (CII) of 2.3, and thus it had the tendency of precipitation of asphaltenes. Adsorption of asphaltene precipitates at the oil-water interface would strengthen the interfacial film, resulting in the formation of more stable emulsion droplets (Becher, 1955; Auflem, 2002). From the SARA analysis too, this crude oil was found to contain 0.43 wt% of asphaltenes.

The emulsions system experienced interesting changes as the water volumetric content was increased to 60%. At flow rate of 20 L/m (or 0.1782 m/s), there were dispersed water-in-oil emulsion droplets, which did not occupy any significant volume fraction. But at flow rate of 40 L/m (or 0.3564 m/s), phase inversion occurred. Phase inversion resulted in the formation of multiple emulsions, where water-in-oil emulsions took up 54% of the volume fraction. Oil-in-water emulsions were dispersed in the sample, and did not aggregate to constitute significant volume fraction. Similar characteristic was observed at flow rate of 60 L/m (or 0.5346 m/s).

Phase inversion became more significant at higher flow rates of 80 L/m (or 0.7128 m/s) and 100 L/m (or 0.8910 m/s). At flow rate of 80 L/m, phase inversion caused water-in-oil emulsions and oil-in-water emulsions to occupy 50% and 10% of volume fractions respectively. At flow rate of 100 L/m, water-in-oil emulsions and oil-in-water emulsions occupied 54% and 14% of volume fractions respectively. Similar to previous trend, higher flow rate produced more stable emulsions, with less percentage of reduction or settled-out.

When the water volumetric content was increased to 80%, all samples showed multiple emulsions, which suggest the occurrence of phase inversion in all samples, including the sample for the lowest flow rate of 20 L/m (or 0.1782 m/s). At the flow rate of 100 L/m (or 0.8910 m/s), significant multiple emulsions were formed, with water-in-oil emulsions occupying 8% of volume fraction and oil-in-water emulsions occupying 15% of volume fraction. At other flow rates below 100 L/m, water-in-oil emulsions occupied not more than

4% of volume fraction, while oil-in-water emulsions did not aggregate to constitute significant volume fraction.

Agreeing with previous trend, higher flow rate resulted in more stable emulsions, with less percentage of reduction or settled-out. However, it is important to note that these results present a new idea on the effect of flow rate on phase inversion. The minimum flow rate for the phase inversion of 60%-water-content system and 80%-water-content system was 40 L/m and 20 L/m, respectively. This shows that for an emulsions system having less dispersed droplets, higher flow rate is required to induce the phase inversion. Further flow rate increment results in more significant phase inversion, which is usually indicated by the presence of multiple emulsions. Thus, it can be put forward that:

i) Phase inversion is affected by the amount of dispersed droplets. As the concentration of dispersed droplets is increased, it will reach a point where the dispersed phase is inverted to become the continuous phase.

ii) Phase inversion is affected by the flow rate. Higher flow rate will bring the emulsions system to an earlier phase inversion. This can probably be caused by the more frequent coalescence of the dispersed phase's droplets at higher flow rate.

iii) Phase inversion depends on the packing nature of the droplets (Alwadani, 2009).

iv) Phase inversion will usually result in multiple emulsions.

At 80% of water volumetric content, due to the excessive amount of water (the corresponding volumetric content of oil was only 20%), all samples had experienced phase inversion, where water had become the continuous phase and oil had become the dispersed phase. Multiple emulsions were significant, especially at higher flow rate. In the case of these multiple emulsions, at low flow rates, the emulsions system seemed to favour the formation of water-in-oil emulsions, rather than oil-in-water emulsions, although water was present in large quantity as the continuous phase.

At the lowest flow rate of 20 L/m (or 0.1782 m/s), water-in-oil emulsions occupied 2% of volume fraction, while oil-in-water emulsions were dispersed. As the flow rate was increased, water-in-oil emulsions occupied more volume fraction, while oil-in-water emulsions also grew and became more aggregated. At flow rate of 100 L/m (or 0.8910 m/s), water-in-oil

emulsions occupied 8% of volume fraction, while oil-in-water emulsions occupied 15% of volume fraction. The droplet size distribution of oil-in-water emulsions was quite irregular. This behaviour can be explained by attributing to the surface tension of oil (measured to be 29.5 mN/m) and interfacial tension of oil-in-water droplets (measured to be ranging from 15 mN/m – 22 mN/m). Higher dissipation energy, which comes from the higher shear rate, is needed to surmount the pressure gradient between the convex and concave sides of an oil-in-water droplet's interface, before the droplet can be formed stably and sustained (Becher, 1955). The interactions of asphaltenes are believed to play an important part at the interfacial films of these multiple emulsions, but unfortunately, this particular area is not fully understood yet.

5.4 Emulsification Effects on Pressure Drop

After circulating the flow of crude oil and water mixtures for 25 minutes, apart from taking samples to observe the extent of emulsification, pressure measurement was also obtained for each different flow rate and different volumetric content ratio of oil and water. Pressure was measured at 8 points along Segments J and K (refer to Figure 14 in Chapter 4), and was recorded once the readings stabilized.

To consider the effect of emulsions on flow pressure drop, pressure difference between Point 8 and Point 5 is taken as the measured pressure drop. At Point 5 and beyond, which is more than 1.69 m from the constriction, the flow is assumed to be fully-developed as it has undergone sufficient entrance length.
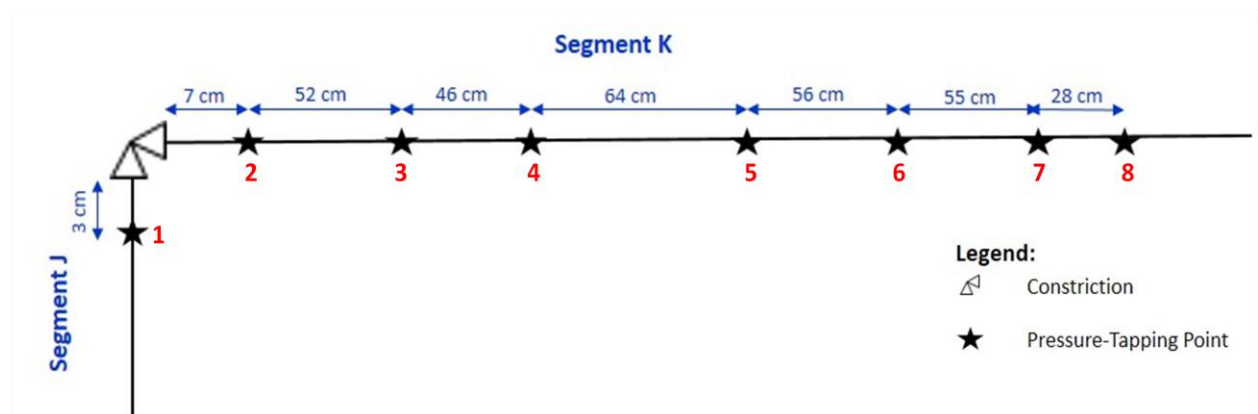
From Figure 14 in Chapter 4: Location of the pressure-tapping points

5.4.1 Flow Pressure Measurement for 0% Water Volumetric Content (100% Oil Volumetric Content)

Table 7: Flow pressure measurement for 0% water volumetric content

Flow Rate (L/m)	Flow Rate (m/s)	Pressure Point 1 (barg)	Pressure Point 2 (barg)	Pressure Point 3 (barg)	Pressure Point 4 (barg)	Pressure Point 5 (barg)	Pressure Point 6 (barg)	Pressure Point 7 (barg)	Pressure Point 8 (barg)
100	0.8910	1.84	1.45	1.53	1.50	1.46	1.43	1.40	1.39
80	0.7128	1.71	1.36	1.44	1.42	1.39	1.36	1.34	1.33
60	0.5346	1.58	1.27	1.34	1.32	1.29	1.26	1.24	1.23
40	0.3564	1.43	1.13	1.18	1.17	1.15	1.13	1.12	1.11
20	0.1782	1.28	1.04	1.08	1.07	1.05	1.03	1.02	1.01

* Each presented value is a mean value, and the standard error of the mean is less than 0.009.

Figure 25: Flow pressure measurement for 0% water volumetric content

5.4.2 Flow Pressure Measurement for 20% Water Volumetric Content (80% Oil Volumetric Content)

Table 8: Flow pressure measurement for 20% water volumetric content

Flow Rate (L/m)	Flow Rate (m/s)	Pressure Point 1 (barg)	Pressure Point 2 (barg)	Pressure Point 3 (barg)	Pressure Point 4 (barg)	Pressure Point 5 (barg)	Pressure Point 6 (barg)	Pressure Point 7 (barg)	Pressure Point 8 (barg)
100	0.8910	1.90	1.50	1.60	1.56	1.51	1.46	1.42	1.40
80	0.7128	1.77	1.4	1.49	1.46	1.42	1.38	1.35	1.33
60	0.5346	1.64	1.31	1.38	1.35	1.31	1.27	1.24	1.23
40	0.3564	1.48	1.19	1.26	1.24	1.21	1.19	1.17	1.16
20	0.1782	1.32	1.06	1.11	1.10	1.08	1.06	1.04	1.04

* Each presented value is a mean value, and the standard error of the mean is less than 0.009.
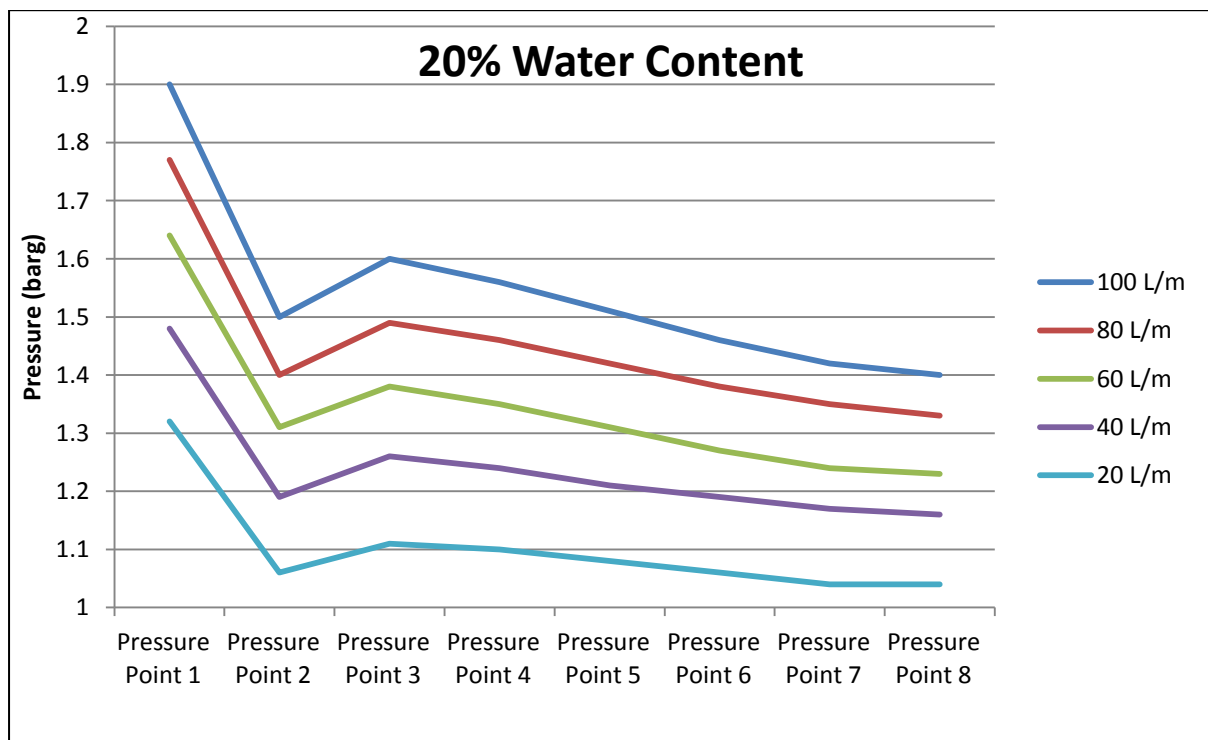
Figure 26: Flow pressure measurement for 20% water volumetric content

5.4.3 Flow Pressure Measurement for 40% Water Volumetric Content (60% Oil Volumetric Content)

Table 9: Flow pressure measurement for 40% water volumetric content

Flow Rate (L/m)	Flow Rate (m/s)	Pressure Point 1 (barg)	Pressure Point 2 (barg)	Pressure Point 3 (barg)	Pressure Point 4 (barg)	Pressure Point 5 (barg)	Pressure Point 6 (barg)	Pressure Point 7 (barg)	Pressure Point 8 (barg)
100	0.8910	1.96	1.57	1.69	1.62	1.56	1.49	1.41	1.39
80	0.7128	1.83	1.47	1.58	1.54	1.48	1.42	1.36	1.34
60	0.5346	1.70	1.38	1.45	1.42	1.35	1.31	1.26	1.24
40	0.3564	1.53	1.25	1.31	1.29	1.25	1.22	1.19	1.18
20	0.1782	1.37	1.13	1.17	1.16	1.13	1.10	1.08	1.08

* Each presented value is a mean value, and the standard error of the mean is less than 0.009.
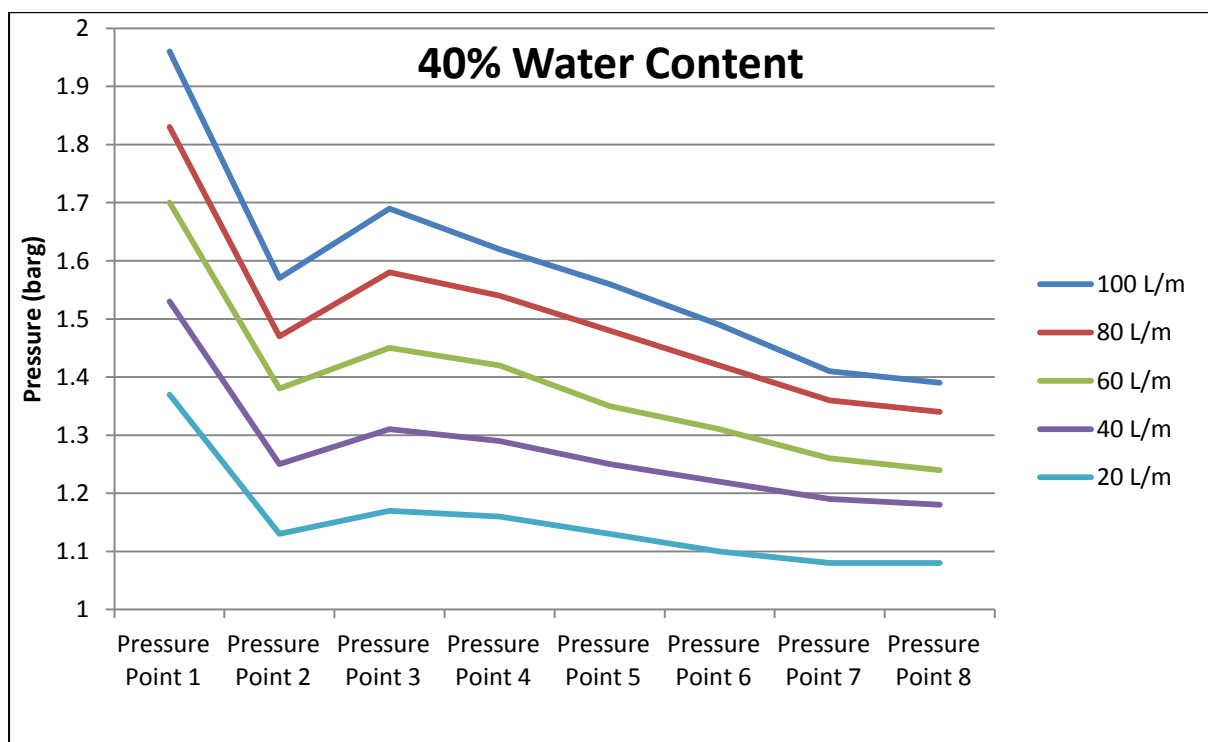
Figure 27: Flow pressure measurement for 40% water volumetric content

5.4.4 Flow Pressure Measurement for 60% Water Volumetric Content (40% Oil Volumetric Content)

Table 10: Flow pressure measurement for 60% water volumetric content

Flow Rate (L/m)	Flow Rate (m/s)	Pressure Point 1 (barg)	Pressure Point 2 (barg)	Pressure Point 3 (barg)	Pressure Point 4 (barg)	Pressure Point 5 (barg)	Pressure Point 6 (barg)	Pressure Point 7 (barg)	Pressure Point 8 (barg)
100	0.8910	2.02	1.62	1.75	1.68	1.62	1.56	1.5	1.48
80	0.7128	1.89	1.51	1.63	1.59	1.53	1.47	1.42	1.41
60	0.5346	1.76	1.44	1.52	1.48	1.41	1.35	1.29	1.28
40	0.3564	1.58	1.29	1.36	1.33	1.29	1.25	1.21	1.19
20	0.1782	1.42	1.18	1.21	1.20	1.17	1.15	1.13	1.12

* Each presented value is a mean value, and the standard error of the mean is less than 0.009.
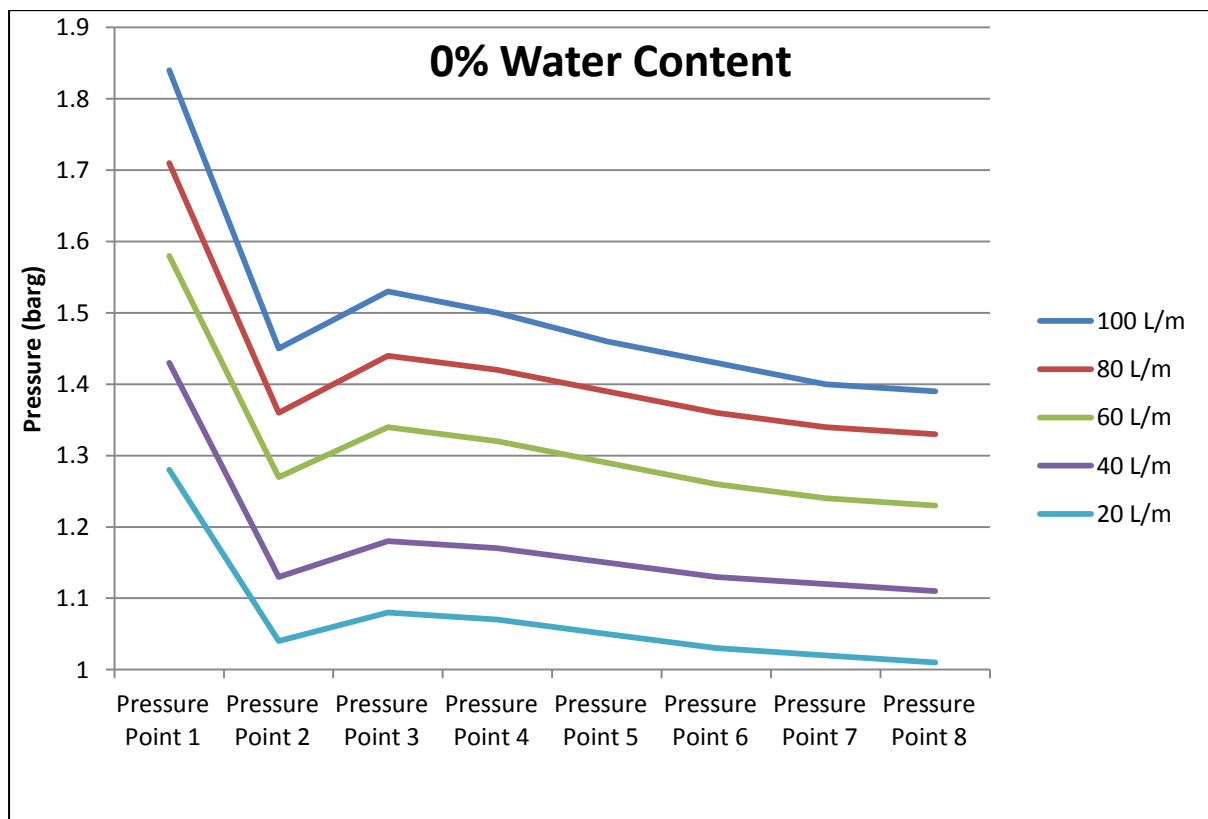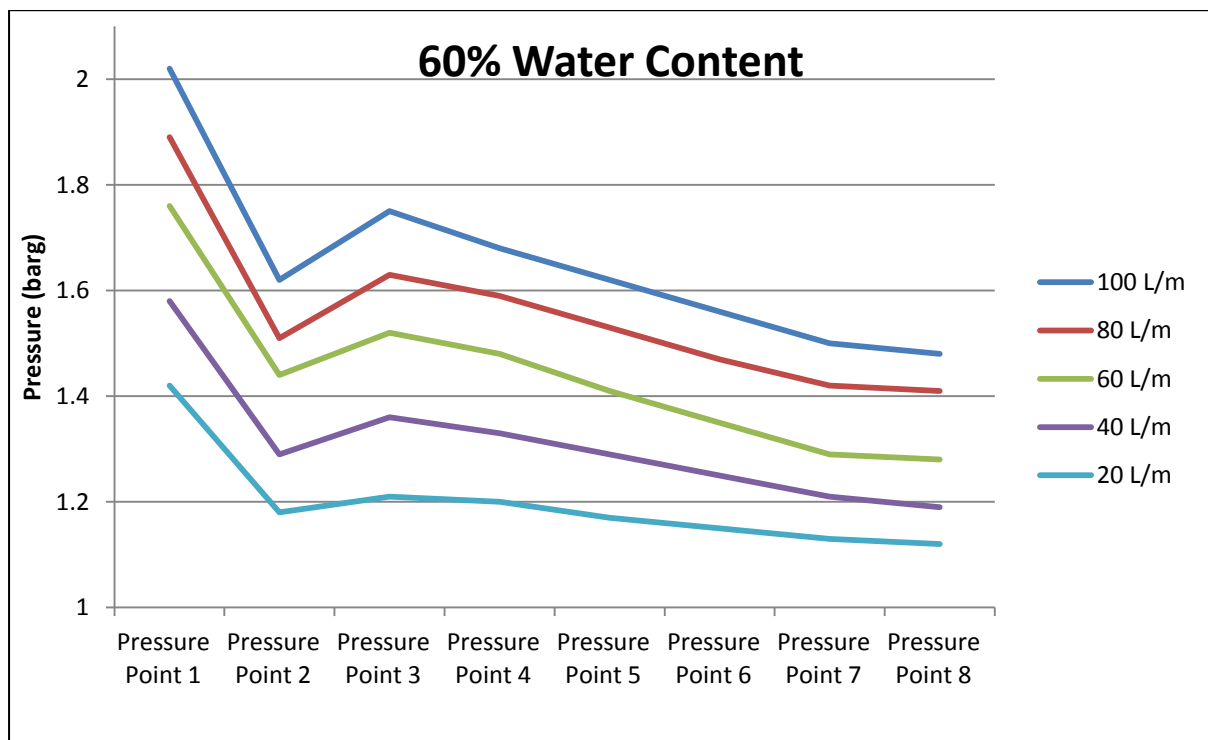

Figure 28: Flow pressure measurement for 60% water volumetric content

5.4.5 Flow Pressure Measurement for 80% Water Volumetric Content (20% Oil Volumetric Content)

Table 11: Flow pressure measurement for 80% water volumetric content

Flow Rate (L/m)	Flow Rate (m/s)	Pressure Point 1 (barg)	Pressure Point 2 (barg)	Pressure Point 3 (barg)	Pressure Point 4 (barg)	Pressure Point 5 (barg)	Pressure Point 6 (barg)	Pressure Point 7 (barg)	Pressure Point 8 (barg)
100	0.8910	2.08	1.68	1.82	1.79	1.74	1.7	1.67	1.66
80	0.7128	1.95	1.57	1.69	1.67	1.64	1.61	1.59	1.59
60	0.5346	1.82	1.47	1.56	1.55	1.53	1.51	1.49	1.49
40	0.3564	1.63	1.34	1.42	1.41	1.39	1.37	1.36	1.36
20	0.1782	1.47	1.22	1.26	1.26	1.25	1.24	1.23	1.23

* Each presented value is a mean value, and the standard error of the mean is less than 0.009.
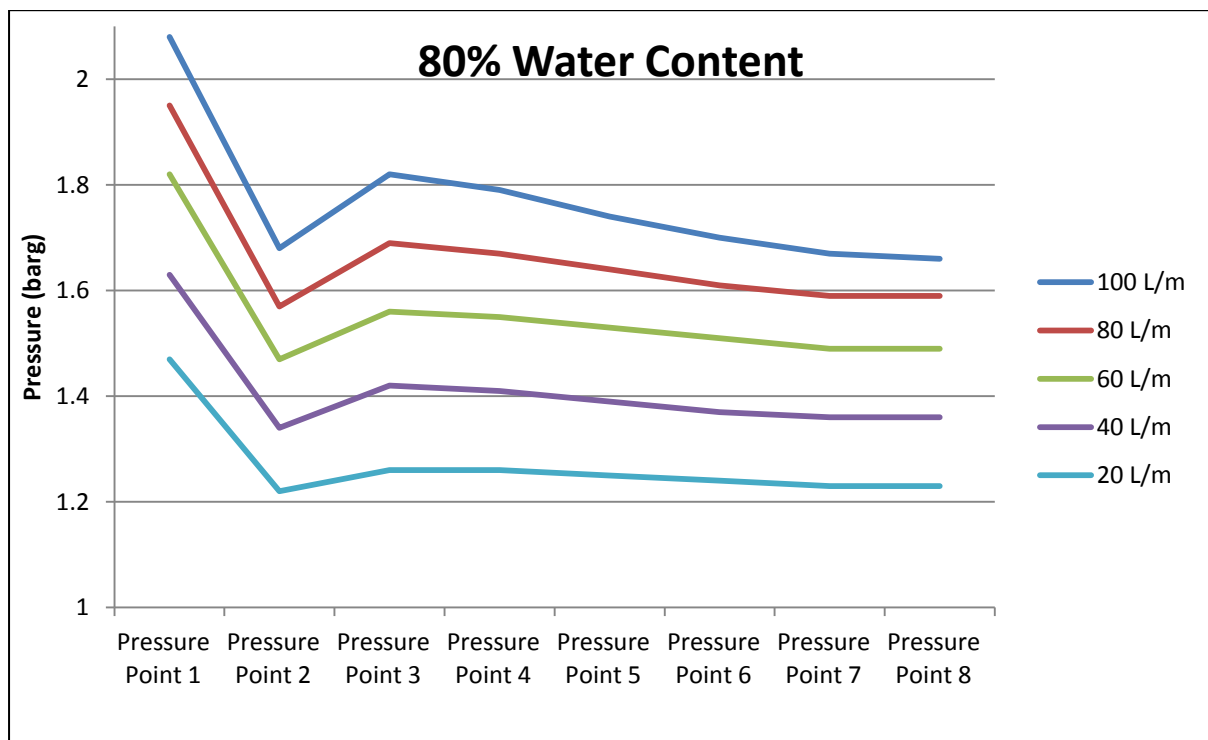
Figure 29: Flow pressure measurement for 80% water volumetric content

5.4.6 Flow Pressure Measurement for 100% Water Volumetric Content (0% Oil Volumetric Content)

Table 12: Flow pressure measurement for 100% water volumetric content

Flow Rate (L/m)	Flow Rate (m/s)	Pressure Point 1 (barg)	Pressure Point 2 (barg)	Pressure Point 3 (barg)	Pressure Point 4 (barg)	Pressure Point 5 (barg)	Pressure Point 6 (barg)	Pressure Point 7 (barg)	Pressure Point 8 (barg)
100	0.8910	2.15	1.73	1.87	1.87	1.86	1.85	1.85	1.84
80	0.7128	2.01	1.62	1.75	1.75	1.74	1.74	1.73	1.73
60	0.5346	1.88	1.53	1.61	1.61	1.6	1.6	1.59	1.59
40	0.3564	1.70	1.39	1.48	1.48	1.47	1.47	1.46	1.46
20	0.1782	1.54	1.27	1.31	1.31	1.30	1.30	1.29	1.29

* Each presented value is a mean value, and the standard error of the mean is less than 0.009.
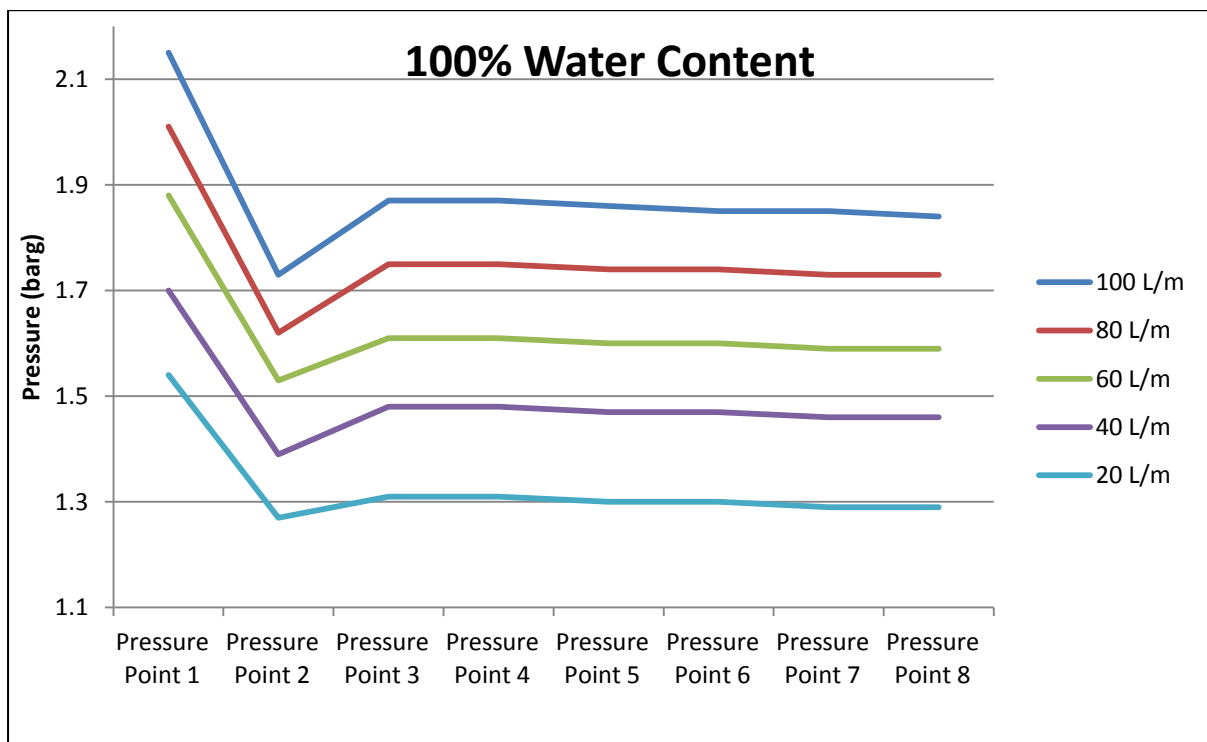
Figure 30: Flow pressure measurement for 100% water volumetric content

5.4.7 Flow Pressure Measurement for 100 L/m (0.8910 m/s) Flow Rate

Table 13: Flow pressure measurement for 100 L/m flow rate

Water Content	Pressure Point 1 (barg)	Pressure Point 2 (barg)	Pressure Point 3 (barg)	Pressure Point 4 (barg)	Pressure Point 5 (barg)	Pressure Point 6 (barg)	Pressure Point 7 (barg)	Pressure Point 8 (barg)
0%	1.84	1.45	1.53	1.5	1.46	1.43	1.4	1.39
20%	1.90	1.50	1.6	1.56	1.51	1.46	1.42	1.4
40%	1.96	1.57	1.69	1.62	1.56	1.49	1.41	1.39
60%	2.02	1.62	1.75	1.68	1.62	1.56	1.50	1.48
80%	2.08	1.68	1.82	1.79	1.74	1.70	1.67	1.66
100%	2.15	1.73	1.87	1.87	1.86	1.85	1.85	1.84

* Each presented value is a mean value, and the standard error of the mean is less than 0.009.

Figure 31: Flow pressure measurement for 100 L/m flow rate

5.4.8 Flow Pressure Measurement for 80 L/m (0.7128 m/s) Flow Rate

Table 14: Flow pressure measurement for 80 L/m flow rate

Water Content	Pressure Point 1 (barg)	Pressure Point 2 (barg)	Pressure Point 3 (barg)	Pressure Point 4 (barg)	Pressure Point 5 (barg)	Pressure Point 6 (barg)	Pressure Point 7 (barg)	Pressure Point 8 (barg)
0%	1.71	1.36	1.44	1.42	1.39	1.36	1.34	1.33
20%	1.77	1.4	1.49	1.46	1.42	1.38	1.35	1.33
40%	1.83	1.47	1.58	1.54	1.48	1.42	1.36	1.34
60%	1.89	1.51	1.63	1.59	1.53	1.47	1.42	1.41
80%	1.95	1.57	1.69	1.67	1.64	1.61	1.59	1.59
100%	2.01	1.62	1.75	1.75	1.74	1.74	1.73	1.73

* Each presented value is a mean value, and the standard error of the mean is less than 0.009.

Figure 32: Flow pressure measurement for 80 L/m flow rate

5.4.9 Flow Pressure Measurement for 60 L/m (0.5346 m/s) Flow Rate

Table 15: Flow pressure measurement for 60 L/m flow rate

Water Content	Pressure Point 1 (barg)	Pressure Point 2 (barg)	Pressure Point 3 (barg)	Pressure Point 4 (barg)	Pressure Point 5 (barg)	Pressure Point 6 (barg)	Pressure Point 7 (barg)	Pressure Point 8 (barg)
0%	1.58	1.27	1.34	1.32	1.29	1.26	1.24	1.23
20%	1.64	1.31	1.38	1.35	1.31	1.27	1.24	1.23
40%	1.70	1.38	1.45	1.42	1.35	1.31	1.26	1.24
60%	1.76	1.44	1.52	1.48	1.41	1.35	1.29	1.28
80%	1.82	1.47	1.56	1.55	1.53	1.51	1.49	1.49
100%	1.88	1.53	1.61	1.61	1.60	1.60	1.59	1.59

* Each presented value is a mean value, and the standard error of the mean is less than 0.009.
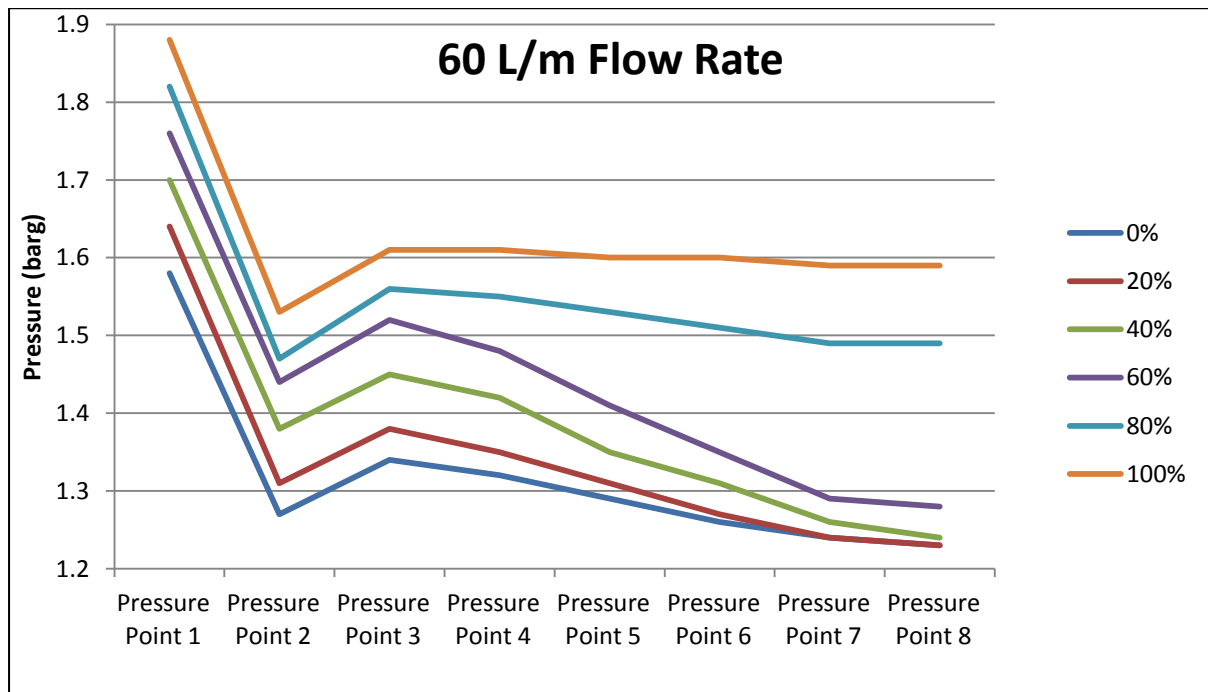
Figure 33: Flow pressure measurement for 60 L/m flow rate

5.4.10 Flow Pressure Measurement for 40 L/m (0.3564 m/s) Flow Rate

Table 16: Flow pressure measurement for 40 L/m flow rate

Water Content	Pressure Point 1 (barg)	Pressure Point 2 (barg)	Pressure Point 3 (barg)	Pressure Point 4 (barg)	Pressure Point 5 (barg)	Pressure Point 6 (barg)	Pressure Point 7 (barg)	Pressure Point 8 (barg)
0%	1.43	1.13	1.18	1.17	1.15	1.13	1.12	1.11
20%	1.48	1.19	1.26	1.24	1.21	1.19	1.17	1.16
40%	1.53	1.25	1.31	1.29	1.25	1.22	1.19	1.18
60%	1.58	1.29	1.36	1.33	1.29	1.25	1.21	1.19
80%	1.63	1.34	1.42	1.41	1.39	1.37	1.36	1.36
100%	1.70	1.39	1.48	1.48	1.47	1.47	1.46	1.46

* Each presented value is a mean value, and the standard error of the mean is less than 0.009.
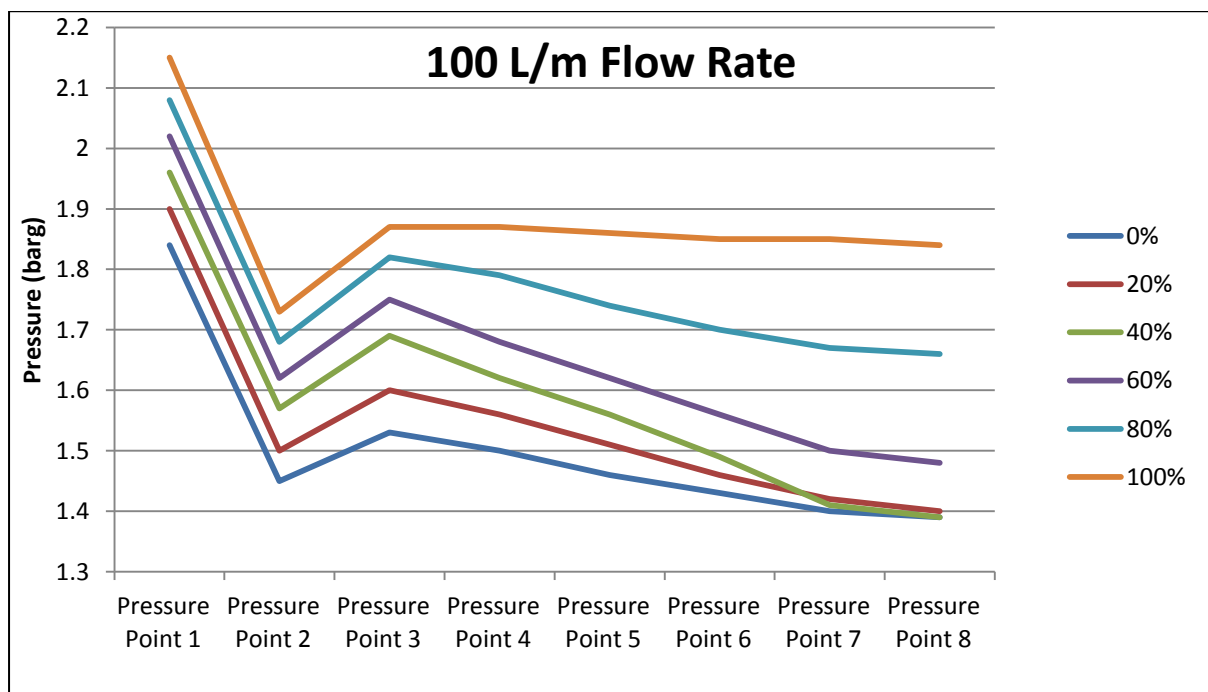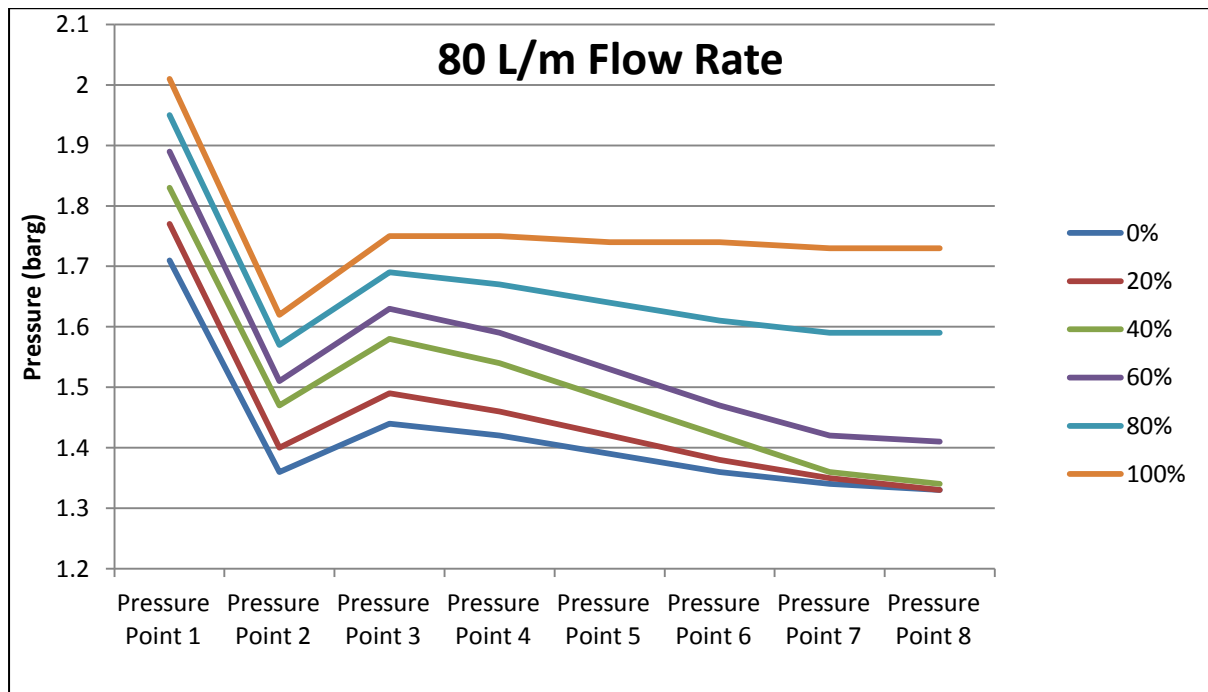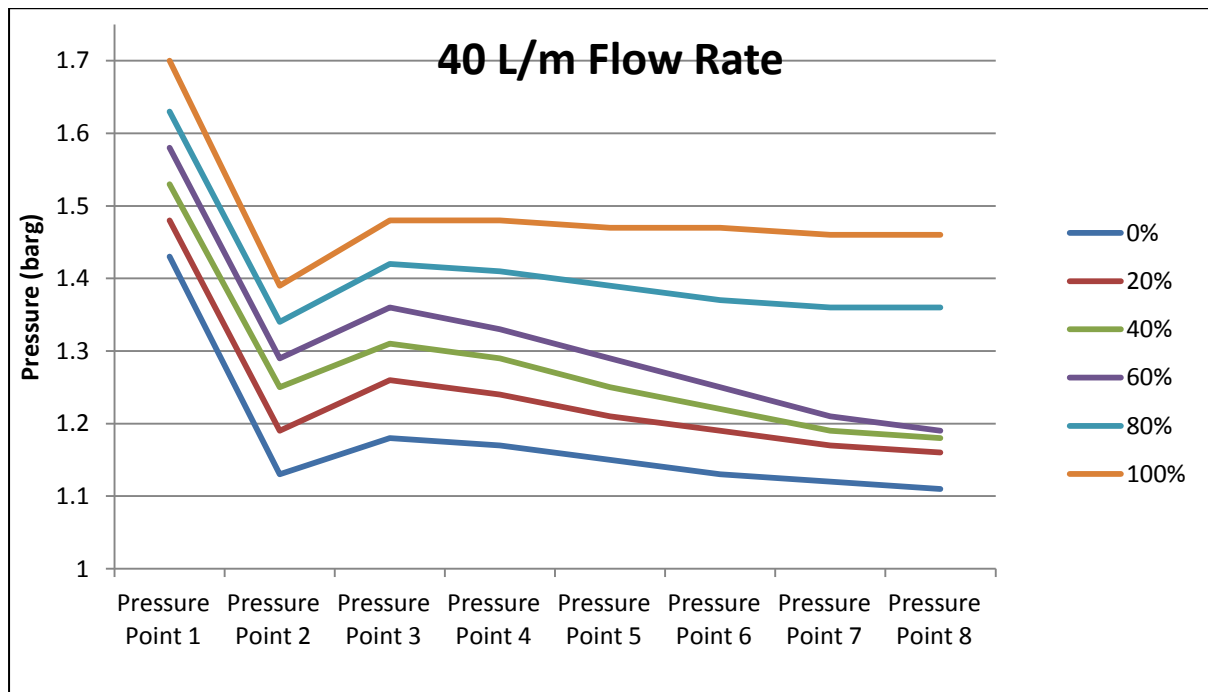

Figure 34: Flow pressure measurement for 40 L/m flow rate

5.4.11 Flow Pressure Measurement for 20 L/m (0.1782 m/s) Flow Rate

Table 17: Flow pressure measurement for 20 L/m flow rate

Water Content	Pressure Point 1 (barg)	Pressure Point 2 (barg)	Pressure Point 3 (barg)	Pressure Point 4 (barg)	Pressure Point 5 (barg)	Pressure Point 6 (barg)	Pressure Point 7 (barg)	Pressure Point 8 (barg)
0%	1.28	1.04	1.08	1.07	1.05	1.03	1.02	1.01
20%	1.32	1.06	1.11	1.1	1.08	1.06	1.04	1.04
40%	1.37	1.13	1.17	1.16	1.13	1.1	1.08	1.08
60%	1.42	1.18	1.21	1.2	1.17	1.15	1.13	1.12
80%	1.47	1.22	1.26	1.26	1.25	1.24	1.23	1.23
100%	1.54	1.27	1.31	1.31	1.30	1.30	1.29	1.29

* Each presented value is a mean value, and the standard error of the mean is less than 0.009.
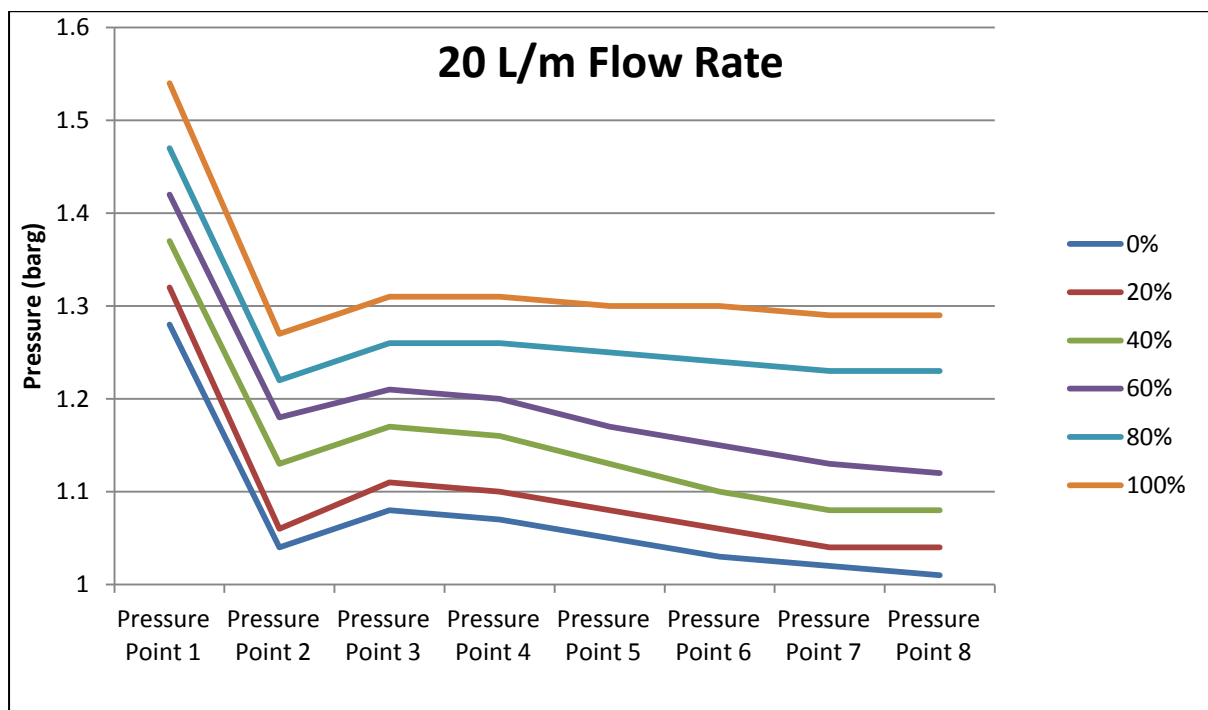
Figure 35: Flow pressure measurement for 20 L/m flow rate

5.4.12 Flow Pressure Drop Profile

The flow pressure drop is taken from the pressure difference between Point 8 and Point 5, where the flow in this section is considered to be fully-developed. The length between Point 8 and Point 5 is 1.39 m.

Table 18: Flow pressure drop profile

Water Content	Pressure Drop for 100 L/m (barg)	Pressure Drop for 80 L/m (barg)	Pressure Drop for 60 L/m (barg)	Pressure Drop for 40 L/m (barg)	Pressure Drop for 20 L/m (barg)
0%	0.07	0.06	0.06	0.04	0.04
20%	0.11	0.09	0.08	0.05	0.04
40%	0.17	0.14	0.11	0.07	0.05
60%	0.14	0.12	0.13	0.1	0.05
80%	0.08	0.05	0.04	0.03	0.02
100%	0.02	0.01	0.01	0.01	0.01
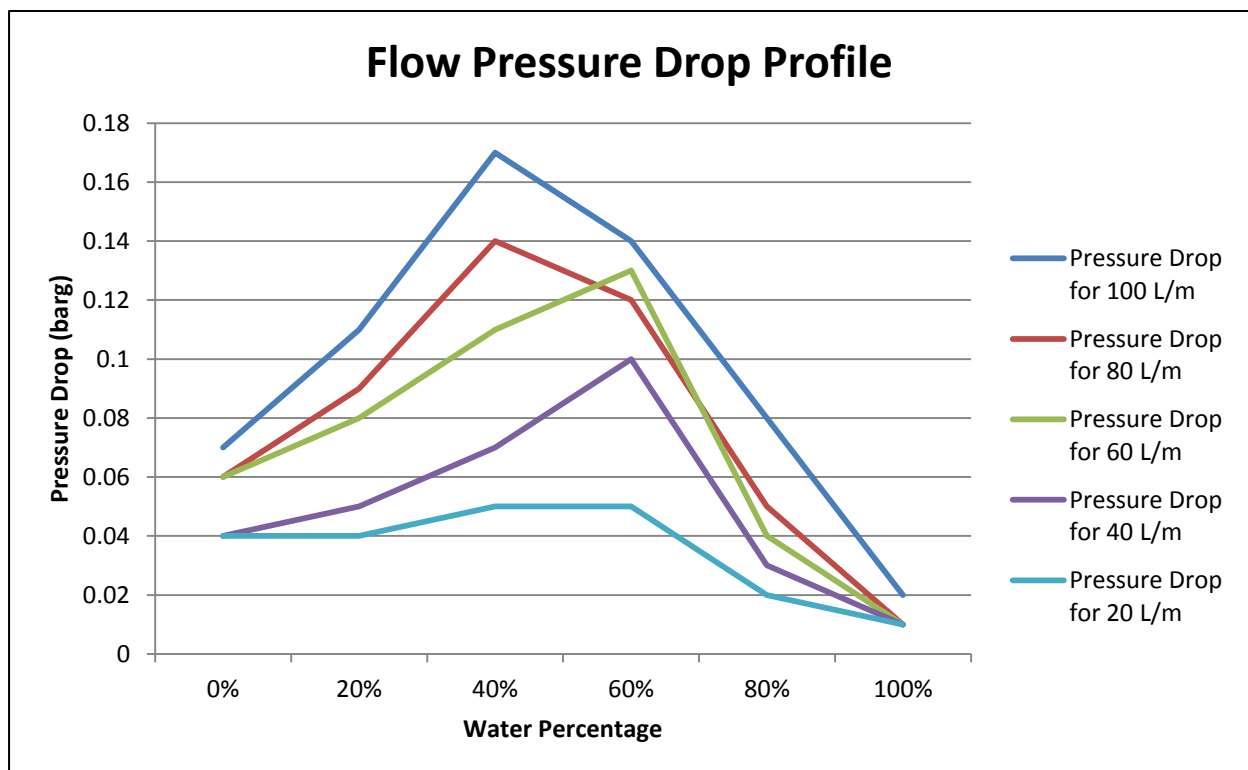
Figure 36: Flow pressure drop profile

5.4.13 Discussion on Flow Pressure Profiles

Sections 5.4.1 to 5.4.6 show the flow pressure profiles at different flow rates, as water volumetric content was increased from 0% to 100%. Generally, the flow pressure profiles exhibited similar trend across Point 1 to Point 8. Point 1, which is located 3 cm before the constriction, gave the highest pressure reading, as the flow started to experience restriction (caused by the constriction and also 90°-bent), with its kinetic energy converted to potential energy, in the form of pressure.

The constriction is defined as the part where the pipe diameter abruptly changes from 2" to 1", with a 90°-bent. This right-angle constriction aims to replicate the usage of choke valves in the oil and gas industry. The flow would experience sudden contraction as it entered into the constriction, and expansion as it left, allowing the Venturi effect to occur. The Venturi effect caused a big pressure drop, and the pressure only started to recover as the flow exited the constriction. Point 2 and Point 3 are located respectively 7 cm and 59 cm after the constriction, and at these 2 points, the pressure could be seen to start recovering.
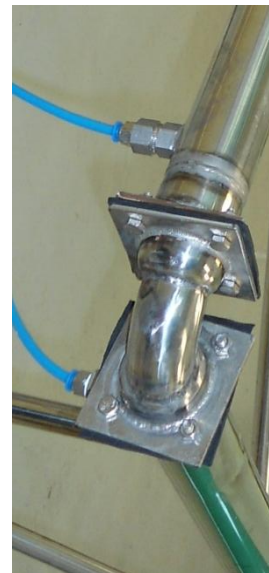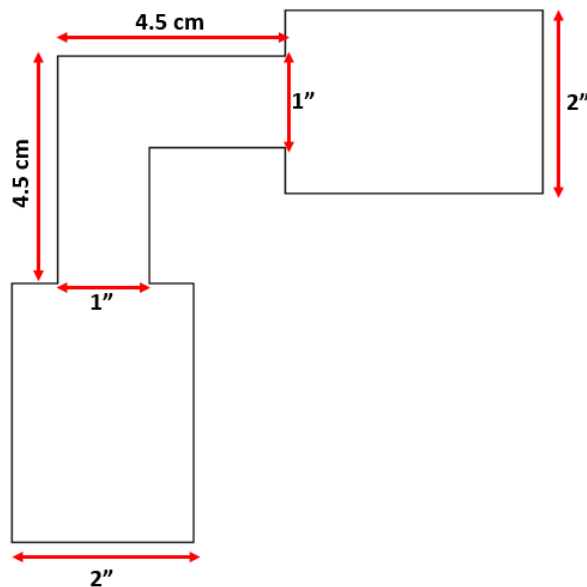
From Figure 9 in Chapter 4: Schematic diagram of the constriction (dimensions are not to scale) and the actual fabricated constriction

Beyond Point 3, the flow pressure had fully recovered, and started to experience pressure loss due to frictional losses, in which emulsions are believed to play a major role. The flow is assumed to be fully-developed at Point 5, which is located 169 cm after the constriction. To verify that 169 cm have sufficiently met the entrance length requirement, the following calculations are performed, with reference to Equations 18 and 19:

Table 19: Verification of entrance length

Pipe Diameter Size	Entrance Length for Pure Crude Oil	Entrance Length for Pure Water
Actual ID: 0.0488 m	At velocity of 0.891 m/s (100 L/m): Re is 9,086.0523 (turbulent flow) The entrance length, ℓ_e is 0.9808 m.	At velocity of 0.891 m/s (100 L/m): Re is 48,712.4099 (turbulent flow) The entrance length, ℓ_e is 1.2976 m.

Thus, from Table 19 above, the length of 169 cm has met the entrance length requirement for both cases of pure crude oil and pure water. The pressure profiles from Point 5 until Point 8 are further analyzed to understand the effect of emulsions on pressure drop.

Throughout Sections 5.4.1 to 5.4.6, it is observed that at higher flow rates, the pressure readings were correspondingly higher. This can be attributed to the higher pump duty, higher pump discharge pressure and total higher energy as the flow rate was increased from 20 L/m to 100 L/m.

Sections 5.4.7 to 5.4.11 show the flow pressure profiles at different water volumetric content, as the flow rate was varied from 100 L/m (or 0.8910 m/s) to 20 L/m (or 0.1782 m/s). As the water volumetric content was increased from 0% to 100% (correspondingly, the oil volumetric content decreased from 100% to 0%), the pressure readings at all points went higher too. This is due to the higher static pressure exerted by water, as water has higher density compared to oil (water density is 1000 kg/m^3, while oil density is 876.8 kg/m^3). The higher static pressure, especially from the tank, resulted in higher suction and discharge pressures of the pump.

Section 5.4.12 shows the flow pressure drop profile for different flow rates, as the water volumetric content was varied from 0% to 100%. This section gives further analysis into the effect of emulsions on pressure drop. As explained earlier, the pressure drop is obtained in a fully-developed regime, which has been determined to be the segment between Point 5 and Point 8. The length of this evaluated fully-developed segment is 1.39 m.

From Figure 36, the pressure drop of pure crude oil (0% water content) was higher than the pressure drop of pure water (100% water content). This can be understood from the viscosity difference between crude oil and water. At temperature of 25 °C, the viscosity of crude oil is 4.7855 cSt, while the viscosity of water is 0.8926 cSt. Liquid with higher viscosity is more resistant towards flow, and it requires more pumping energy to overcome the pressure drop.

As the water content was increased in stages from 0% to 100%, the pressure drop profile increased to a maximum peak, and subsequently reduced to the pressure drop value of pure water. This observation is attributed to the presence of emulsion droplets in the system, which affects the flow viscosity. Previous research findings have shown that:

a) Emulsion droplets will increase the flow viscosity, due to hydrodynamic forces and interactions of the droplets (Krieger and Dougherty, 1959; Lee, 1969; Otsubo and Prud'homme, 1994; Zaki, 1997)

b) Flow viscosity depends on the viscosity of the continuous phase and emulsions, apart from being affected by emulsion droplet size distribution (Kokal, 2005; Ashrafizadeh and Kamran, 2010)

As the water content was increased to 20%, water-in-oil emulsion droplets started to form (refer to Section 5.3). At higher flow rates, more stable water-in-oil emulsion droplets were formed, resulting in higher flow viscosity and flow pressure drop. The trend continued as the water content was further increased to 40%.

At water content of 40%, maximum peak pressure drop was observed for flow rates of 100 L/m (or 0.8910 m/s) and 80 L/m (0.7128 m/s). This peak pressure drop indicates maximum water-in-oil emulsion droplets, and the system had reached the phase inversion point, agreeing with the research by Keleşoğlu et al. (2012). Further increment of water content resulted in phase inversion, with the formation of oil-in-water emulsions, water-in-oil emulsions and multiple emulsions.

However, samples with lower rates of 20 L/m to 60 L/m were only able to attain the maximum peak pressure drop at water content of 60%. This suggests that lower flow rate has a later phase inversion point, in addition to less stable emulsion droplets. This can be related with the reduced interactions and less coalescence between emulsion droplets at lower velocity. At water content of 60% and beyond, all samples had experienced phase inversion. The presence of unstable emulsions, irregular size distribution of emulsion droplets, non-aggregated emulsions with less dense packing, and water as the continuous phase contributed to lower pressure drop after the phase inversion. This observation supports the earlier findings on the drag-reducing characteristics of unstable emulsion (Pal, 1993; Nädler and Mewes, 1997). The pressure drop decreased to the final value of pressure drop of pure water, which was around 0.01 – 0.02 barg.

Comparing the flow rates, sample with flow rate of 100 L/m (or 0.8910 m/s) had the most significant change in pressure drop. At water content of 40%, it reached maximum peak pressure drop with value of 0.17 barg. The pressure drop had increased 142.86% from the pressure drop value of pure crude oil. Meanwhile, sample with flow rate of 20 L/m (or 0.1782 m/s) had the least change in pressure drop. At water content of 60%, it reached maximum peak pressure drop with value of 0.05 barg. The pressure drop only increased 25% from the pressure drop value of pure crude oil. This observation strengthens the hypothesis of the effect of emulsions on pressure drop. Sample with flow rate of 20 L/m had the least amount of emulsions, due to its low velocity and the correspondingly low dissipation energy to form the emulsions (Becher, 1955).

The flow pressure drop profile, as shown in Figure 36, is a good production optimization tool for the upstream oil industry. It accounts for the presence and effect of emulsions, thus answering the uncertainty described in Section 1.2 (Problem Statement). Oil-producing platforms aim to produce at optimum flow rate and discharge pressure, *i.e.* the highest possible flow rate that can be achieved without causing pressure limitation to the export pumps. With the flow pressure drop profile, the maximum pressure drop for a pipeline can be estimated more accurately, given the water and crude content flowing in it. The optimum values of flow rate can be chosen from the intersection of flow pressure drop profile and pump performance curve charts.

5.5 Dissipation Energy in Emulsification

The pressure drop data obtained in Section 5.4.12 can be further analyzed to calculate the friction factor. The equation for Fanning friction factor, f, is given as (Som and Biswas, 2003):

$$f = \frac{\Delta PD}{2L\rho V^2} \tag{25}$$

where ΔP stands for pressure drop, D stands for internal diameter of the pipe, L stands for the length of the measured pressure drop, ρ stands for density, and V stands for velocity.

In Chapter 2, it has been pointed out in Equation 3 that the dissipation energy to disperse the emulsion droplets in cylindrical pipes is related to the Fanning friction factor from the following relationship (Johnsen and Rønningsen, 2003).

$$E = 2f \frac{V^3}{D} \tag{3}$$

Higher dissipation energy facilitates the formation of more stable emulsion droplets.

Table 20: Calculation of dissipation energy values

Water Content	Dissipation Energy for 100 L/m, m^2 / s^3	Dissipation Energy for 80 L/m, m^2 / s^3	Dissipation Energy for 60 L/m, m^2 / s^3	Dissipation Energy for 40 L/m, m^2 / s^3	Dissipation Energy for 20 L/m, m^2 / s^3
0	5.12	3.51	2.63	1.17	0.58
20%	7.82	5.12	3.41	1.42	0.57
40%	11.77	7.75	4.57	1.94	0.69
60%	9.44	6.47	5.26	2.70	0.67
80%	5.26	2.63	1.58	0.79	0.26
100%	1.28	0.51	0.38	0.26	0.13
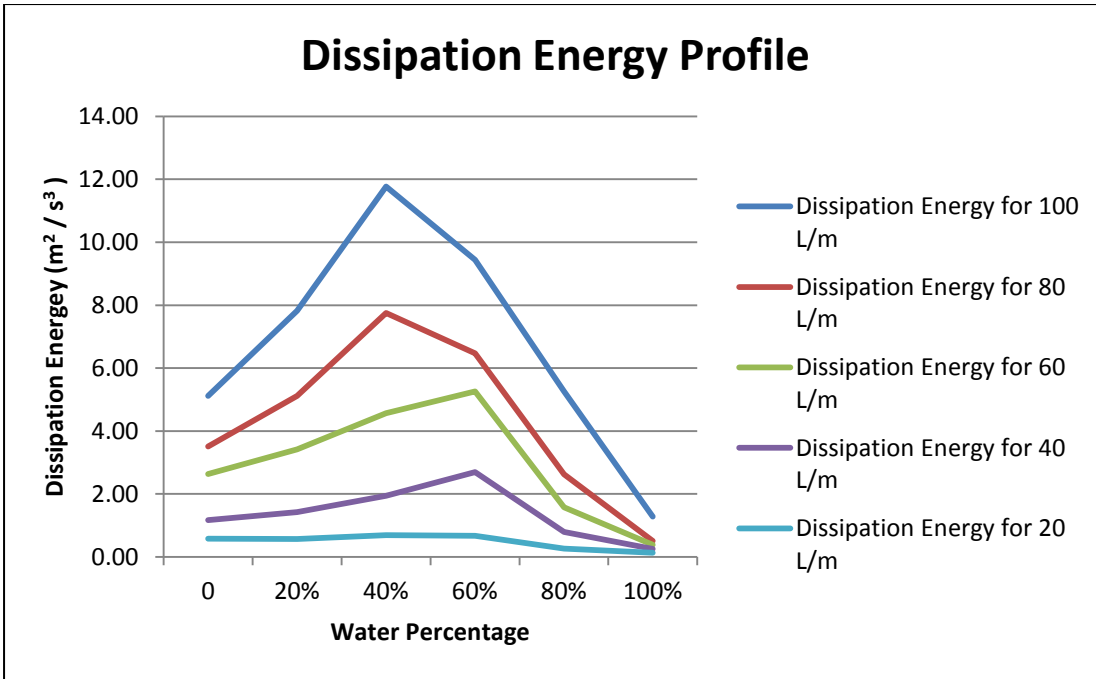
Figure 37: Dissipation energy profile

The dissipation energy profile shares trend similarity with the pressure drop profile (compare Figure 37 and Figure 36). This highlights the significant relationship between dissipation energy, formation of emulsions and the corresponding flow pressure drop. The highest dissipation energy resulted in maximum emulsification and maximum pressure drop.

Equation 25 and Equation 3 can be re-written as:

$$E = \frac{\Delta PV}{L\rho} \tag{26}$$

where E stands for dissipation energy, ΔP stands for pressure drop, V stands for velocity, L stands for the length of the measured pressure drop, and ρ stands for density.

From Equation 26, it can be deduced that the dissipation energy is directly proportional to the pressure drop and velocity.

5.6 Friction Factor and Flow Regime

Equation 25 also allows friction factor to be calculated, and the friction factor profile is plotted in Figure 38.
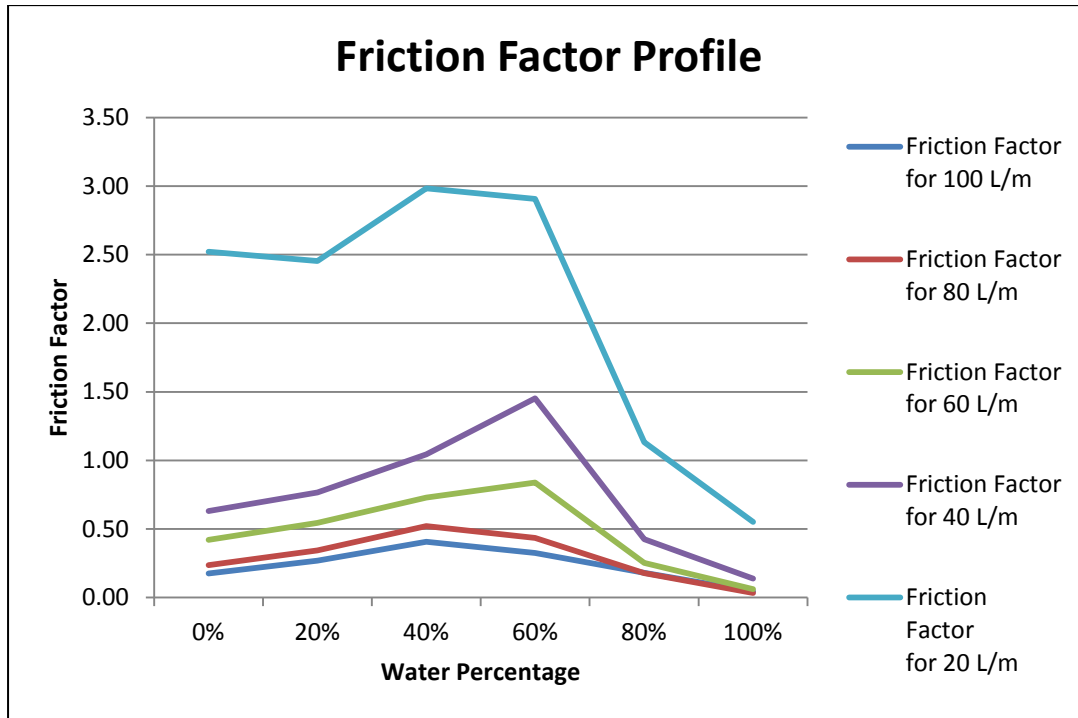
Figure 38: Friction factor profile

The friction factor profile shows the relationship between friction factor and water content percentage. The presence of emulsions affects the friction factor, and this can be understood from the effect of emulsions on flow pressure drop.

For all cases of water volumetric ratios and flow rates, it is calculated that only turbulent flow regime (Re > 4000) was experienced, except at the lowest flow rate of 20 L/m, where transitional flow regime (2100 < Re < 4000) occurred for low water content runs. Figure 39 shows the relationship between Reynolds number and flow rate.
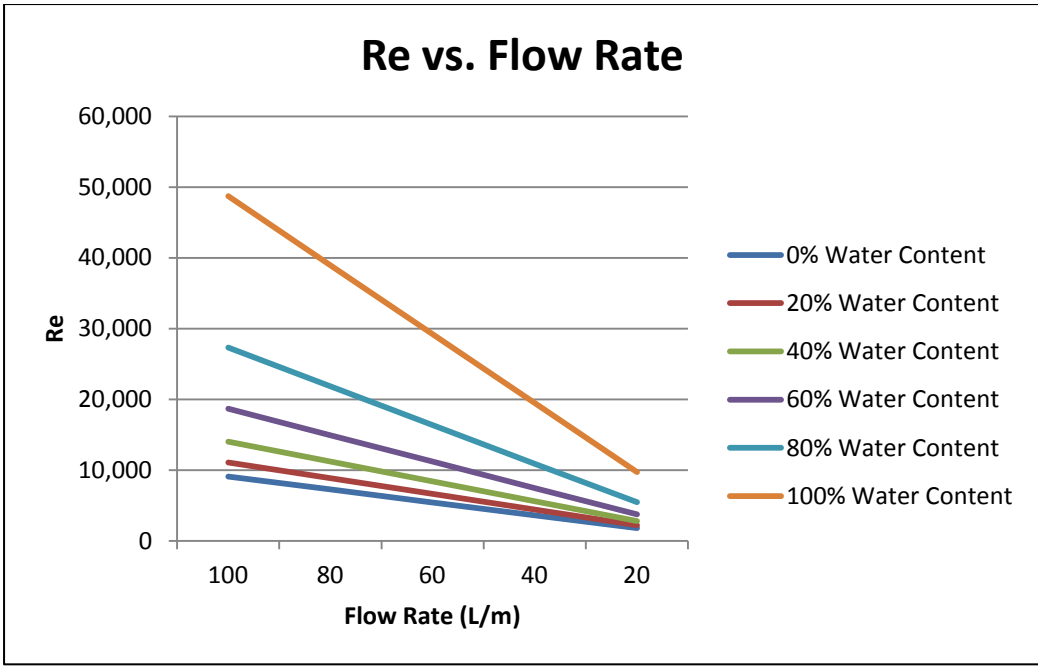
Figure 39: Re vs. Flow Rate

Laminar flow regime was not feasible to be tested, as flow rate below 20 L/m would cause inaccuracy to the flow meter and low flow condition for the pump (can result in pump's overheating and permanent damage).

CHAPTER 6

CONCLUSION AND RECOMMENDATIONS

6.1 Conclusion

Pipeline emulsions flow is an inevitable occurrence in the oil production industry, as the conditions for emulsions formation exist naturally. Apart from shutting-in the wells or opening up other reservoir zones, there is not much control that we can have on the presence of water or other emulsions-favourable fluids. However, the formation of emulsions can still be controlled by manipulating the flow rate or kinetic energy.

This research has met the stated objectives to analyze the formation and stability of emulsions in a continuous flow loop, to determine the phase inversion, to establish the effect of emulsions formation on pressure drop, as well as the relationship with dissipation energy.

Higher flow rate, and correspondingly higher kinetic energy, has resulted in the formation of more stable emulsion droplets. At lower flow rate, there are more emulsions droplets which destabilize and settle out. Also, this research presents a new idea that phase inversion is affected by flow rate, where higher flow rate will bring the emulsions system to an earlier phase inversion. In the laboratory experiment, samples with 60% water volumetric content experienced phase inversion at flow rate above 80 L/m. Samples run with lower flow rate were only able to achieve phase inversion when the water volumetric content was increased to 80%. This can probably be caused by the more frequent coalescence of the emulsion droplets at higher flow rate.

Phase inversion can be determined as the point with maximum pressure drop, as the water volumetric content is increased in water-in-oil emulsions system. Further addition of water will result in the phase inversion from water-in-oil emulsions to oil-in-water emulsions. After the phase inversion, the pressure drop starts to decrease, until it reaches the pressure drop of pure water. Although multiple emulsions are present, the pressure drop still decreases because of the presence of unstable emulsions, irregular size distribution of emulsion droplets, non-aggregated emulsions with less dense packing, and water as the continuous

phase. This trend is more significant at higher flow rate, where more emulsion droplets are present.

The effect of emulsions on pressure drop has been established too, and a flow pressure drop profile is presented, showing the pressure drop at various water volumetric contents for different flow rates. This flow pressure drop profile, which is based on the experimental data, can be generalized for any water-and-oil emulsions system. Apart from flow pressure drop profile, the analysis of pressure drop data allows dissipation energy profile to be drawn. The dissipation energy profile shows the amount of energy required in forming the emulsions. Higher presence of emulsions requires more dissipation energy, and results in more pressure drop. The dissipation energy is directly proportional to the pressure drop and velocity.

In the laboratory experiment, sample with flow rate of 100 L/m reached maximum peak pressure drop at water volumetric content of 40%. The pressure drop had increased 142.86% from the pressure drop value of pure crude oil. Meanwhile, for sample with flow rate of 20 L/m, its maximum peak pressure drop was only attained at water volumetric content of 60%, and it was 25% higher than the pressure drop value of pure crude oil. The sample with flow rate of 20 L/m had the least amount of stable emulsions, lower pressure drop and later inversion point. It can be deduced that higher dissipation energy is required to form more emulsions, and correspondingly, the pressure drop (a measurable variable) will be higher.

In Malaysian offshore brownfields, a big majority of the pipelines are transporting around 10% - 50% of water (PETRONAS, 2015). In the industry, the pipeline transportation system often fails to take into account the effect of emulsions, causing non-optimized operating variables. To mitigate the unwanted formation of emulsions and higher additional pressure loss, the optimum values of flow rate and pump discharge pressure can be chosen from the combination of flow pressure drop profile and pump performance curve charts. The flow pressure drop profile, which is highly dependent on the crude characteristics, should be constructed for a specific pipeline transportation system, and be utilized to improve the overall operations. It is recommended to flow at high flow rate to deliver the crude, but not exceeding the maximum pressure drop that limits the pumps' discharge pressure.

6.2 Recommendations

For future research purposes, it is recommended to:

a) Determine the droplet size distribution of emulsions and characterize the emulsions, to study further into the stability of emulsions.

b) Investigate the molecular interactions at the interfacial films of emulsion droplets, as this will give more understanding on crude oil components that are responsible for emulsification and the stability of emulsions.

APPENDIX

Full crude compositional analysis by gas chromatography:

Table 21: Full crude compositional analysis

No.	Component	Wt%	Mol%
1	C1	0.000	0.000
2	CO2	0.000	0.000
3	C2	0.006	0.037
4	C3	0.071	0.321
5	IC4	0.081	0.279
6	C4	0.201	0.693
7	Neopentane	0.003	0.009
8	IC5	0.285	0.792
9	C5	0.303	0.842
10	2,2-Dimethylbutane*	0.000	0.000
11	2,3-Dimethylbutane*	0.000	0.000
12	Cyclopentane	0.164	0.385
13	2-Methylpentane	0.278	0.652
14	3-Methylpentane*	0.000	0.000
15	C6	0.533	1.252
16	Methylcyclopentane	0.575	1.251
17	2,4-Dimethypentane	0.035	0.077
18	Benzene	0.102	0.221
19	Cyclohexane	0.735	1.599
20	2-Methylhexane*	0.000	0.000
21	3-Methylhexane*	0.000	0.000
22	1,T-3-Dimethylcyclopentane*	0.000	0.000
23	1,C-3-Dimethylcyclopentane*	0.000	0.000

24	1,T-2-Dimethylcyclopentane*	0.000	0.000
25	C7	1.509	3.283
26	Methylcyclohexane	2.139	4.109
27	Ethylcyclopentane*	0.000	0.000
28	Toluene	0.487	0.936
29	2-Methylheptane*	0.000	0.000
30	1-Cis-3-Dimethylcyclohexane*	0.000	0.000
31	3-Methylheptane	0.975	1.873
32	1-Methyl-T-3-Ethylcyclopentane*	0.000	0.000
33	1-Trans-2-Dimethylcyclohexane*	0.000	0.000
34	C8	1.900	3.650
35	Ethylcyclohexane*	0.000	0.000
36	Ethylbenzene	0.473	0.785
37	Meta&Para-Xylene	0.813	1.348
38	Ortho-Xylene	0.220	0.365
39	2-Methyloctane*	0.000	0.000
40	3-Methyloctane*	0.000	0.000
41	C9	2.307	3.827
42	1-Methyl-3-Ethylbenzene*	0.000	0.000
43	1,3,5-Trimethylbenzene*	0.000	0.000
44	n-Propylbenzene*	0.000	0.000
45	1-Methyl-2-Ethylbenzene*	0.000	0.000
46	C10	3.967	5.928
47	n-Butylbenzene	0.458	0.623
48	C11	3.346	4.557
49	C12	4.319	5.372
50	C13	4.679	5.354
51	C14	5.341	5.629
52	C15	8.246	8.015
53	C16	5.789	5.222

54	C17	4.607	3.893
55	C18	5.125	4.088
56	C19	4.232	3.222
57	C20	3.209	2.337
58	C21	3.076	2.117
59	C22	2.323	1.525
60	C23	2.210	1.391
61	C24	2.125	1.285
62	C25	2.054	1.192
63	C26	1.747	0.974
64	C27	1.802	0.963
65	C28	1.971	1.017
66	C29	1.959	0.976
67	C30	2.382	1.148
68	C31	1.496	0.697
69	C32	1.665	0.751
70	C33	1.120	0.490
71	C34	0.767	0.325
72	C35	0.380	0.157
73	C36+	5.410	2.166
	TOTAL	**100.000**	**100.000**

* Considered as pseudo-components, due to co-elution with other components

REFERENCES

Abdel-Aal, H.K., Aggour, M., and Fahim, M.A. (2003). *Petroleum and gas field processing.* New York, U.S.A: Marcel Dekker.

Ahmed, N.S., Nassar, A.M., Zaki, N.N., and Gharieb, H.K. (1999). Formation of fluid heavy oil-in-water emulsions for pipeline transportation. *J. Fuel, 78*, 593–600.

Ali, M.F. and Alqam, M.H. (2000). The role of asphaltenes, resins and other solids in the stabilization of water in oil emulsions and its effects on oil production in Saudi oil fields. *Fuel 79,* 1309 – 1316.

Alwadani, M. S. (2009). *Characterization and rheology of water-in-oil emulsion from deepwater fields*. (MSc. Thesis). Rice University.

Ashrafizadeh, S.N. and Kamran, M. (2010). Emulsification of heavy crude oil in water for pipeline transportation. *Journal of Petroleum Science and Engineering*, *71*, 205 – 211.

Ashrafizadeh, S.N., Motaee, E. and Hoshyargar, V. (2012). Emulsification of heavy crude oil in water by natural surfactants. *Journal of Petroleum Science and Engineering, 86–87*, 137–143.

Aske, N., Kallevik, H., and Sjöblom, J. (2002). Water-in-crude oil emulsion stability studied by critical electric field measurements. Correlation to physico-chemical parameters and near-infrared spectroscopy. *J. Pet. Sci. Eng.,* 36, 1 – 17.

Asomaning, S. and Watkinson, A.P. (1999). Deposit formation by asphaltene-rich heavy oil mixtures on heat transfer surfaces. *Proceedings of the International Conference on Mitigation of Heat Exchanger Fouling and Its Economic and Environmental Implications, July, 1999* (pp. 283-287). Banff, Alberta, Canada: Banff Centre.

Auflem, I. H. (2002). *Influence of asphaltene aggregation and pressure on crude oil emulsion stability*. (Doktor Ingeniør Thesis). Norwegian University of Science and Technology.

Aveyard, R., Binks, B.P., Fletcher, P.D.I. and Ye, X. (1992). The resolution of emulsions, including crude oil emulsions, in relation to HLB behaviour. In. Sjöblom, J. (Ed.), *Emulsions - A fundamental and practical approach* (pp. 97-110). Netherland: Kluwer Academic Publishers.

Becher, P. (1955). *Principles of emulsion technology*. New York: Reinhold

Becker, J. R. (1997). *Crude oil waxes, emulsions, and asphaltenes* (pp. 126-129). Oklahoma: PennWell Publishing Company.

Bennett, C.A., Appleyard, S., Gough, M., Hohmann, R.P., Joshi, H.M., King, D.C... Stomierowski, S.E. (2006). Industry recommended procedures for experimental crude oil preheat fouling research. *Heat Transfer Eng., 27*, 28-35.

Bhardwaj, A. and Hartland, S. (1998). Studies on build up of interfacial film at the crude oil/water interface. *J. Dis. Sci. Tech.*, *19(4),* 465-473.

Binks, B.P. (1993). Surfactant monolayers at the oil-water interface. *Chemistry and Industry (July), 14,* 537-541.

Boukadi, F., Singh, V., Trabelsi, R., Sebring, F., Allen, D., and Pai, V. (2012). Appropriate separator sizing: A modified Stewart and Arnold method. *Modelling and Simulation in Engineering*, 721814. DOI: 10.1155/2012/721814

Briceno, M., Isabel, R.M., Bullón, J., and Salager, J.L. (1997). Customizing drop size distribution to change emulsion viscosity. *2nd World Congress on Emulsion - 2ème Congrès Mondial de l'Emulsion CME2* (Paper 2-1-094). Bordeaux, France.

Broughton, G. and Squires, L. (1938). The viscosity of oil–water emulsions. *J. Phys. Chem. 42,* 253–263.

Cengel, J. A., A. A. Faruqui; J. W. Finnigan, C. H. Wright, and J. G. Knudsen. (1962). Laminar and turbulent flow of unstable liquid-liquid emulsions. *AIChE* J., *8(3),* 335.

Charles, M., Govier, G.W. and Hodgson, G. W. (1961). The horizontal flow of equal density oil-water Mixtures. *Can. J. Chem. Engng., 39,* 27-36.

Cheng, D.C.-H. and Heywood, N.I. (1984). Flow in pipes. I. Flow of homogeneous fluids. *Phys. Technol. 15*, 244–251.

Darby, R. (1996). *Chemical engineering fluid mechanics*. Marcel Dekker, Inc.

Devold, H. (2013). *Oil and gas production handbook: An introduction to oil and gas production, transport, refining and petrochemical industry.* ABB.

Einstein, A. (1906). Eine neue bestimmung der moleküldimensionen, *Ann. Physik, 19*, 289-306.

Ese, M.H., Galet, L., Clausse, D. and Sjöblom, J. (1999). Properties of Langmuir Surface and Interfacial Films Built up by Asphaltenes and Resins: Influence of Chemical Demulsifiers. *J. Coll. Int. Sci.*, *220,* 293-301.

Fingas, M., Fieldhouse, B., Bobra, M., and Tennyson, E. (1993). The physics and chemistry of emulsions. *Proceedings of the Workshop on Emulsions.*Washington, D.C.: Marine Spill Response Corporation.

Gafonova, O.V. (2000). *Role of Asphaltenes and Resins in the Stabilization of Waterin-Hydrocarbon Emulsions*. The University of Calgary: MSc. Thesis.

Grace, R. (1992). Commercial Emulsion Breaking. In L.L. Schramm (Ed.), *Emulsions fundamentals and applications in the petroleum industry* (pp. 313-338). Washington DC: American Chemical Society.

Industrial Grade 09 Computer Electronics Owner's Manual. (2010). USA: GPI.

Johnsen, E.E. and Rønningsen, H.P. (2003). Viscosity of live water-in-crude oil emulsions: Experimental work and validation of correlations. *Pet. Sci. Eng., 38,* 23–36.

Keleşoğlu, S., Pettersen, B.H. and Sjöblom, J. (2012). Flow properties of water-in-North Sea heavy crude oil emulsions. *Journal of Petroleum Science and Engineering*, *100,* 14- 23.

Kilpatrick, P.E., and Spiecker, P.M. (2001). Asphaltene Emulsion. In J. Sjöblom (Ed.), *Encyclopedic handbook of emulsion technology* (pp. 707-730). New York: Marcel Dekker

Kokal, S. (2005). Crude-oil emulsions: A state-of-the-art review. *SPE Production and Facilities, SPE 77497-PA.* http://dx.doi.org/10.2118/77497-PA.

Krieger, I.M. and Dougherty, T.J. (1959). A mechanism for non-Newtonian flow in suspensions of rigid spheres. *Trans. Soc. Rheol. 3*, 137–152.

Krawczyk, M.A., Wasan. D.T., and Shetty, C. (1991). Chemical demulsification of petroleum emulsions using oil-soluble demulsifiers. *Ind. Eng. Chem. Res. 30(2),* 367–375.

Lamb, M.S. and Simpson, W.C. (1963). Pipeline transportation of wax laden crude oil as water suspensions. *Proc. Sixth World Petroleum Congress, 19 – 26 June*. Germany.

Lee, D.I. (1969). The viscosity of concentrated suspensions. *Trans. Soc. Rheol. 13*, 273–288.

Lee, R. F. (1999). Agents which promote and stabilize water-in-oil emulsions. *Spill Science & Technology Bulletin*, 5(2), 117-126.

Lim, J.S., Wong, S.F., Law, M.C., Samyudia, Y. and Dol, S.S. (2015). A Review on the effects of emulsions on flow behaviours and common factors affecting the stability of emulsions. *Journal of Applied Sciences, 15*, 167-172. DOI: 10.3923/jas.2015.167.172.

Marsden, S.S. and Raghavan, R. (1973). A system for producing and transporting crude oil as an oil/water Emulsion. *Journal of the Institute of Petroleum, 59, 570*, 273-278.

Mat, H., Samsuri, A., Wan Rahman, W. A. and Siti, I.R. (2006). *Study on demulsifier formulation for treating Malaysian crude oil emulsion*. Universiti Teknologi Malaysia, Malaysia.

Merchant, Jr. and Sylvia, M.L. (1988). *US Patent No. 4737265 A*. Water based demulsifier formulation and process for its use in dewatering and desalting crude hydrocarbon oils.

Messick M.A. (1982). *US Patent 4343323 A*. Pipeline transportation of heavy crude oil.

Mouraille, O., Skodvin, T., Sjöblom, J., and Peytavy, J.L. (1998). Stability of water-in-crude oil emulsions, role played by the state of salvation by asphaltenes and by waxes. *J. Dispersion Sci. Technol.*, 19, 339 – 367.

Nädler, M. and Mewes, D. (1997). Flow induced emulsification in the flow of two immiscible liquids in horizontal pipes. *Int. J. Multiphase Flow*, *23*, 55-68.

NRT Science & Technology Committee. (1997). *Emulsion breakers and inhibitors for treating oil spills* [Fact Sheet].

Omer, A. and Pal, R. (2010). Pipeline flow behavior of water-in-oil emulsions with and without a polymeric additive in the aqueous phase. *Chem. Eng. Technol., 33(6),* 983-992.

Omer, A. and Pal, R. (2013). Effects of surfactant and water concentrations on pipeline flow of emulsions. *Ind. Eng. Chem. Res., 52,* 9099 – 9105.

Otsubo, Y. and Prud'homme, R.K. (1994). Effect of drop size distribution on the flow behaviour of oil-in-water emulsions. *Rheol. Acta, 33,* 303–306.

Pal, R. (1987). *Emulsions: Pipeline flow behaviour, viscosity equations and flow measurement.* (PhD Thesis). Univ. of Waterloo, Ontario.

Pal, R. (1993). Pipeline flow of unstable and surfactant-stabilized emulsions. *AIChE J., 39,* 1754-1764

Pal, R. (1998). Effects of droplet size and droplet size distribution on the rheology of oil-in-water emulsions. In *Proceedings of the 7ᵗʰ UNITAR International Conference for Heavy Crude and Tar Sands* (No. 1998.053).

Pal, R. (2007). Mechanism of turbulent drag reduction in emulsions and bubbly suspensions. *Ind. Eng. Chem. Res., 46(2),* 618-622.

Pal, R. and Hwang, C.-Y.J. (1999). Loss coefficients for flow of surfactant-stabilized emulsions through pipe components. *Trans IChemE 77 (Part A),* 685 – 691

Pal, R. and Rhodes, E. (1989). Viscosity / concentration relationships for emulsions. *J. Rheol., 33(7),* 1021-1045.

Pal, R., Bhattacharya and Rhodes, E. (1986). Flow behaviour of oil-in-water emulsions. *Can. J. Chem. Engng 64, 3-10.*

Pal, R., Yan, Y., and Masliyah, J.H. (1992). In L.L. Schramm (Ed.), *Emulsions fundamentals and applications in the petroleum industry* (pp. 141-145). Washington DC: American Chemical Society.

Paso, K., Silset,A., Sørland,G., Goncalves, M.A.L., and Sjöblom, J. (2009).Characterization of the formation ,flow ability, and resolution of Brazilian crude oil emulsions. *Energy Fuels 23(1),* 471–480.

PETRONAS. (2015). Annual Crude Pipeline Network Capacity Report (Internal Report).

Pilehvari, A., Saadevandi, B., Halvaci, M. and Clark, P. E. (1988). Oil/water emulsions for pipeline transport of viscous crude oils. In *SPE Annual Technical Conference and Exhibition, 2-5 Oct* (Paper SPE 18218). http://dx.doi.org/10.2118/18218-MS.

Plasencia, J., Pettersen, B., and Nydal, O.J. (2013). Pipe flow of water-in-crude oil emulsions: Effective viscosity, inversion point, and droplet size distribution. *Journal of Petroleum Science and Engineering, 101,* 35-43.

Plegue, T. H., Frank, S. G., Fruman, D. H. and Zarkin, J. L. (1989) Concentrated viscous crude oil-in-water emulsions for pipeline transport. *Chem. Engng Comm,. 82,* 111-122.

Porter, M.R. (1994). Use of surfactant theory. In *Handbook of surfactants* (pp. 26-93). United Kingdom: Blackie Academic & Professional.

Pouplin, A., Masbernat, O., Decarre, S., and Line, A. (2010). Transition to turbulence in a dispersed liquid-liquid horizontal flow. In *Proceedings of the 7th International Conference on Multiphase Flow ICMF 2010*. Tampa, FL, USA.

Richardson, E. (1933). Viscosity of emulsions. *Kolloid-Z, 65*, pp. 32

Rose, S. C. and Marsden Jr, S. S. (1970). The flow of North Slope crude oil and its emulsions at low temperatures. In *SPE 45th Annual Fall Meeting and Exhibition*, 4-7 Oct (Paper SPE 2996). http://dx.doi.org/10.2118/2996-MS.

Russel T., Hodgson, G. W. and Govier G. W. (1959). Horizontal pipeline flow of mixtures of oil and water. *Can. J. Chem. Eng., 37*, 9-17.

Sakka, S. (2002*). Sol–gel science and technology topics in fundamental research and Applications* (Vol. 1, pp. 33-35). New York: Springer.

Sanchez, L. E. and Zakin, J. L. (1994) Transport of viscous crudes as concentration oil-in-water emulsions. *Ind. Engng Chem. Res. 33*, 3256-3261.

Schorling, P. C., Kessel, D.G. and Rahimian, I. (1999). Influence of crude oil resin/asphaltene ratio on the stability of oil/water Emulsion. *Colloids and Surfaces, 152*, 95-102.

Schramm, L. L. (1992). Petroleum emulsions. In L.L. Schramm (Ed.), *Emulsions fundamentals and applications in the petroleum industry* (pp. 1045). Washington DC: American Chemical Society.

Schubert, H. and Armbruster, H. (1992). Principles of formation and stability of emulsions. *International Chemical Engineering, 32(1),* 14-28.

Sherman, P. (1970). *Industrial rheology.* London: Academic Press.

Sifferman T.R. (1981). *US Patent No. 4265264 A*. Method of transporting viscous hydrocarbons.

Simon, R. and Poynter W.G. (1970). *US Patent No. 3519006 A*. Pipelining oil/water mixtures.

Sjöblom, J. (2006). *Emulsions and emulsion stability* (2nd ed.). London, UK: Taylor & Francis.

Sjöblom, J., Johnsen, E.E., Westvik, A., Ese, M-H., Djuve, J., Auflem, I.H. and Kallevik, H. *et al.* (2001). Demulsifiers in the oil industry. In J. Sjöblom (Ed.), *Encyclopedic handbook of emulsion technology*. New York: Marcel Dekker.

Sjöblom, J., Mingyuan, L., Christy, A.A., and Gu, T. (1992). Water-in-crude oil emulsions from the Norwegian continental shelf. 7 - Interfacial pressure and emulsion stability. *Colloids and* Surfaces, 66, 55-62.

Sjöblom, J., Mingyuan, L., Hoiland, H., and Johansen, E.J. (1990). Water-in-crude oil emulsions from the Norwegian continental shelf. Part III - A comparative destabilization of model systems. *Colloid and Surfaces*. *46,* 127-139.

Som, S.K. and Biswas, G. (2003). *Introduction to fluid mechanics and fluid machines* (2nd ed.). New Delhi: Tata McGraw-Hill.

Speight, J.G. (1994). Chemical and physical properties of petroleum asphaltenes. In T.F. Yen and G.V. Chilingarian (Eds.), *Asphaltenes and Asphalt* (1). Amsterdam, Elsevier Science.

Speight, J. G. (2014). *The chemistry and technology of petroleum* (5th ed.). U.S., Boca Raton: Taylor & Francis.

Tadros, T.F. (1994). Fundamental principles of emulsion rheology and their applications. *Colloids Surf. A, 91*, 39-55.

Tadros, T. F., and Vincent, B. (1983). Emulsion stability. In P. Becher (Ed.), *Encyclopaedia of emulsion technology* (Vol 1). New York: Marcel Dekker.

Tambe, D.E., and Sharma, M.M. (1993). Factor controlling the stability of colloid-stabilized emulsions: An experimental investigation. *J. Coll. Int. Sci. 157*, 244-253.

Taylor, G.I. (1932). The viscosity of a fluid containing small drops of another liquid. *Prec. R. Soc.* A, 138, 41-48.

Wilkes, J. (1999). *Fluid mechanics for chemical engineers*. US: Prentice Hall.

Wong, S.F., Lim, J.S. and Dol, S.S. (2015a). Crude oil emulsion: A review on formation, classification and stability of water-in-oil emulsions. *Journal of Petroleum Science and Engineering, 135,* 498-504. DOI: 10.1016/j.petrol.2015.10.006.

Wong, S.F., Law, M.C., Samyudia, Y. and Dol, S.S. (2015b). Rheology study of water-in-crude oil emulsions. *Chemical Engineering Transactions, 45,* 1411-1416. DOI:10.3303/CET1545236.

Yaghi, B.M., and Al-Bemani, A. (2002). Heavy crude oil viscosity reduction for pipeline transportation. *Energy Sources, 24*, 93–102.

Yang, F., Niu, Q., Lan, Q., and Sun, D. (2007). Effect of dispersion pH on the formation and stability of pickering emulsions stabilized by layered double hydroxides particles. *J. Colloid Interface Sci., 306 (2),* 285–295.

Zaki, N., Schorling, P.C., and Rahimian, I. (2000). Effect of asphaltene and resins on the stability of water-in-crude-oil emulsions. *Petroleum Sci. Tech.*, *18*, 945-963.

Zaki, N. (1997). Surfactant stabilized crude oil-in-water emulsions for pipeline transportation of viscous crude oils. *Colloids Surf., A Physicochem. Eng. Asp., 125 (1)*, 19–25.

Zaki, N.N., Abdel-Raouf, M.E. and Abdel-Azim, A.A.A. (1996). Propylene oxide-ethylene oxide block copolymer as demulsifier for water-in-oil emulsion - Effect of molecular weight and hydrophilic-lipophylic balance on the demulsification efficiency. *Journal of Monatshefte für Chemie*. 127, 621-629.

Zakin, J. L., Pinaire, R. and Borgmeyer, M. E. (1979). Transport of oils as oil-in-water emulsions. *J. Fluids Eng., 101(1),* 100-104.

Zhang, J., Chen, D., Yan, D., Yang, X. and Shen, C. (1991). Pipelining of heavy crude oil as oil-in-water emulsions. In *SPE Production Operations Symposium, 7-9 April* (SPE 21733*).* Oklahoma City, Oklahoma. http://dx.doi.org/10.2118/21733-MS.